# THE ELUCIDATION OF SINGLE ELECTRON TRANSFER (SET) MECHANISMS IN THE REACTIONS OF NUCLEOPHILES WITH CARBONYL COMPOUNDS

by

Larry E. Brammer, Jr.

Dissertation submitted to the Faculty of the

Virginia Polytechnic Institute and State University

in partial fulfillment of the requirements for the degree of

DOCTOR OF PHILOSOPHY

IN

CHEMISTRY

APPROVED:

James M. Tanko, Chairman

Mark R. Anderson

Karen J. Brewer

Harry W. Gibson

James F. Wolfe

June, 1996

Blacksburg, Virginia

Key Words: Radical anions, Single electron transfer, Electrochemistry, Nucleophilic substitution, Ketyl anion

# THE ELUCIDATION OF SINGLE ELECTRON TRANSFER (SET) MECHANISMS IN THE REACTIONS OF NUCLEOPHILES WITH CARBONYL COMPOUNDS

by

Larry E. Brammer, Jr.

James M. Tanko, Chairman

Chemistry

(ABSTRACT)

The chemistry of the radical anion generated from 1,1-dimethyl-5,7-di-*t*-butylspiro[2,5]octa-4,7-dien-6-one (**20**) was studied electrochemically using cyclic and linear sweep voltammetry (CV, LSV). The reduction potential of **20** was estimated to be -2.5 V vs. 0.1 M $Ag^+/Ag$, similar to the reduction potentials observed for aryl ketones and enones. LSV results for the reduction of **20** are consistent with the occurrence of substrate reduction followed by a subsequent chemical step (an EC mechanism). The broadness of the reduction wave and variation of peak potential with sweep rate suggest that the rate limiting step is heterogeneous electron transfer. Ring opening of the radical anion generated from **20** results in a 9:1 ratio of the 3° and 1° distonic radical anions. The rate constant for ring opening has been estimated to be $k \geq 10^7\ s^{-1}$, with a calculated (AM1) enthalpy of ring opening of $\Delta H^\circ > -15$ kcal/mol. The facile nature of radical anion ring opening can be ascribed to the relief of cyclopropyl ring strain in conjunction with the establishment of aromaticity. On this basis, the regiochemistry of the ring

opening of the radical anion derived from **20** suggests that polar and SET pathways can be differentiated based upon the regiospecificity of cyclopropyl ring opening.

In reactions between **20** and nucleophiles known to react via SET with carbonyl compounds, **20** successfully produced products characteristic of SET pathways. However, subsequent studies of the reaction between **20** and thiophenoxide, a nucleophile purported to undergo SET, produced no evidence for a SET pathway.

It was discovered that ring opened products may also be formed by competing polar pathways involving a carbocationic intermediate, especially in protic solvents. In dipolar aprotic solvents, ring opening occurs primarily via an $S_N2$ process, with nucleophilic attack occurring preferentially at the least hindered carbon. The strengths and weaknesses of **20** as a SET probe are discussed.

## ACKNOWLEDGEMENTS

I would like to extend my sincerest gratitude to Dr. James (Jimbo) M. Tanko for his patience, understanding, and guidance during my graduate work. My warmest thanks are extended to Mrs. Linda Tanko for making Blacksburg feel more like home. I would like to thank my committee for their help, encouragement, and critical reviews of my work. I would like to extend a measure of gratitude to Dr. Arthur Guinness, Dr. Darin Dotson and Dr. Paul Higgs for keeping me focused on the overall goals of this endeavor and Mr. Trent Selby for being an excellent fishing companion when I needed to unwind. My warmest regards are extended to the gentlemen who participated in intramural softball, especially the other senior citizen on the team who helped keep the first base side of the field invincible, Harry, we played, we ached, and we almost conquered.

I would like to thank the office staff who helped me trudge through the unavoidable bureaucracy, especially Mrs. Vicki Hutchinson a true fellow Appalachian American. Finally, I would like to thank my mother and father for listening to me complain, providing a shoulder to cry on, and for their unwavering support throughout my many endeavors, it is finally over.

# TABLE OF CONTENTS

# LIST OF ILLUSTRATIONS

# LIST OF TABLES

# CHAPTER 1. HISTORICAL OVERVIEW

Single electron transfer (SET) has emerged as a major mechanistic pathway in the addition of nucleophiles to carbonyl compounds. Detection of SET pathways is seldom simple as often the same products are produced regardless of the pathway taken ( SET or polar), **Figure 1**.

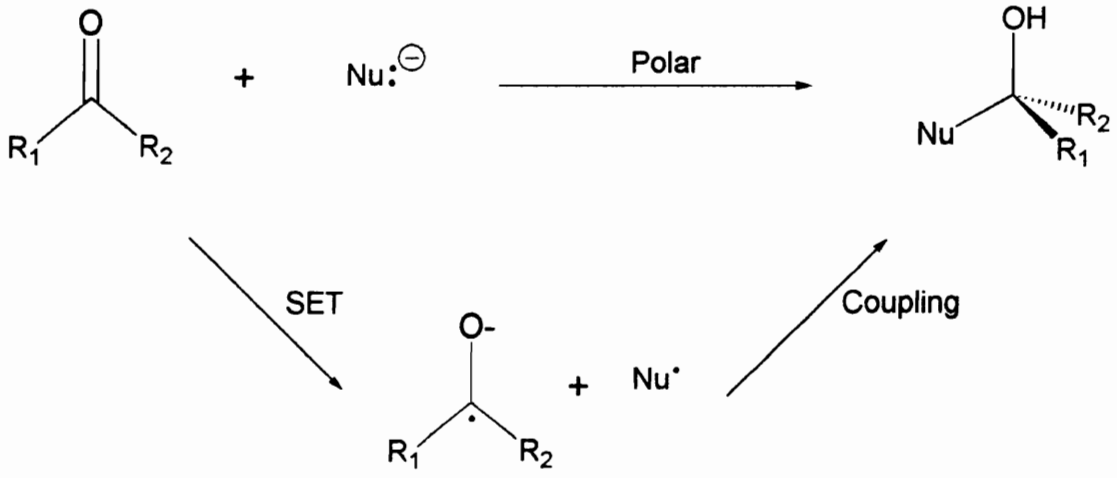


**Figure 1: Comparison between SET and polar pathways.**

Unique to a SET pathway is the formation of paramagnetic intermediates. Several methods have been employed to identify or trap these intermediates to allow the detection of a SET pathway.

A popular method for elucidation of SET pathways utilizes electron paramagnetic resonance spectroscopy (EPR) to detect the paramagnetic intermediate.[1,2,3,4] This method

allows detection of radicals and radical anions present at very low concentrations. Spectroscopic observation of a radical intermediate does not necessarily mean that the intermediate is involved in the reaction pathway leading to product formation. Experimental evidence has shown that in some cases, the EPR active species was an intermediate leading to a "blind" pathway not involved in product formation.[5,6] To avoid this type of error, researchers have turned their attention toward the incorporation of functional groups (*i.e. "probes")* into the substrate whose transformation lead to unique products when electron transfer occurs.

The probes used for identification of SET pathways fall into two general categories: fragmentation probes and rearrangement probes. Fragmentation probes involve substituents which lead to fragmentation and formation of a stable anion after electron transfer has occurred. Identification of a SET pathway is then made through product analysis, **Scheme 1**.

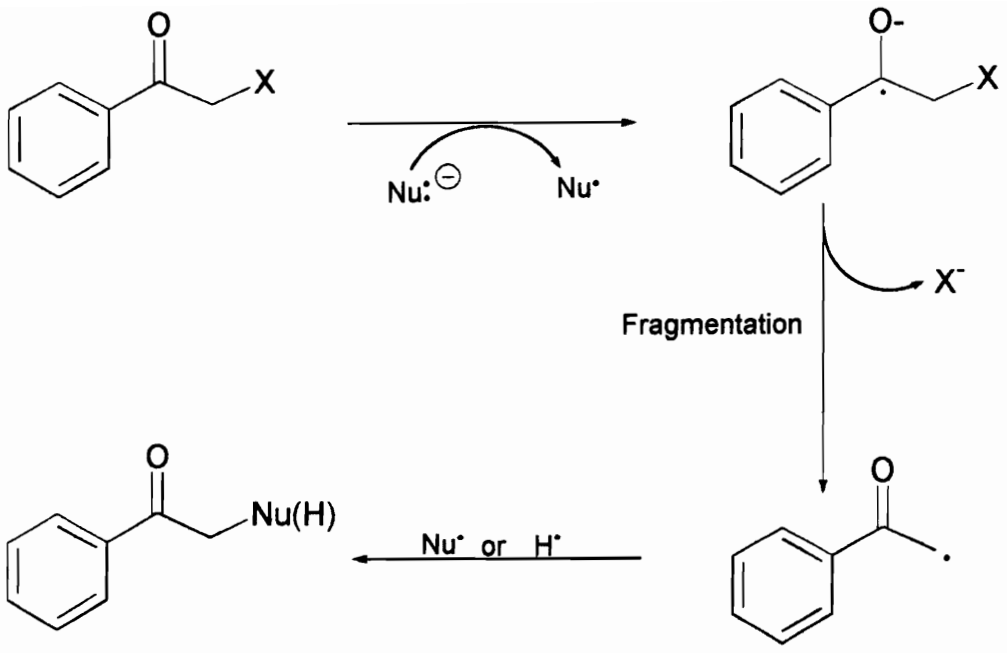


**Scheme 1**

While it is ambiguous as to whether products obtained from a 1,2 addition process indicate a SET pathway or a polar pathway, it is presumed that products obtained from a formal Nu·/neutral radical coupling ($ArCOCH_2Nu$) or a hydrogen atom abstraction ($ArCOCH_3$) are formed from the radical produced through a SET pathway.[7,8] Nu·/radical coupling is advantageous because it shows that SET was the pathway which produced the products. A direct nucleophilic ($S_N2$) substitution pathway at the α-carbon can not be discounted as an alternative mechanism for formation of $ArCOCH_2Nu$. The presence of the products observed from hydrogen atom addition, pinacol coupling of the radical anions, or radical dimerization can only serve to show that a SET reaction has occurred;

however, the SET reaction could also be a side reaction not involved in the product determining pathway.

The success of this approach in the identification of SET relies on the reversibility of the fragmentation step ($k_1$) and its rate being faster than any competitive process involving the radical anion (e.g., $k_2$ and $k_3$, **Figure 2**).

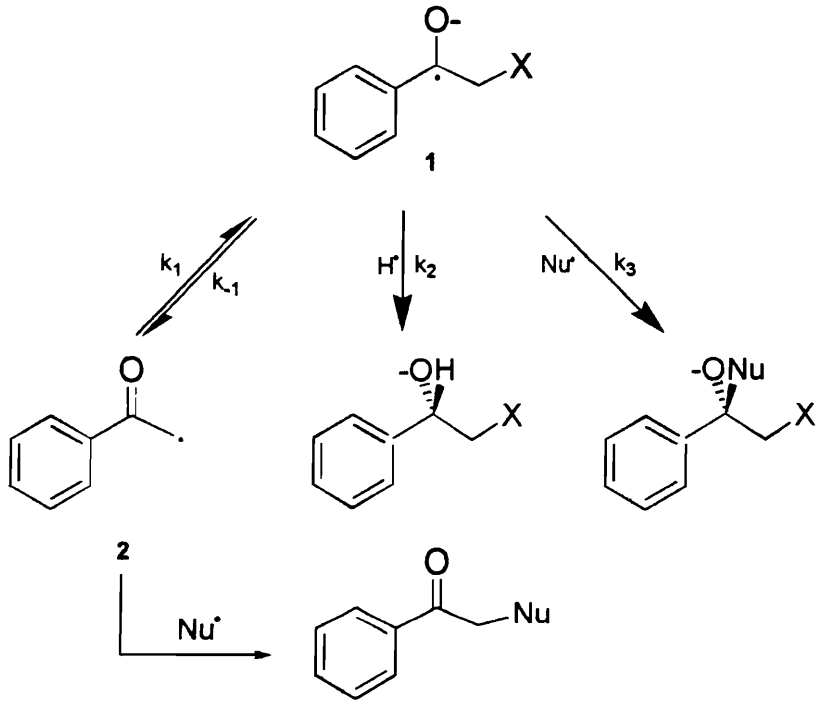


**Figure 2: Competing reactions of radical anions generated via electron transfer from Nu˙.**

The fragmenting moiety can be placed on the aromatic ring as well as alpha to the carbonyl. If a nucleophile is too basic to be used with substrates that contain α-hydrogens due to competing enolization of the ketone, monosubstituted benzophenones can be

utilized.[9] In addition, placement of the fragmenting moiety on the aromatic ring eliminates any possibility of $S_N2$ attack at the α-carbon.

Tanner *et. al.*[9], have determined the rates of fragmentation for a number radical anions generated from α-substituted acetophenones, *ortho*, *meta*, and *para* substituted acetophenones, and *ortho*, *meta*, and *para* substituted benzophenones. The results of this study are shown in **Table 1**.

**Table 1: Rate constants of fragmentation of radical anions generated from susbstituted acetophenones and benzophenones in acetonitrile at room temperature.[9]**

$$RX^{\bullet -} \xrightarrow{k_{fx}} R^{\bullet} + X^{\ominus}$$

| $PhCOCH_2X^{\bullet -}$ (1) | | $X\text{-}C_6H_4COCH_3^{\bullet -}$ (2) | | $X\text{-}C_6H_4COC_6H_5^{\bullet -}$ (3) | |
|---|---|---|---|---|---|
| X | $k_{fx}$ ($s^{-1}$) | X | $k_{fx}$ ($s^{-1}$) | X | $k_{fx}$ ($s^{-1}$) |
| Br | $> 10^9$ | *m*-Cl | 15 | *p*-Cl | 29 |
| Cl | $> 10^9$ | *p*-Cl | $3 \times 10^3$ | *o*-Cl | 61 |
| F | $5.2 \times 10^9$ | *o*-Cl | $3 \times 10^5$ | *m*-Br | $7.9 \times 10^2$ |
| OCOPh | $6.3 \times 10^9$ | *m*-Br | $8 \times 10^3$ | *p*-Br | $6 \times 10^4$ |
| $OCOCH_3$ | $9.6 \times 10^8$ | *p*-Br | $3.2 \times 10^7$ | *m*-I | $2.5 \times 10^6$ |
| OPh | $9.5 \times 10^6$ | *o*-Br | $5.1 \times 10^9$ | | |
| *p*-$TolSO_2$ | $5.3 \times 10^8$ | *m*-I | $1.9 \times 10^8$ | | |
| SPh | $9.3 \times 10^6$ | *p*-I | $3.5 \times 10^9$ | | |

The fragmentation of α-substituted acetophenone radical anions (**1**) is shown to proceed with rate constants ranging from ca $10^7$ to > $10^9$ $s^{-1}$ depending upon the nature of the leaving group. Radical anions generated from *ortho*, *meta*, and *para* substituted acetophenones (**2**) are shown to fragment with rate constants ranging from 15 to $10^9$ $s^{-1}$. Again the rate constants are influenced by the nature of the leaving group; however, they are also influenced by the placement of the fragmenting group on the aromatic ring. The rates of fragmentation of radical anions generated from *ortho*, *meta*, and *para* substituted benzophenones (**3**) are generally seen to be slower than the corresponding acetophenones with rate constants ranging from 29 to $10^6$ $s^{-1}$. Aromatic ring substituted substrates show two general trends in the observed fragmentation data. The rate of halide expulsion is faster in the *ortho* and *para* positions than that observed for the *meta* position. This is because the spin density is greater at the *ortho* and *para* positions, compared to the *meta*. The rate constant depression observed in the monosubstituted benzophenone radical anions stems from delocalization of the radical into both aromatic rings, **Scheme 2**.

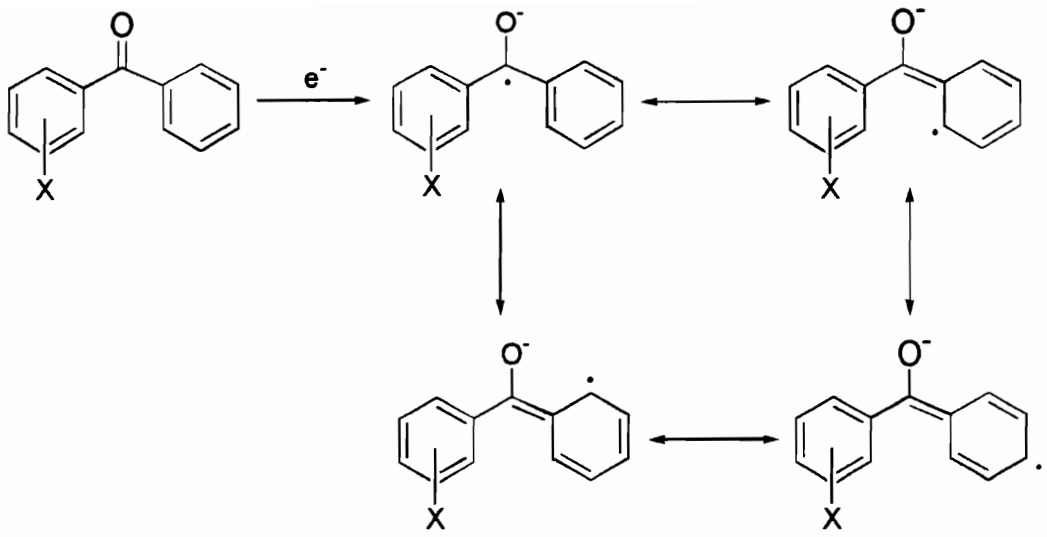

**Scheme 2**

Data from this study combined with the findings of several other groups have shown that it is possible for a fragmentation probe of this type to identify SET pathways in the reaction of nucleophiles with carbonyl compounds.[10,11,12,13,14,15] Subsequently, these fragmentation probes have been successful in identifying SET pathways in reactions of carbonyl compounds with Grignard reagents[16] and lithium dialkylcuprates[7].

Rearrangement probes allow trapping of a paramagnetic intermediate through a unimolecular rearrangement. Following the formation of a radical or radical anion intermediate, a structural rearrangement occurs that allows formation of products that can be ascribed solely to a SET process. Commonly, these probes are based on radical rearrangements involving cyclization or ring opening reactions. However, rearrangement probes can also be based on processes as simple as the isomerization of a double bond.

Investigation of double bond E,Z isomerization has met with limited success in identifying SET in reactions of nucleophiles with α,β-unsaturated ketones.[17,18,19] The major assumption with this approach is that formation of a radical anion intermediate will cause subsequent rearrangement from a less stable to a more stable double bond through a *beta* centered radical (**4**), **Scheme 3**.

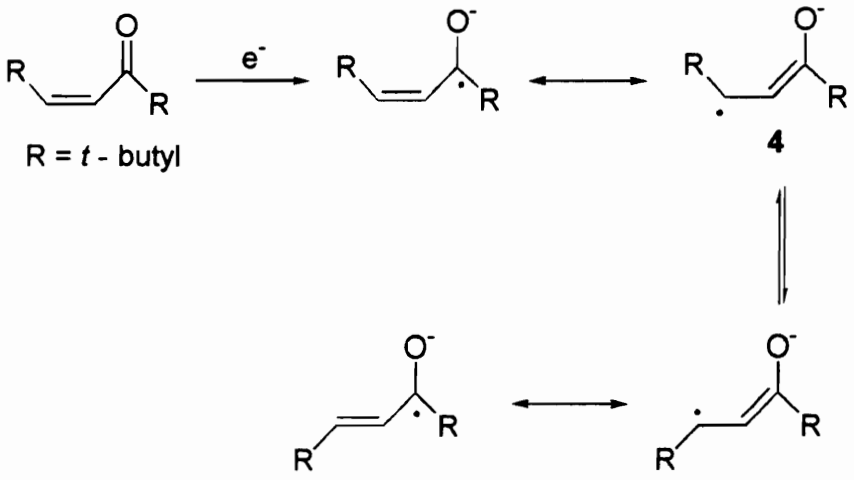


**Scheme 3**

As a result, differentiation between SET and nucleophilic addition is determined based on the appearance of 1,2 addition products in which double bond isomerization has occurred, **Figure 3**.

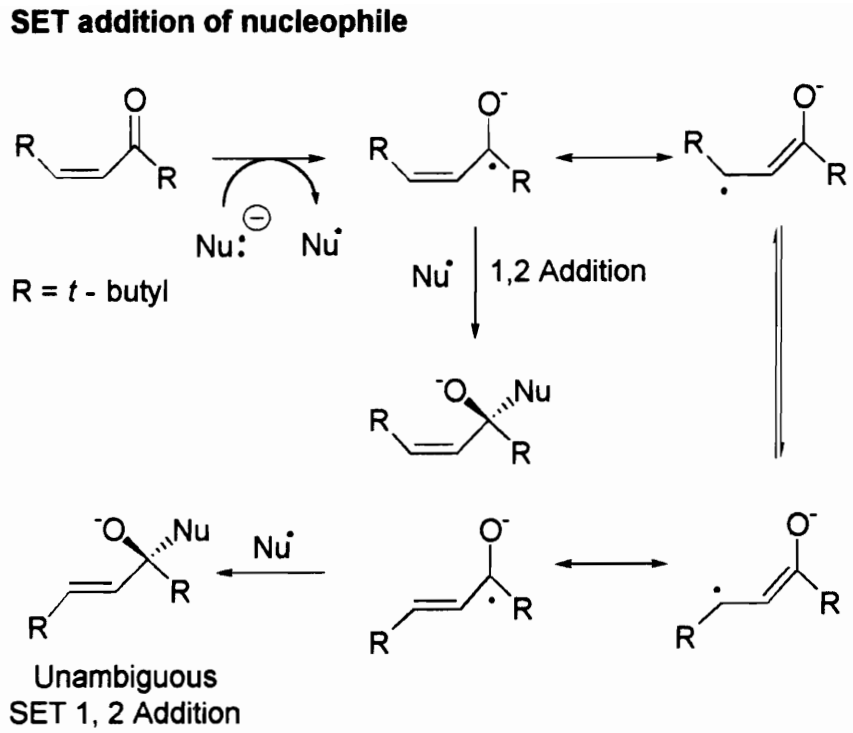


**Figure 3: E,Z isomerization resulting from SET addition of the nucleophile.**

The E,Z isomerization of a double can only show the occurrence of a SET process in the addition of a nucleophile, however, radical isomerization could occur in an SET reaction not related to the product forming pathway, specifically through an SET induced isomerization of starting material, **Figure 4**.

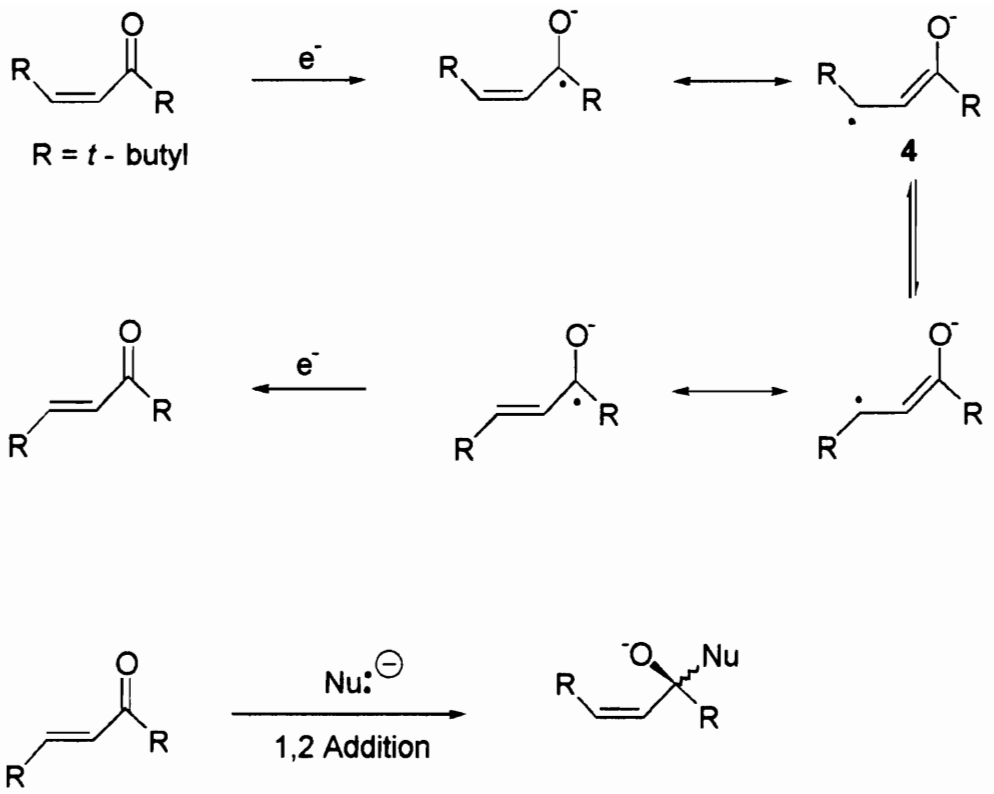


**Figure 4: E,Z double bond isomerization followed by nucleophilic addition.**

A second problem is encountered with this type of probe in the identification of SET arises if a reversible 1,4 nucleophilic addition is possible, **Scheme 4**.

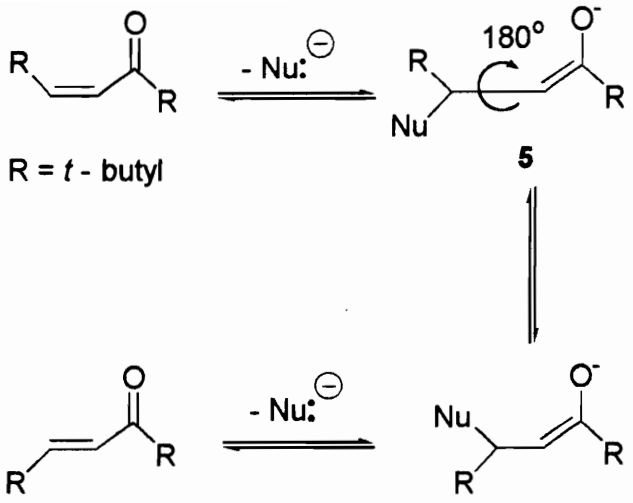


**Scheme 4**

A 1,4-Michael addition of the nucleophile to the starting material would result in the analogous enolate ion, **5**. If this reaction is reversible bond rotation in enolate **5** can lead to isomerized starting material. Subsequent 1,2-nucleophilic addition would then provide an indication that SET has occurred and could lead to the misidentification of a polar process as a SET process. Therefore, without further evidence supporting a SET pathway as the product-determining pathway, results obtained from studies using substrates of this type are ambiguous at best.

Probes that can undergo cyclization have been used extensively for the identification of SET in the reaction of nucleophiles with carbonyl compounds. The working hypothesis behind probes of this type is that radical intermediates formed as a consequence of SET will undergo cyclization onto a remote unsaturated functionality in a

manner different from what would be observed in a polar reaction. Differentiation between a polar pathway and a SET pathway can then be afforded by product analysis.

Many of the probes designed to undergo cyclization during a SET process are based upon the the $\Delta^5$-hexenyl $\rightarrow$ cyclopentylcarbinyl radical rearrangement, **Equation 1**.

**Eqn. 1**

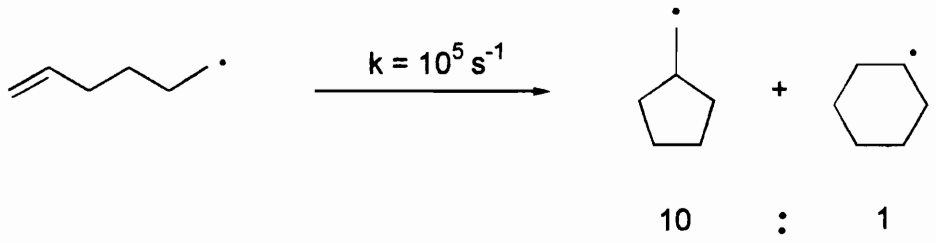


The rate constant for the $\Delta^5$-hexenyl $\rightarrow$ cyclopentylcarbinyl radical rearrangement has been determined to be ca. $10^5$ $s^{-1}$ at 0° C, yielding the cyclopentylcarbinyl radical and cyclohexyl radical in a 10:1 ratio.[20] The rate constant for ring closure[21] of the analogous anionic species was found to be slower by a factor of $10^8$-$10^{10}$ due to the localization of the negative charge by the counter-ion (cation) . Therefore, the appearance of cyclization products may indicate the presence of a radical intermediate associated with a SET pathway. Generally, a remote C=C substituent is incorporated into the structure of the nucleophile to trap the neutral free radical produced after electron transfer.[22,23,24,25,26] However, the C=C substituent can also be incorporated into the structure of the carbonyl compound.[27,28] Regardless of the placement of the probe substituent, identification of

SET pathways can be based on the appearance of a cyclopentylcarbinyl substituent in the products, **Figure 5**.

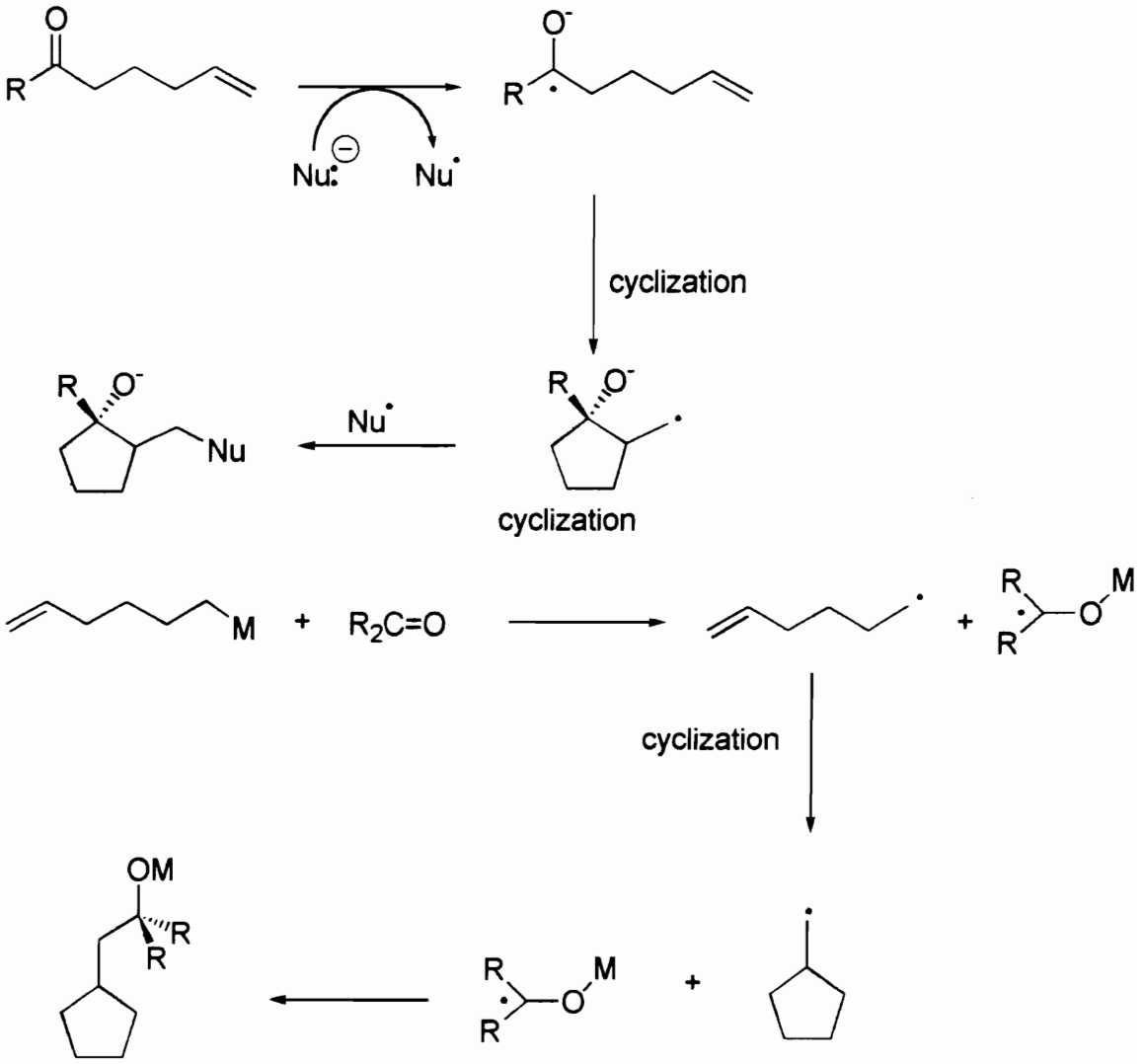


**Figure 5: Elucidation of SET pathways based on the $\Delta^5$-hexenyl → cyclopentylcarbinyl and related rearrangements.**

However, caution must be used in assuming that cyclization is the result of a SET pathway. Studies have shown that that the $\Delta^5$-hexenyl organometallic compounds can autocyclize.[21,29] Also cyclization must be unequivocally shown to occur in the pathway leading to product formation and not in a side reaction. If reaction conditions allow anionic cyclization to become a competing reaction with radical cyclization, results obtained from a probe of this type are meaningless. Fortunately, Garst and Hines[29] found that differentiation between anionic and radical cyclization could be afforded through the use of 1-methyl-5-hexenyl organometallic reagants. Anionic and radical cyclizations of this substrate provide different cis/trans ratios in the ring cyclization process. Differentiation between SET is then afforded by comparing the cis to trans cyclization ratio of the cyclopentyl ring. A ratio of 4.5 to 1 cis to trans is considered to indicate 100% radical character, **Equation 2**.[29]

**Eqn. 2**

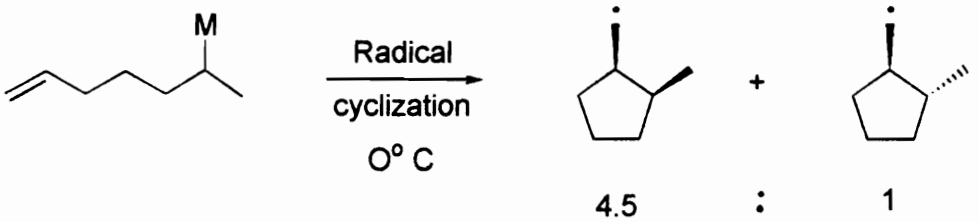


Even though a probe of this type allows differentiation between radical and anionic cyclizations, it still does not indicate that the cyclization is occurring in the product forming pathway. A reversible electron transfer could occur with a reverse rate constant

slow enough to allow cyclization to occur. Upon cyclization, nucleophilic attack could then occur at the carbonyl giving the false impression that product formation occurred as a result of SET, **Figure 6**.

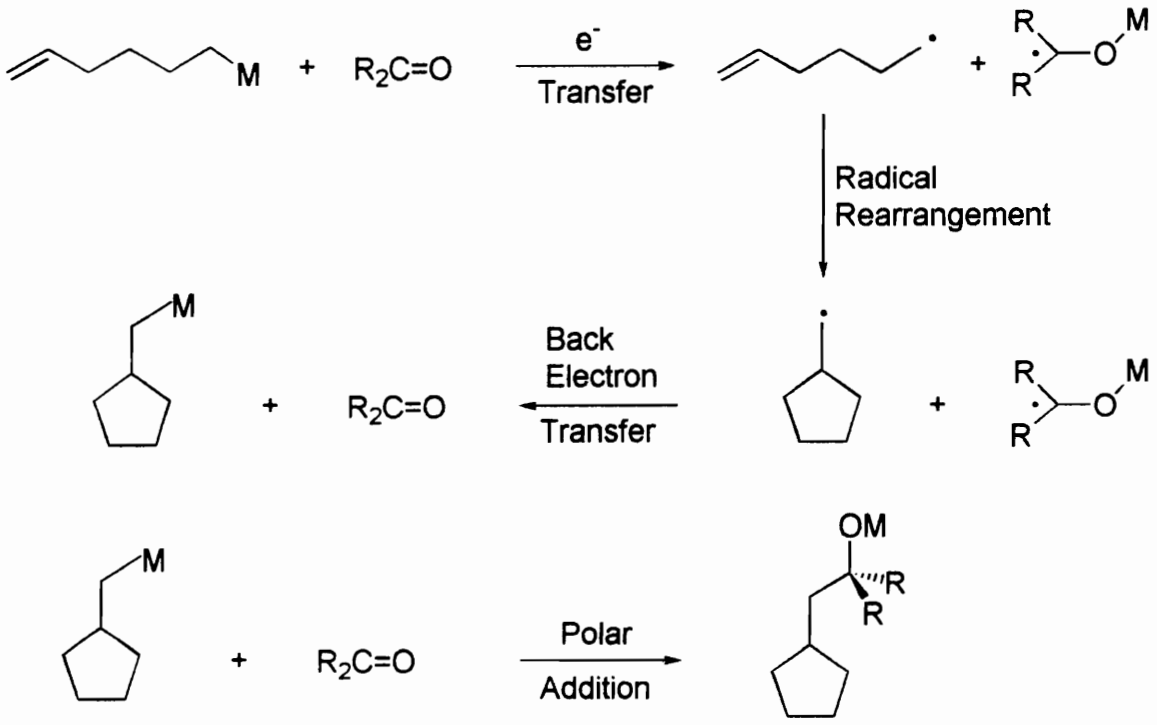


**Figure 6: Rearrangement mechanism of the $\Delta^5$-hexenyl radical resulting in misidentification of SET.**

Several studies have employed substituents capable of undergoing cyclization analogous to the $\Delta^5$-hexenyl system in reactions between organometallic compounds and carbonyl compounds and successfully shown that SET is operating to some extent in these types of reactions, **Figure 7**.[22,23]

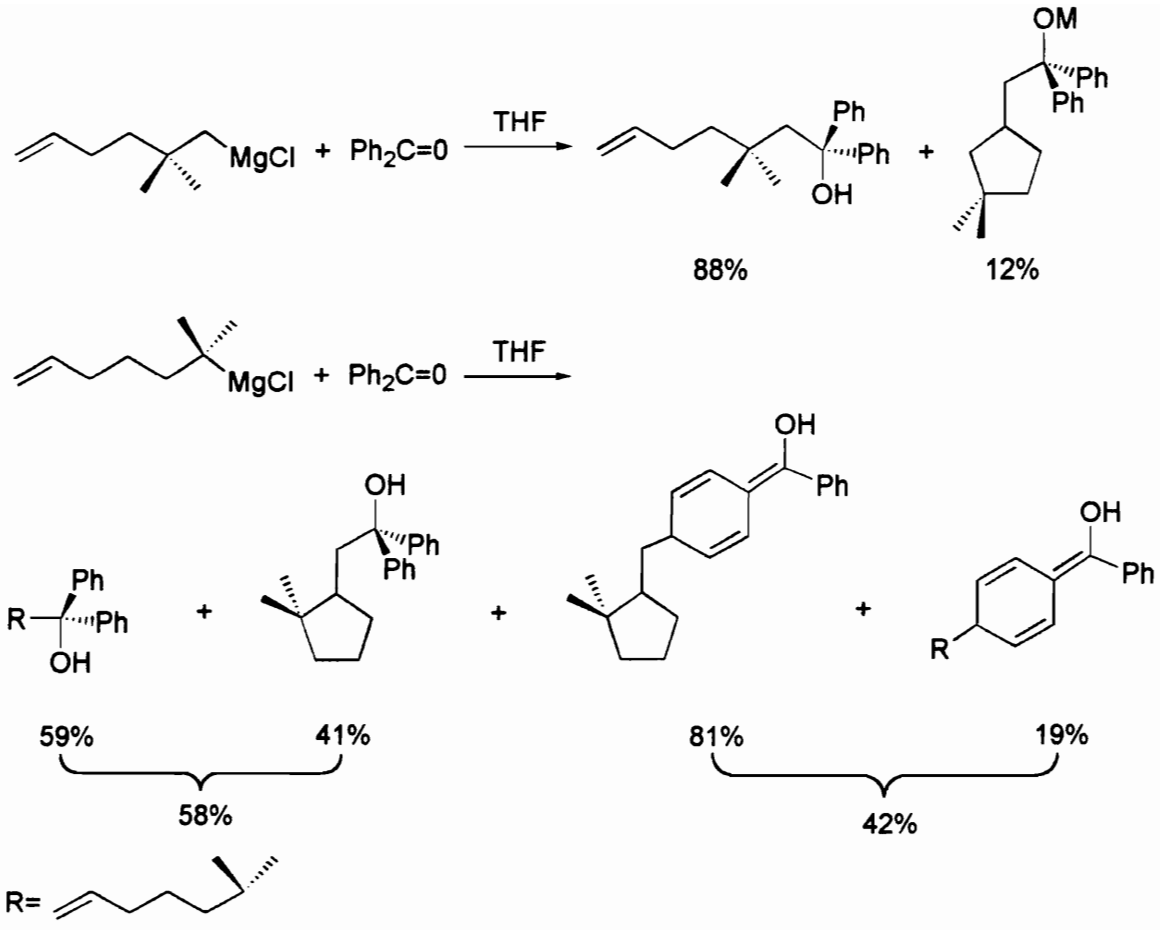


**Figure 7: Successful detection of SET utilizing the $\Delta^5$-hexenyl → cyclopentylcarbinyl radical rearrangement.**

A popular SET probe that employs ring opening to infer the presence of a radical intermediate is based upon the cyclopropylcarbinyl → homoallyl radical rearrangement, **Equation 3**.

**Eqn. 3**

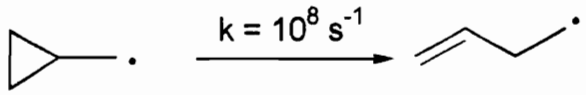


Cyclopropylcarbinyl radical ring opening is very facile and found to occur at a rate constant of $1.2 \times 10^8$ $s^{-1}$ at 25° C.[20,30] Ring closure of the homoallyl radical occurs 5 orders of magnitude slower with a rate constant of $4.9 \times 10^3$ $s^{-1}$. The rates of ring opening for the gem-dimethylcyclopropylcarbinyl radical and the cis or trans methylcyclopropylcarbinyl radical to their corresponding 3° and 2° radicals are also found to be of comparable rates.[31]

Unlike the $\Delta^5$-hexenyl system, the use of cyclopropylcarbinyl derived organometallic reagents as nucleophiles is limited due to the large amount of rearrangement products seen in the generation of the organometallic species, unless extremely low temperatures are maintained, **Figure 8**.[32,33,34,35]

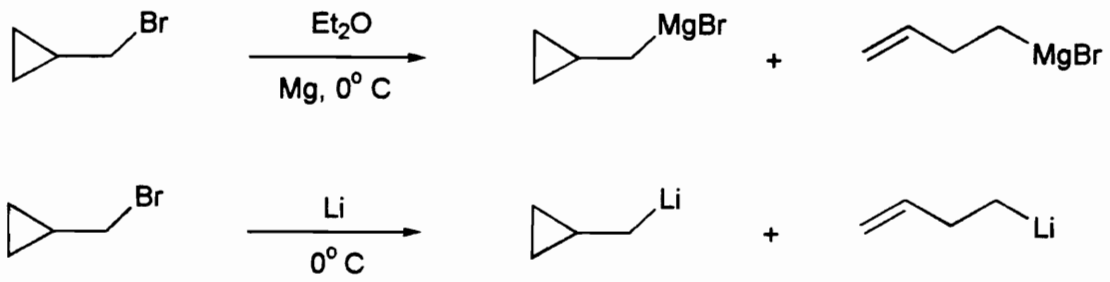


**Figure 8: Rearrangement reactions of cyclopropylcarbinyl organometallic reagents.**

Traditionally the method employed for identification of a SET process in the reactions of nucleophiles with ketones has been through incorporation of a cyclopropylcarbinyl group into the structure of the ketone such that formation of a radical intermediate will result in ring opening, **Scheme 5**.[36,37,38]

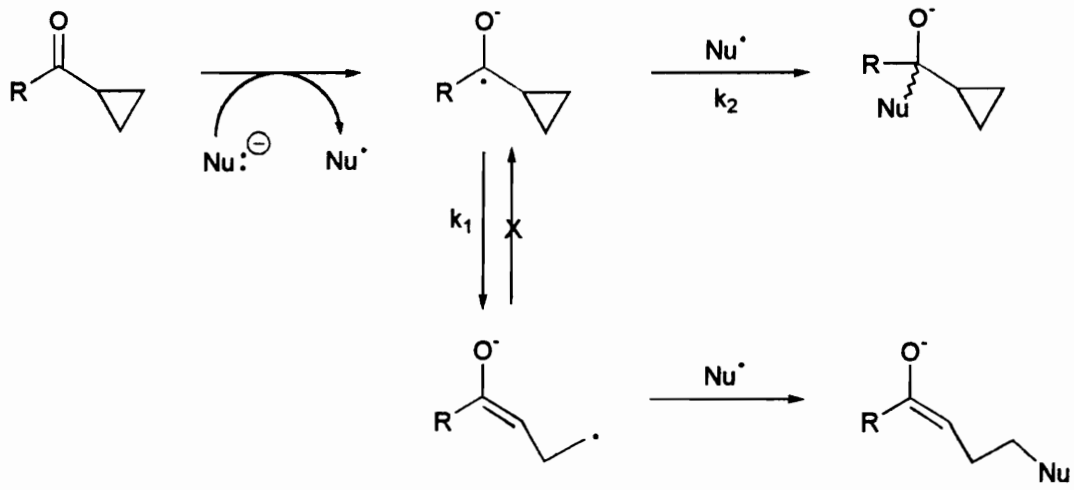


**Scheme 5**

In order for a ring opening probe to be successful in the identification of SET in the reactions of carbonyl compounds with nucleophiles, the rate of ring opening ($k_1$) must be faster than the competing radical/radical anion reaction ($k_2$) and the ring opening should be irreversible.

It is often assumed that upon generation of the ketyl anion, the relief of cyclopropyl ring strain will provide the same thermodynamic and kinetic driving force

exhibited by the cyclopropylcarbinyl radical. However, experimental results pertaining to the ring opening of the cyclopropyl group in a number of substituted and unsubstituted cyclopropyl phenyl radical ketyl anions has shown this assumption to be erroneous.

**Table 2: Rate constants and enthalpies of cyclopropyl ring opening for selected cyclopropyl ketyl anions.**[36,37,38]

| Reaction | $k_1$ $s^{-1}$ | $\Delta H^\circ$ kcal/mol |
|---|---|---|
| 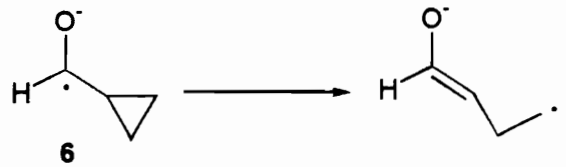 **6** | | - 11 |
| 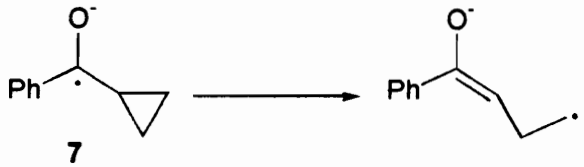 **7** | ≤ 2 | + 11 |
| 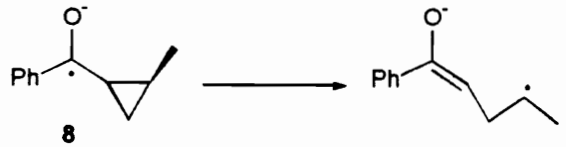 **8** | | + 2.5 |
| 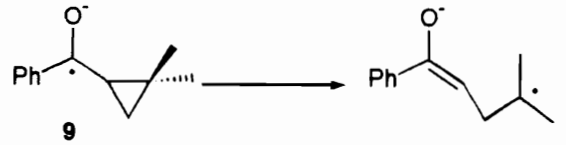 **9** | | - 2.5 |
| 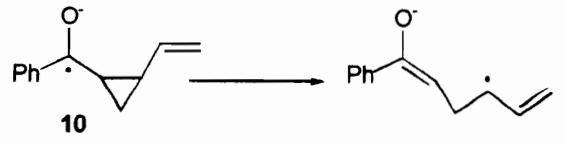 **10** | ≥ 5 x $10^5$ | -2 |
|  **11** | 1 x $10^7$ | -2 |

**Table 2** shows the rate constants for ring opening of cyclopropyl phenyl ketone and several substituted analogs. As shown the rate constants for ring opening range from 2 to $10^7$ $s^{-1}$.[36]

Tanko et. al.[37] have shown that cyclopropyl groups whose only substituents on the cyclopropane ring are either an H or alkyl undergo a slow, reversible ring opening. Furthermore, the radical anion produced from cyclopropyl phenyl ketone has an equilibrium that favors the ring closed radical ketyl anion ($K_{eq}$= 2 x $10^{-8}$), **Scheme 6**.[38]

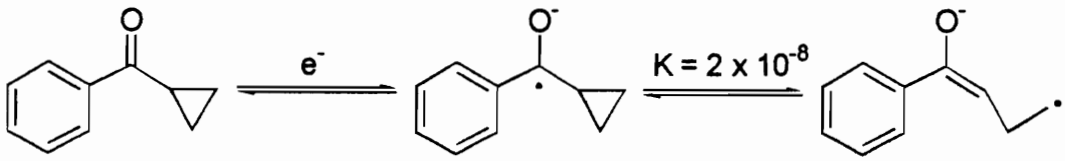


**Scheme 6**

The slow reversible ring opening can be attributed to the loss of resonance of the radical into the aromatic ring which occurs as the result of ring opening, **Scheme 7**.

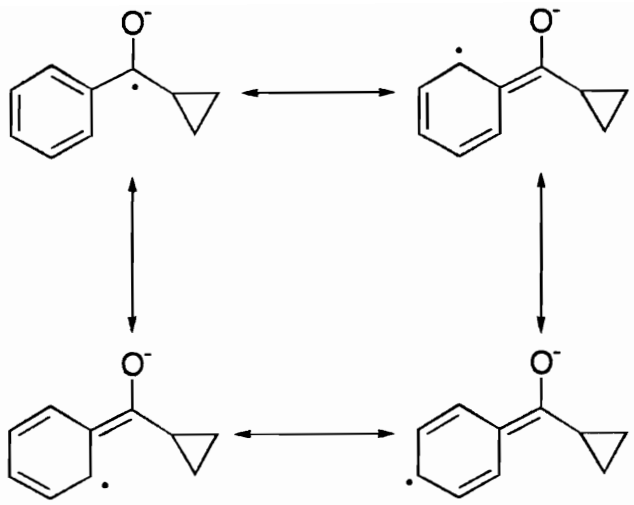

**Scheme 7**

Though energy is gained from the relief of ring strain in the ring opening of the cyclopropyl group, it is not enough to compensate the loss in resonance energy. Comparison of the calculated values of $\Delta H^{\circ}$ (AM1 SCF-MO), **Table 2**, for ring opening of substrates **7** - **11** to that calculated for substrate **6** shows ring opening to be more endothermic by a minimum of 8.5 kcal/mol. This attests to the stabilizing ability of the phenyl group upon the ring closed radical ketyl anion. Experimental evidence to the delocalization of the radical into the aromatic ring is provided through EPR studies of the ring closed radical anion. The EPR spectra of **7** exhibits high values of $a^{H}$ for the *ortho* and *para* positions of the aromatic ring and hindered rotation around the $C_{Ar}$-C=O,[36] indicating extensive delocalization of the radical into the aromatic ring. In order to

compensate for the loss of resonance energy, substituents better able to stabilize a radical intermediate were attached to the cyclopropyl ring.

Attachment of a phenyl group onto the cyclopropyl ring was shown to be able to partially compensate for the loss of resonance energy. This was seen through the increased rate constant for ring opening of **11**, ca $10^6$-$10^7$ $s^{-1}$, comparable to that of the cyclopropylcarbinyl neutral free radical ring opening.[36,39] However, studies by Tanner et. al.[38] have shown the cyclopropyl ring opening in the one electron reduction of (+)-*trans*-1-benzoyl-2-phenylcyclopropane (**12**) to be reversible, **Scheme 8**.

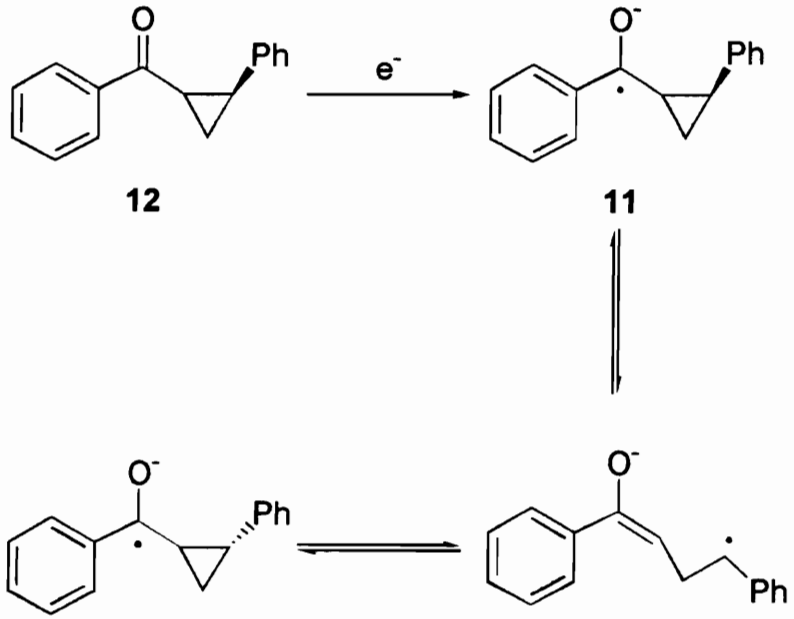


**Scheme 8**

The reversibility of the ring opening precludes the use of **12** as a SET probe.

A lower limit of $10^5$ $s^{-1}$ was found for the rate of ring opening of the radical ketyl anion (**10**) generated from 1-benzoyl-2-vinylcyclopropane (**13**).[36] The rate of ring opening of the ketyl anion approaches that observed for the cyclopropylcarbinyl radical. However, it would not be possible to discern whether addition to the vinyl substituent occurred from a nucleophilic or SET process, **Figure 9**.

**Path A (Polar pathway for ring opening)**

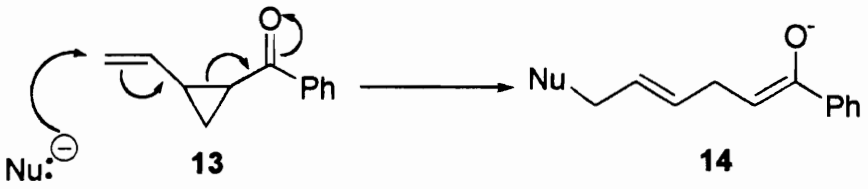


**Path B (SET pathway for ring opening)**

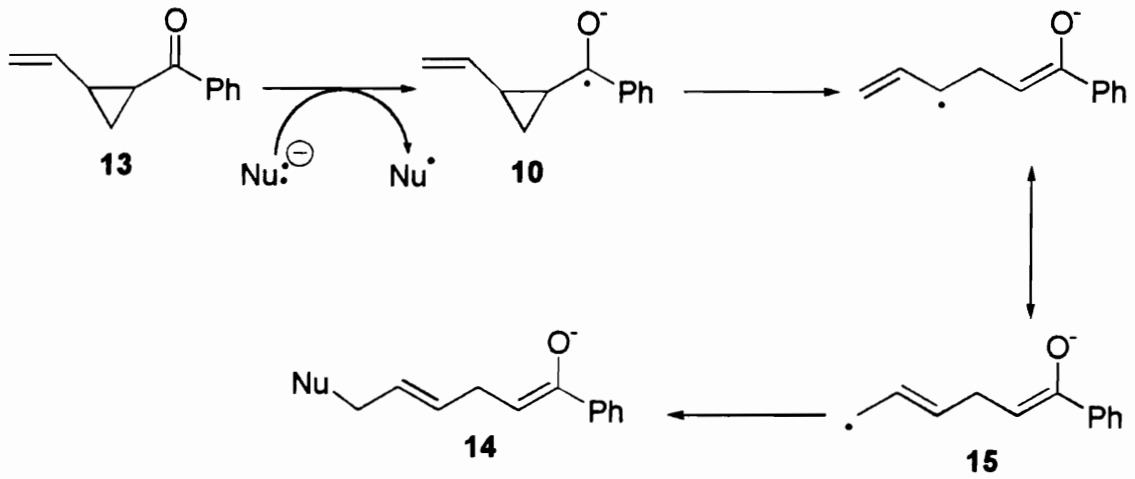


**Figure 9: SET vs. polar addition in the reactions of nucleophiles with 1-benzoyl-2-vinylcyclopropane.**

As shown in **Figure 9** there are two possible ways a nucleophile may react with **13**. Path A illustrates direct nucleophilic attack across the double in a Michael type addition reaction. Path B illustrates a SET pathway resulting in the ring opened allylic radical anion **15**. Radical coupling to **15** with Nu· results in formation of **14**, also produced in Path A. Therefore, results obtained from **13** would be ambiguous regarding the occurrence of SET.

From the available experimental data it became clear that substrates such as cyclopropyl phenyl ketone were not going to unambiguously detect a SET pathway in the reactions of nucleophiles and carbonyl compounds, due to the reversibility of the ring opening reactions, the inability or slowness of the ring opening process, or due to the ambiguity that would arise in product analysis (i.e., the same product arises from a polar pathway). Therefore, a substrate needed to be developed which upon reduction would yield a radical anion whose ring opening would be thermodynamically more favorable and which (hopefully) might remove the ambiguity that existed in earlier SET probes. A possible resolution of the discrepancies associated with SET probes was found by Liotta et. al. in their investigation into the reactions of 2,5-dimethyl-4-ethylenedioxycyclohexadienone, **16**, with organometallic nucleophiles.[40]

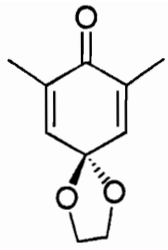

**16**

The use of **16** as a probe for the detection of SET is based on the premise that following reaction mechanism occurs upon electron transfer, **Figure 10**.

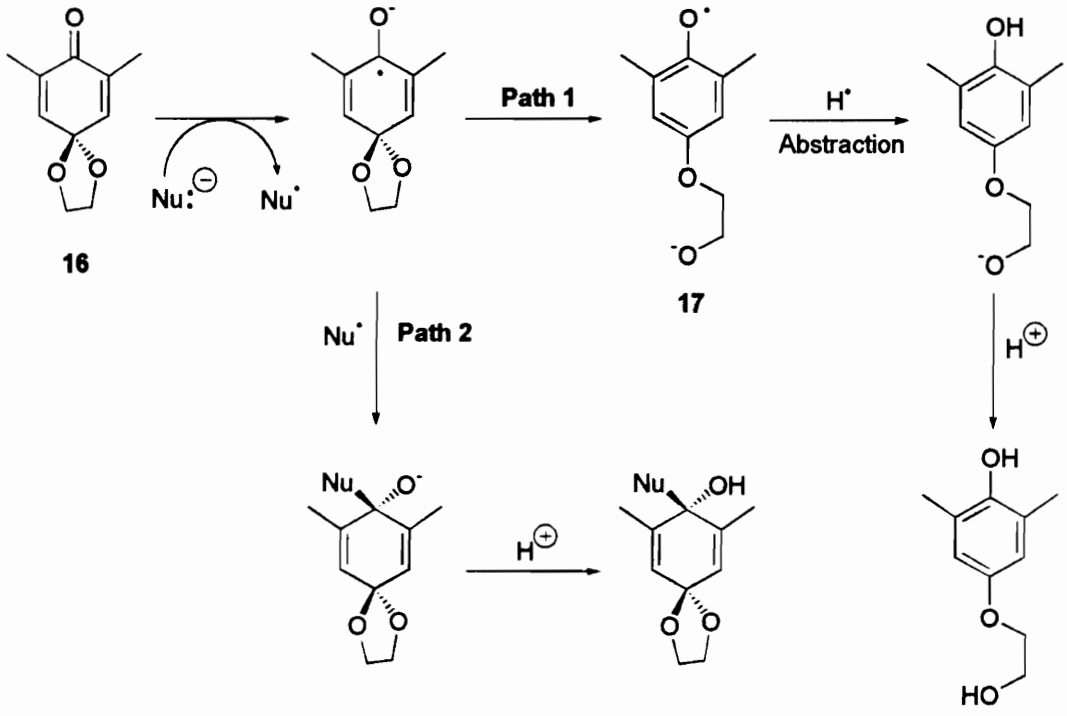


**Figure 10: Utilization of 2,5-dimethyl-4-ethylenedioxyhexadienone as a SET probe.**

Upon electron transfer, two possibilities exist for reaction of the radical anion. Ring opening (path 1) allows establishment of aromaticity resulting in the formation of **17**. Alternatively a rapid 1,2 addition could occur (path 2) leaving the ethylenedioxy moiety intact. Path 1 allows identification of SET by the formation of the phenol through hydrogen atom abstraction. However, 1,2 addition products could be a result of either direct nucleophilic attack or a SET process. Since it is not possible to discern between 1,2 addition products formed from a SET or nucleophilic attack, it would be impossible to unambiguously identify the pathway responsible for the production of these 1,2 addition products.

This probe has been successfully used for the identification of SET in reactions involving several organometallic nucleophiles. However, one pitfall associated with this probe is that it relies upon hydrogen abstraction from either the solvent or the nucleophile by the phenoxy radical to identify a radical pathway resulting from electron transfer. Since Nu· is not captured, it is impossible to categorically state that the phenoxy radical was formed in the pathway leading to product formation.

In 1991 research began in our lab into the utilization of 5,7-di-*t*-butylspiro[2,5]octa-4,7-dien-6-ones **18** - **20** as possible probes for the detection of SET in addition reactions of nucleophiles with enones.

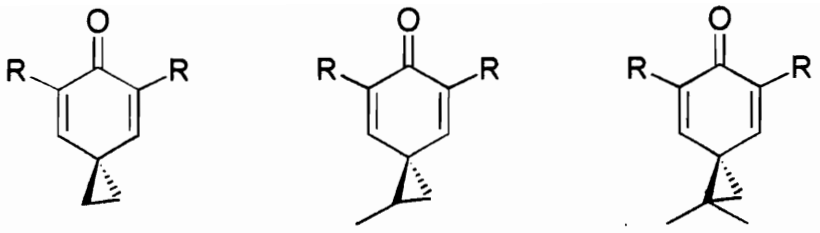

**18** **19** **20**

R = *t* - butyl

These substrates seemed ideal candidates for use as SET probes for several reasons. Upon generation of a radical anion intermediate, relief of cyclopropyl ring strain would work in conjunction with the establishment of aromaticity to afford a very facile ring opening, $\Delta H^{\circ}$ = -31 kcal/mol (AM1 SCF-MO), **Scheme 9**.[41]

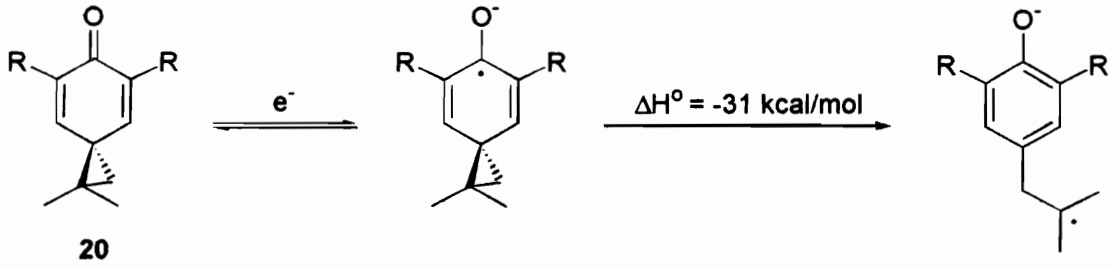


**20**

R = *t* -butyl

**Scheme 9**

Some control of the rate of ring opening should be available in substrates **19** and **20**. This control would be a consequence of the added stabilization resulting from formation of the

corresponding secondary (**21**) or tertiary radical (**22**) upon ring opening to the 2-phenylethyl radical. Since the relief of cyclopropyl ring strain would work in conjunction with establishment of aromaticity, it might be possible to attain rate constants comparable to those observed for the cyclopropylcarbinyl → homoallyl radical rearrangement, **Figure 11**.

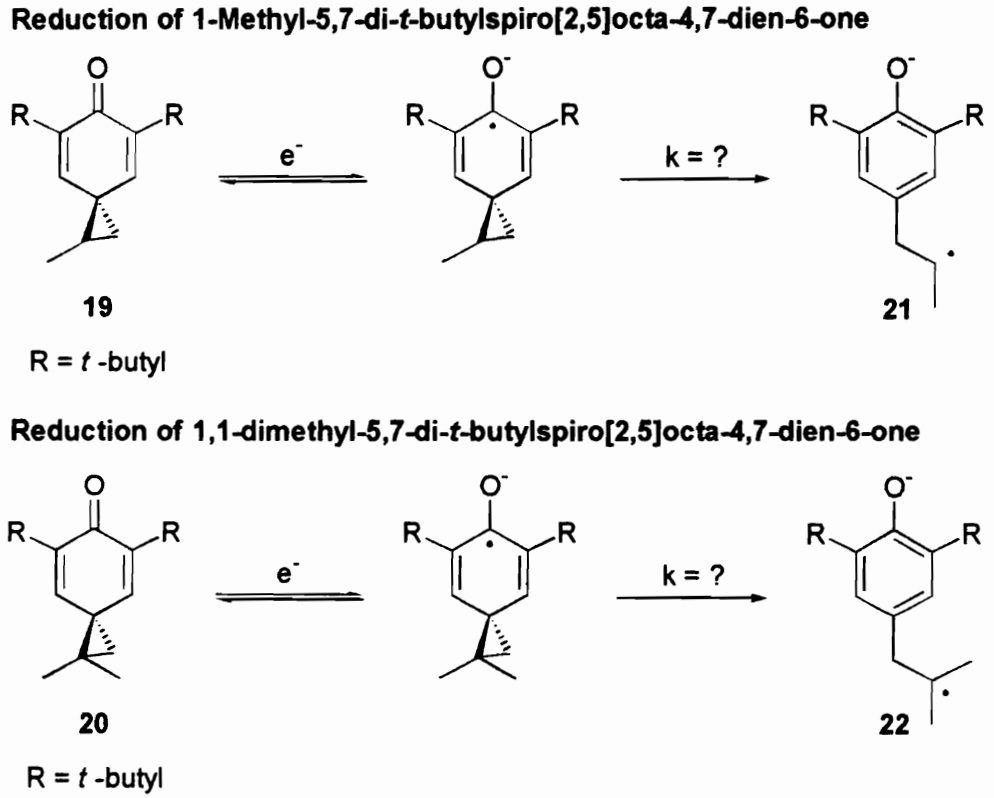


**Figure 11: Hypothesized cyclopropyl ring opening for the radical anions generated from 19 and 20.**

The resulting carbon radical provides an added bonus not available in the α-ethylenedioxy radical, **17**. Formation of the subsequent carbon radicals should allow coupling to Nu·,

provided disproportionation does not occur, ring opening is irreversible, and the lifetimes of the radicals are long enough to allow coupling. This would show that SET was involved in the product forming pathway and not a side reaction.

In addition, substrates **19** and **20** may be used to detect SET based upon the regiospecificity of the reaction. Reactions of 1-benzoyl-2,2-dimethylcyclopropane have shown that nucleophilic attack on the cyclopropane ring occurs at the least hindered position[7], while radical pathways resulted in ring opening to the tertiary radical, resulting in an isomeric product, **Scheme 10**.[42]

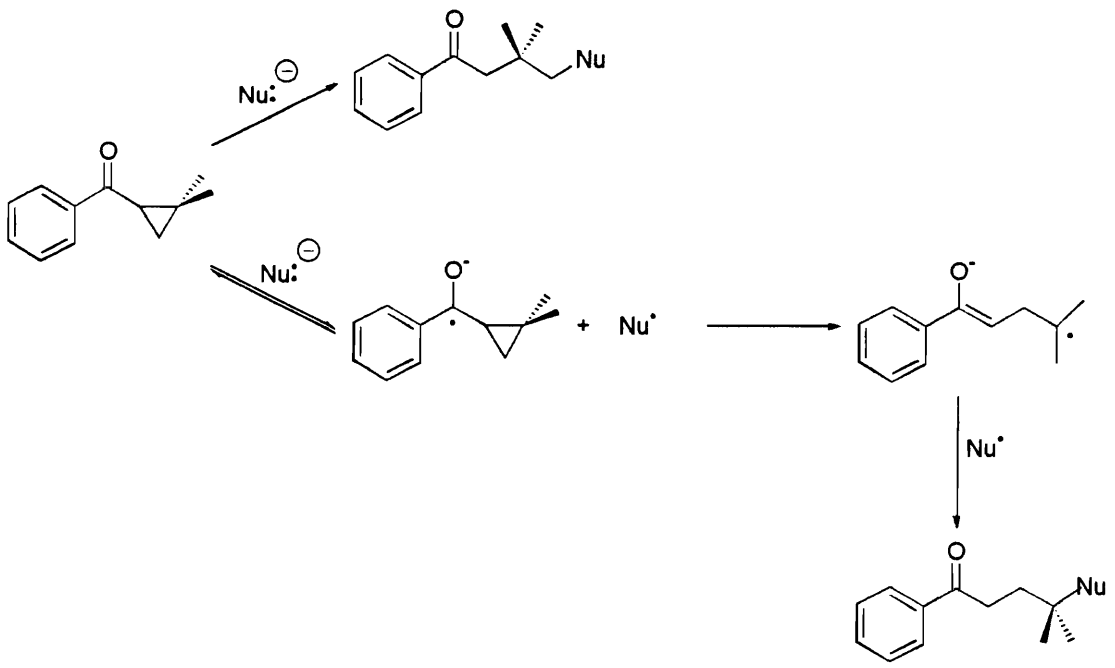


**Scheme 10**

The establishment of aromaticity as a result of cyclopropyl ring opening should cause the rate of cyclopropyl ring opening in **19** and **20** to occur at rates significantly greater than the ring opening of the radical ketyl anion derived from 1-benzoyl-2,2-dimethylcyclopropane. Therefore, if the same reactivity pattern is exhibited by substrates **19** and **20** as observed in 1-benzoyl-2,2-dimethylcyclopropane, then SET and nucleophilic pathways can be differentiated by the regiospecificity of nucleophilic addition, **Figure 12**.

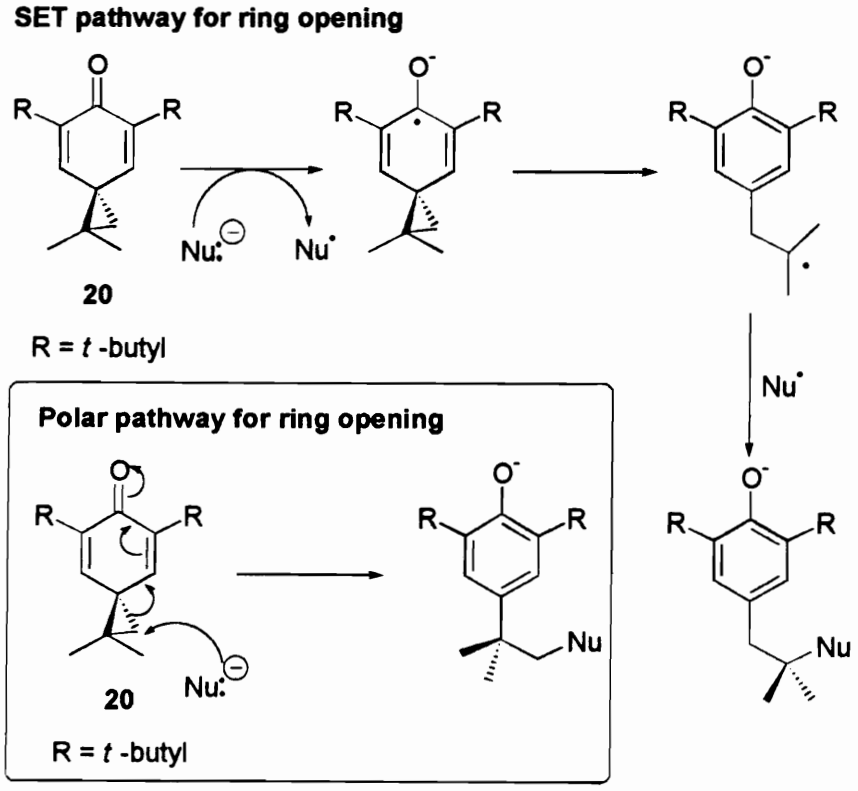


**Figure 12: Detection of SET based upon the regiospecificity of cyclopropyl ring opening.**

## SUMMARY

In the past 30 years many techniques and substrates have been purported to identify reactions that occur through single electron transfer pathways. However, upon further scrutiny, it is usually found that results are ambiguous at best.

In the utilization of a rearrangement probe for the detection of SET pathways several criteria must be met. Rearrangement of the probe substituent should be fast and irreversible, and should lead to products that can be solely ascribed to SET. It is believed that through the use of 5,7-di-*t*-butylspiro[2,5]octa-4,7-dien-6-ones all of these criteria can be met.

It was our goal in this study to characterize and utilize 5,7-di-*t*-butylspiro[2,5]octa-4,7-dien-6-ones as SET probes and to show that they were unambiguously able to differentiate between SET and nucleophilic pathways based upon the regiospecificity of the reaction. Characterization of the spiro[2,5]octadienones was accomplished by cyclic voltammetric, linear sweep voltammetric, and bulk electrolytic techniques. Once the rate and regiospecificity of radical ring opening was determined, the spiranes were allowed to react with several nucleophiles which independent evidence has shown react with carbonyl compounds via SET pathways in order to assess whether use of these substrates would allow differentiation between SET and polar pathways.

# CHAPTER 2. CHEMISTRY OF RADICAL ANIONS GENERATED FROM 1,1-DIMETHYL-5,7-DI-*t*-BUTYLSPIRO[2,5]OCTA-4,7-DIEN-6-ONES.

## INTRODUCTION

Voltammetric methods are extremely useful techniques for the investigation of reactions involving electron transfer. Voltammetry provides a method for generation of a reactive species via electron transfer and then furnishes a means to monitor the kinetics of its subsequent reactions.[43,44]

Voltammetric techniques employ a working electrode for generation and monitoring of the reactive species. Although the composition of the working electrode can be quite diverse, for our purposes the working electrode was limited to either gold or carbon. The potentials of the working electrode are standardized by referencing them to an electrode comprised of materials that have an accurately measured redox couple. All measurements acquired in this study were referenced to 0.1 M $Ag^+/Ag$.

One of the most common voltammetry methods is cyclic voltammetry (CV). In a CV experiment, the voltage of a working electrode is varied in a linear fashion from an initial potential ($E_i$) to a switching potential ($E_s$) and then to a final potential ($E_f$) over a period of time (T) (frequently $E_i = E_f$). The change in voltage ($\delta E$) as a function of the change in time ($\delta T$) is defined as the sweep rate ($\nu$) of the experiment. A plot of E versus T produces the triangular waveform shown in **Figure 13**.[45]

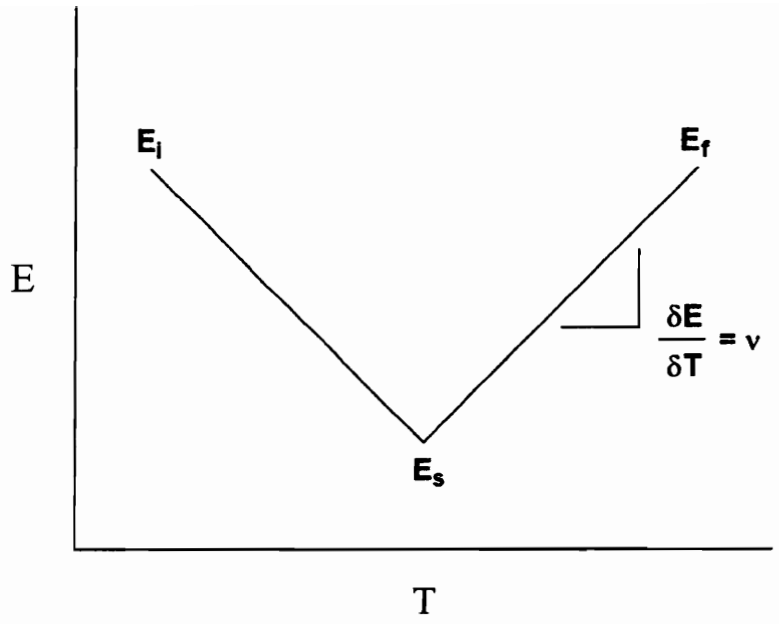


**Figure 13: Variation of potential with time in a CV experiment.**

The voltammogram of a CV experiment is recorded as a plot of current (I) vs. potential (E). Systems exhibiting fast and reversible heterogeneous electron transfer produce a voltammogram such as that shown in **Figure 14**.[45]

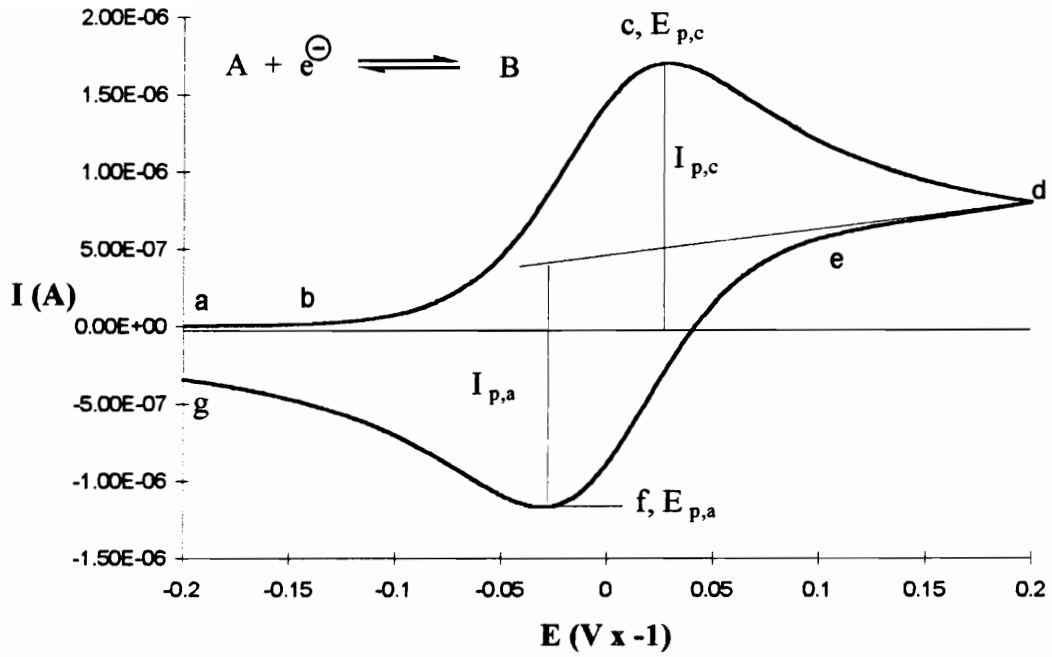


**Figure 14: Typical I vs. E plot obtained from a reversible electron transfer process.**

The voltammogram depicted in **Figure 14** corresponds to a CV experiment in which the substrate is first reduced and then the resulting reduction product is oxidized in the return sweep of the experiment.

The initial potential, $E_i$, is identified by point a. This potential is positive relative to the reduction potential of the substrate. From $E_i$, the electrode potential is varied linearly to more negative potentials reaching a point (point b) where cathodic current begins to flow and reduction of the substrate at the electrode surface begins. Further negative increase in the electrode potential causes the current to rise sharply between b and c until maximum cathodic current flow is reached at the reductive peak potential, $E_{p,c}$,

c. At this point the substrate is being reduced as fast as it can diffuse to the electrode surface. From c to point d cathodic current flow decays as the substrate is depleted in the vicinity of the electrode. The switching potential, $E_s$, is reached at point d at which time the potential of the electrode is scanned in a positive direction. From points d to e reduction of the substrate is still occurring since the electrode potential is still negative of the reduction potential of the substrate; however, between points e and f the potential of the electrode becomes sufficiently positive to allow the flow of anodic current and begin the oxidation of the electrogenerated species. Anodic current reaches it's maximum value at the oxidation peak potential, $E_{p,a}$ (point f). Between points f and g the decay of anodic current is observed as all of the reduced species is oxidized in the vicinity of the working electrode. Completion of the CV experiment occurs upon reaching the final potential, $E_f$.[45]

When the electron transfer is fast and reversible, **Equation 4**, the concentrations of A and B at the electrode surface are governed by the Nernst equation, **Equation 5**.

**Eqn. 4**

$$A + e^- \underset{\text{Fast Reversible}}{\overset{k_s}{\rightleftharpoons}} B$$

**Eqn. 5**

$$E = E^{o} - RT/nF \left( \ln ([B]/[A]) \right)$$

Where: $E^{o}$ = standard reduction potential of the substrate
R = the gas constant
T = temperature in Kelvin
F = Faraday's constant
E = electrode potential
n = number of electrons

The Nernst equation demonstrates that the concentration of reactant and product at the electrode surface is directly affected by the potential of the electrode. At the initial potential of a CV experiment a ratio exists between the concentrations of A and B in which the concentration of B is very small. When the potential of the working electrode is changed to more negative values, the concentration of B must increase to satisfy the Nernst equation; current therefore flows. In the reverse scan the potential residing on the electrode is being changed in a positive direction; therefore, to satisfy the Nernst equation, the concentration of A must begin increasing relative to the concentration of B. At the final potential of the CV experiment the initial concentrations of A and B are reestablished.

Cyclic voltammetry is able to provide a plethora of information concerning the nature of the electron transfer and any follow-up chemical reaction that may occur. This information is provided through accurate determination of the cathodic peak potential ($E_{p,c}$), the anodic peak potential ($E_{p,a}$), the cathodic peak current ($I_{p,c}$), and the anodic peak current ($I_{p,a}$). These values provide a method to ascertain the chemical and electrochemical reversibility of the voltammogram in a CV experiment based on the peak

widths exhibited in the voltammogram, the ratio of the anodic/cathodic current, and the shift in $E_p$ as a function of sweep rate. Once these diagnostics have shown that the voltammogram is electrochemically reversible, the standard reduction potential, $E^o$, can be determined for the redox couple.

Peak widths in a cyclic voltammogram are defined as the differences between the peak potentials, $E_p$, and the half peak potentials exhibited in the voltammogram, $E_{p/2}$. The half peak potential is the potential coinciding with the point where $I_p$ is half of it's maximum value. For a system exhibiting a fast, reversible electron transfer, $E_p - E_{p/2} = 59/n$ mV (where n is the number of electrons involved in the redox couple). The peak width is independent of sweep rate. The difference between $E_{p,a}$ and $E_{p,c}$ should also equal 59/n mV. If diagnostics show that the electron transfer of the redox couple is reversible, determination of the standard reduction potential, $E^o$, of a substrate is available from $E_{p,a}$ and $E_{p,c}$, **Equation 6**.[45]

**Eqn. 6**

$$(E_{p,c} + E_{p,a}) / 2 = E^o$$

Determination of the electrochemical reversibility of the electron transfer in a particular redox process is accomplished through careful scrutiny of the peak widths and peak shifts displayed in the voltammogram. However, peak widths relay no information regarding the chemical reversibility of the redox process. Determination of the chemical

reversibility of the redox process is provided by the current ratios, $-( I_{p,a}/ I_{p,c})$, displayed in the voltammogram.

For a chemically reversible system the ratio of $-(I_{p,a}/ I_{p,c}) = 1$. If current ratios much less than 1 are observed, then a reaction involving the electrogenerated species is occurring during the lifetime of the CV experiment. As a result, the electrogenerated species is unavailable for oxidation in the reverse sweep of the CV experiment and the current ratio will be less than 1, $-(I_{p,a}/ I_{p,c}) < 1$. Therefore, current ratios are able to provide a qualitative assessment of the stability of the electrogenerated species.

A large number of possibilities exist to categorize the nature of the reactions following the electron transfer; however, this study will only be concerned with those involving a unimolecular follow-up homogeneous chemical step, specifically transformations proceeding through an EC mechanism, **Figure 15**.

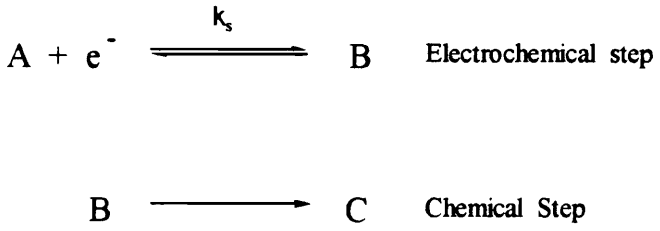


**Figure 15: The EC mechanism.**

In an EC mechanism, reduction of the substrate (E) is immediately followed by a chemical step (C) that decreases the amount of reduced material available for subsequent

oxidation. The ratio of $-(I_{p,a}/ I_{p,c})$ will be dependent upon the rate of the chemical step and the sweep rate. As the rate of the chemical step increases, the $-(I_{p,a}/ I_{p,c})$ ratio will approach 0. If the rate of the chemical step ( $k_c$) is fast enough, kinetic control of the EC mechanism can become dependent upon the rate of the heterogeneous electron transfer ($k_s$). In systems exhibiting no reverse current, linear sweep voltammetry (LSV) may be utilized to determine the species involved in the chemical step and determine a rate law for their reaction.

A LSV experiment is simply half of a cyclic voltammetry experiment. The absence of a reverse current in the voltammogram makes the return sweep unnecessary; therefore, the final potential and the switching potential are the same, **Figure 16**.

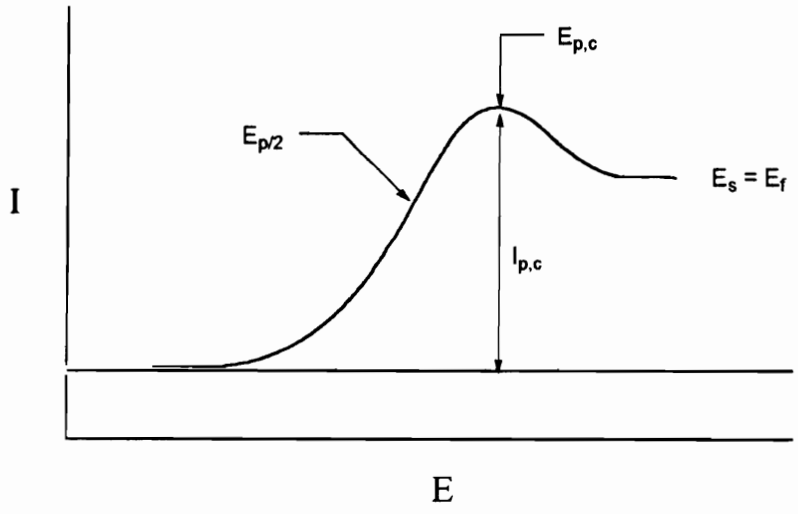


**Figure 16: Typical voltammogram observed in linear sweep voltammetry.**

From a LSV experiment $E_{p,c}$, $I_{p,c}$, and $E_{p/2}$ can be extracted. However, the real utility of a LSV experiment is in its ability to provide data that allows determination of the reaction order for the follow-up homogeneous reaction.[46,47] Combined with electrolytic techniques, the rate law and mechanism of decay of an electrogenerated species can be identified.

In an EC mechanism, there are a number of ways in which B can be consumed in a follow-up chemical reaction. Regardless of the method of reaction, if the chemical step is rate limiting, the Nernst equation will be obeyed at the electrode surface. The consumption of B in a chemical reaction means that more B has to be made in order to satisfy the Nernst equation. Maximum cathodic current will therefore occur at potentials more positive relative to those observed for reversible systems. As the sweep rate is increased the shift in $E_{p,c}$ decreases (i.e., becomes more negative). The shift in $E_{p,c}$ is directly related to the consumption of the reduced species and can therefore be utilized to determine the reaction order of it's consumption.

For a given chemical reaction, **Equation 7**, a plot of $E_{p,c}$ versus logv will produce a graph in which the slope is directly related to the reaction order of B, **Equation 8**.

**Eqn. 7**

$$A + e \rightleftharpoons B \quad (\text{fast, reversible})$$

$$aA + bB + cC \longrightarrow \text{Products}$$

**Eqn. 8**

$$-\frac{\delta E_p}{\delta \log \nu} = \frac{1}{b+1}\left(\ln \frac{RT}{nF}\right) = \frac{1}{b+1}\left(59.2\ \text{mV}\right)$$

Once b has been determined, the slope from a plot of $E_{p,c}$ versus $\log C_x$, where $C_x$ is the concentration of either A ($C_A$), **Equation 9**, or C ($C_C$), **Equation 9A**, is directly related to the reaction orders of A or C.

**Eqn. 9**

$$\frac{\delta E_p}{\delta \log C_A} = \frac{a+b+1}{b+1}\left(\ln \frac{RT}{nF}\right) = \frac{a+b+1}{b+1}\left(59.2\ \text{mV}\right)$$

**Eqn. 9A**

$$\frac{\delta E_p}{\delta \log C_c} = \frac{c+b+1}{b+1}\left(\ln \frac{RT}{nF}\right) = \frac{c+b+1}{b+1}\left(59.2\ \text{mV}\right)$$

Once the experimental values have been measured, the rate law of the chemical reaction can be determined (**Table 3**).

**Table 3: Theoretical response for first and second order rate laws based upon Eqns. 7-9.**

| Rate Law | $\delta E_p/\delta \log v$ (mV/decade) | $\delta E_p/\delta \log C_A$ (mV/decade) |
|---|---|---|
| k[B] | -29.5 | 0 |
| $k[B]^2$ | -19.7 | 19.7 |
| k[A][B] | -29.5 | 29.5 |

In this way the reaction orders of the electrode generated species and any other substrate involved in the chemical reaction can be deconvoluted to allow determination of the rate law.

To characterize the systems under study, we had to concern ourselves with the two limiting cases of an EC mechanism, rate limiting chemical step ($k_c$) in which the responses summarized in **Table 3** are observed, or rate limiting heterogeneous electron transfer ($k_s$). Differentiation between the two limiting cases is afforded through careful analysis of the voltammogram peak width and the change of peak potential as a function of sweep rate.

Systems exhibiting a rate limiting chemical step are governed by the Nernst equation. As a result, $\delta E_{p,c}/\delta \log v$ can be used as a diagnostic for a rate limiting chemical step. For systems proceeding through an EC mechanism in which the chemical step is rate limiting, $E_p$ (the reduction potential) will shift to more negative values as the sweep rate is increased, **Equation 10.**[45]

**Eqn. 10**

$$\delta E_{p,c}/\delta \log \nu = -29.5 \text{ mV/decade.}$$

The peak width exhibited in the voltammogram provides further diagnostics to evaluate the rate limiting step of an EC mechanism. Peak width diagnostics for systems exhibiting rate limiting $k_c$ are shown in **Equation 11** and **Equation 12.**

**Eqn. 11**

$$E_p - E_{p/2} = 59/n \text{ mV}$$

Where: n = number of electrons transferred.

**Eqn. 12**

$$E_p - E_{1/2} = 29 \text{ mV}$$

Where: $E_{1/2}$ = the standard potential for the redox couple, $E^o$.

These values show no dependence on the sweep rate of the experiment. When the chemical reaction is slow enough, a portion of the reduced species will be available for oxidation; therefore, an oxidation wave is observed. In systems undergoing a rate limiting chemical step, the difference in the cathodic and anodic peak potentials should equal to 59/n mV. Since a rate limiting chemical step is governed by the Nernst equation, there is a large similarity between the values above and those observed for a system exhibiting

reversible heterogeneous electron transfer. However, when the rate limiting step is heterogeneous electron transfer, $k_s$, this is not the case.

Non-Nernstian behavior is exhibited by systems in which the heterogeneous electron transfer, $k_s$, is rate limiting.[48] However, some of the same behavior is exhibited in the voltammogram when the heterogeneous electron transfer is rate limiting as is observed in a voltammogram exhibiting a rate limiting chemical step. As in the case when the chemical step is rate limiting, a negative shift in $E_p$ is observed with increasing sweep rate and $E_p - E_{p/2}$ is independent of sweep rate. The LSV of a system exhibiting rate limiting heterogeneous electron transfer are characterized by broad peaks in the voltammograms, **Equation 13.**

**Eqn. 13**

$$E_p - E_{p/2} = 47.7/\alpha n$$

where: n = number of electrons transferred.
$\alpha$= the transfer coefficient ($0 \leq \alpha \leq 1$).

The broadness of the peak is not dependent on the sweep rate of the experiment. The diagnostic shift of $E_p$ for a system with rate limiting heterogeneous electron transfer is shown in **Equation 14**.

**Eqn. 14**

$$\delta E_{p,c}/\delta \log v = -30/\alpha n \text{ mV/decade}$$

where: n = number of electrons transferred.
$\alpha$= the transfer coefficient ($0 \leq \alpha \leq 1$).

As a consequence of the heterogeneous electron transfer being rate limiting, the diagnostics for rate limiting heterogeneous electron transfer are dependent on the number of electrons involved in the transfer, and on the transfer coefficient, $\alpha$.

The transfer coefficient of an electrochemical process describes the symmetry of the transition state during heterogeneous electron transfer.[48] The transfer coefficient can be determined from a plot of $E_p$ vs. sweep rate or from the peak widths exhibited in the voltammogram. As a result, the transfer coefficient can be obtained using **Equation 15** or **Equation 16**.

**Eqn. 15**

$$\alpha = (F/RT)( \delta E_{p,c}/\delta \ln v)$$

**Eqn. 16**

$$\alpha = (RT/F)(1.85/(E_{p/2}-E_p)$$

Values of the transfer coefficient can range from 0 to 1 (typically ($0 \leq \alpha \leq 1$). A description of what these values infer about the transition state for heterogeneous electron transfer is shown in **Figure 17**.

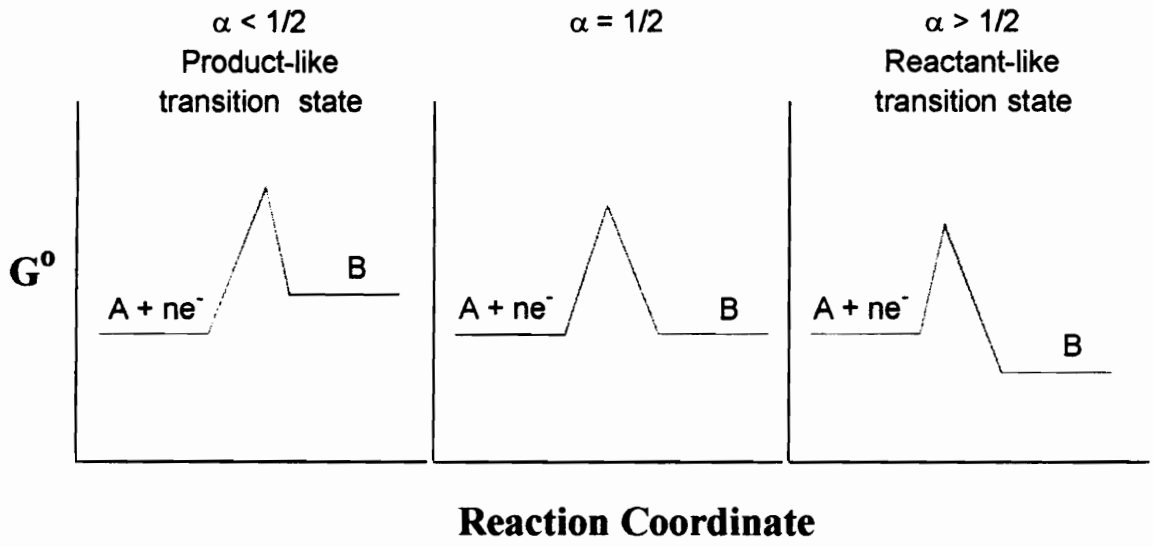


**Figure 17: Effect of the transfer coefficient on the transition state of heterogeneous electron transfer.**

The value of the transfer coefficient can also be used to determine whether the heterogeneous electron transfer proceeds in a concerted or step-wise method. Saveant has suggested that the transfer coefficient is diagnostic of concerted vs. stepwise electron transfer/bond cleavage in several arylmethyl halides.[49] It was shown that substrates possessing transfer coefficients ranging from 0.2 - 0.3 exhibited concerted halogen cleavage with electron transfer. However, substrates exhibiting transfer coefficient values of 0.5 have been shown to proceed through a discrete radical anion intermediate prior to

halogen cleavage. The transfer coefficient can therefore be a very powerful tool in the characterization of substrates exhibiting rate limiting heterogeneous electron transfer.

In summary CV is a very powerful method for the generation and characterization of reactive species produced via electron transfer. Characterization of substrates exhibiting irreversible voltammograms due to follow-up chemical reactions is afforded through the use of LSV. Utilizing LSV, the rate limiting step of an EC mechanism can be determined. LSV permits the determination of the reaction order of all species involved in a first or second order reaction and establishment of a rate law for the chemical step when that step is rate limiting. Thus, LSV emerged as a very powerful method for characterization of the substrates that we investigated.

# SYNTHESES OF 5,7-Di-*t*-BUTYLSPIRO[2,5]OCTA-4,7-DIEN-6-ONES

The syntheses of **19** and **20** were accomplished through modification of previously published syntheses, **Scheme 11**.[50,51,52,53]

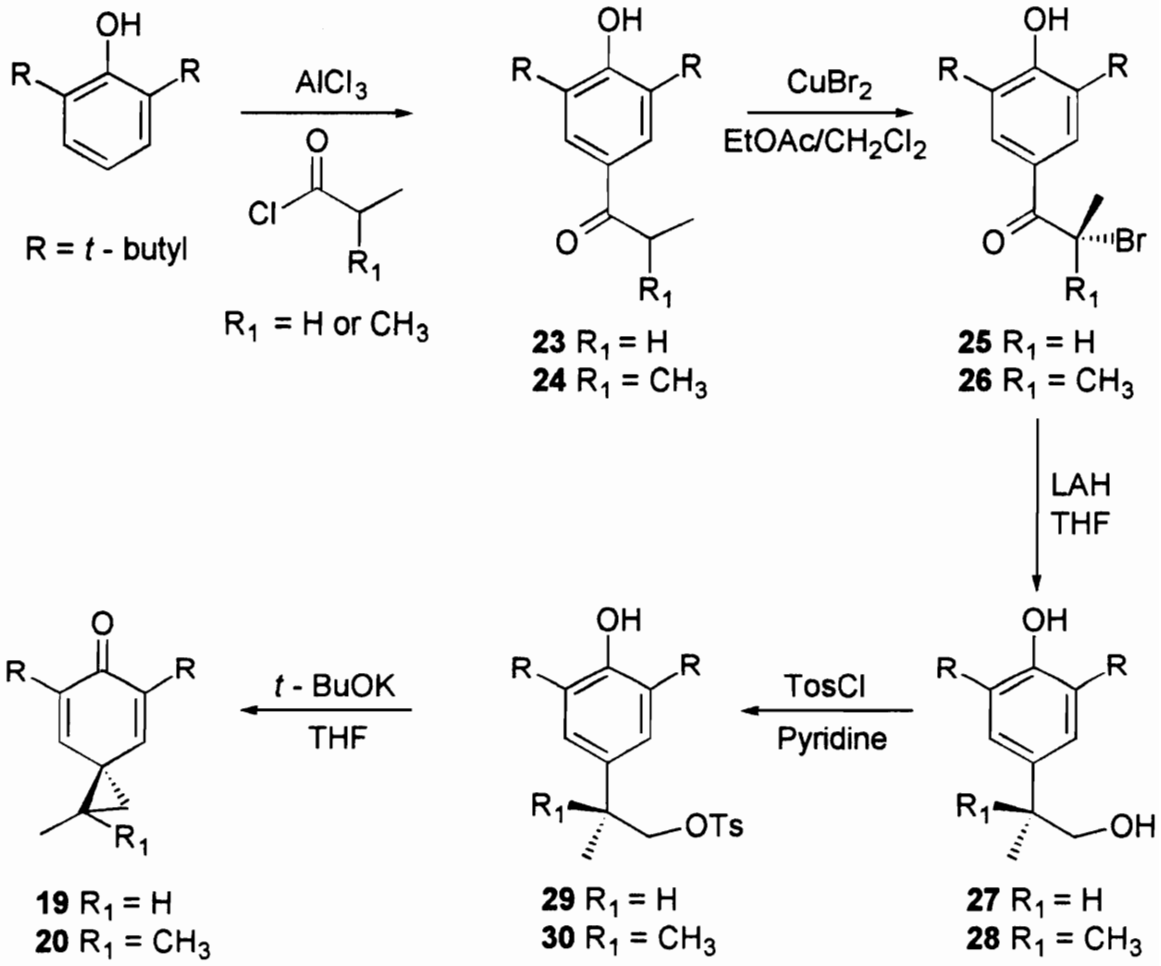


**Scheme 11**

The initial reaction of this synthesis is a Friedel-Crafts acylation reaction. The spirooctadienone produced in the overall reaction depends upon the identity of the acid chloride used in this step. Synthesis of **19** is afforded through the use of propionyl chloride, while **20** is obtained utilizing *iso*-butanoyl chloride. The synthesis of the ketone is complicated by the occurrence of a retro Friedel-Crafts acylation reaction. To insure optimal yields of ketones **23** and **24** reaction times were kept to approximately 1 minute and temperatures were kept below -10° C.

Bromides **25** and **26** were obtained through an α-bromination reaction of the ketone utilizing copper(II)bromide ($CuBr_2$). The proposed mechanism of this reaction is shown in **Scheme 12**.

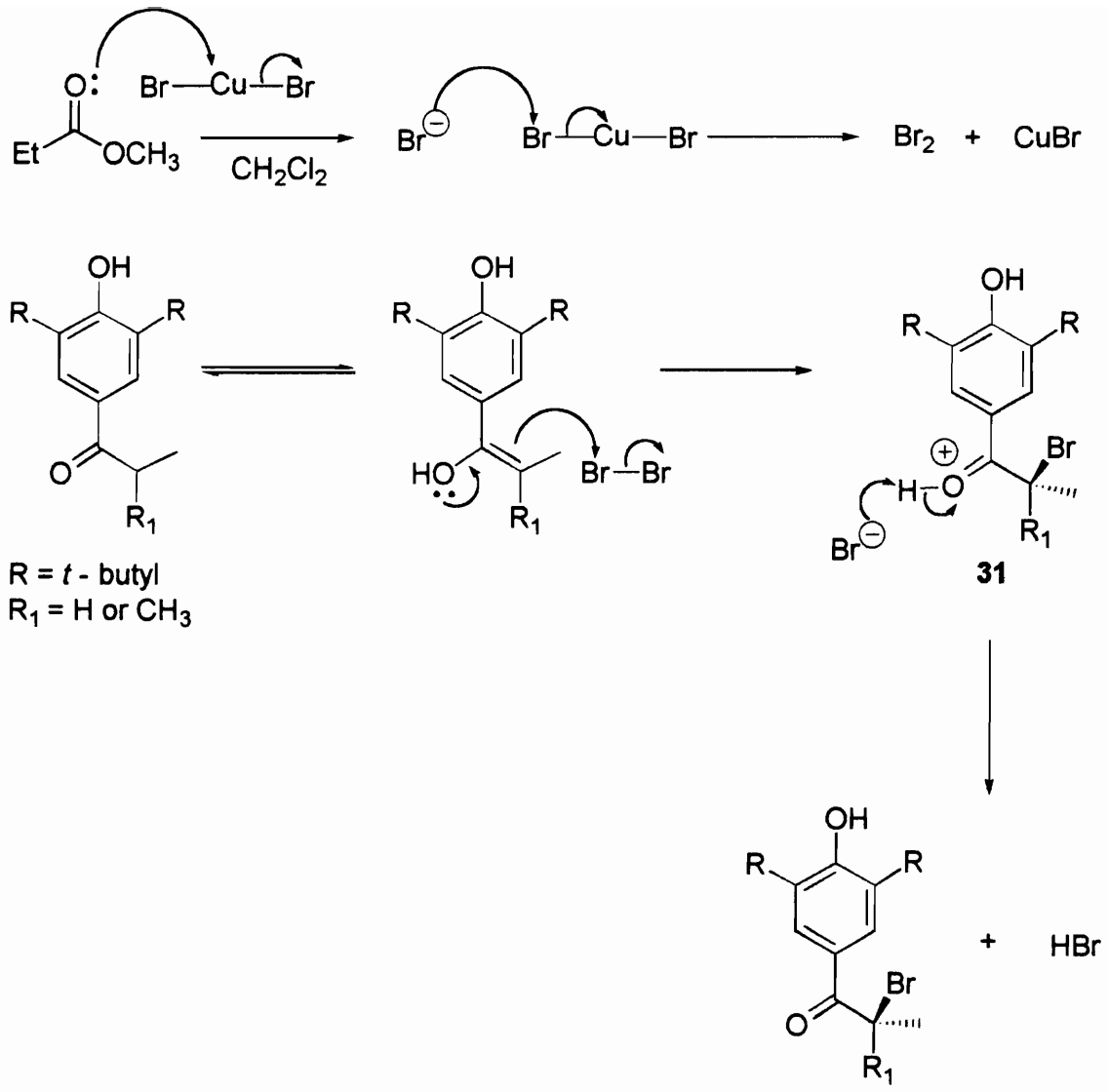


**Scheme 12**

In this reaction ethyl acetate coordinates to copper(II)bromide resulting in expulsion of bromide. Bromide can then interact with another molecule of copper(II)bromide resulting in the formation of bromine and copper(I)bromide. The enol tautomer then reacts with

bromine resulting in the protonated α-brominated ketone (**31**). Reaction of **31** with bromide results in the subsequent α-brominated ketones, **25** or **26**.

Conflicting reports to the identity of the alcohols produced in the LAH reduction of **25** or **26** were present in the literature.[51,53] The alcohols produced in the original synthesis were identified as the 2° and 3° alcohols from the proposed mechanism shown in **Scheme 13**.[51]

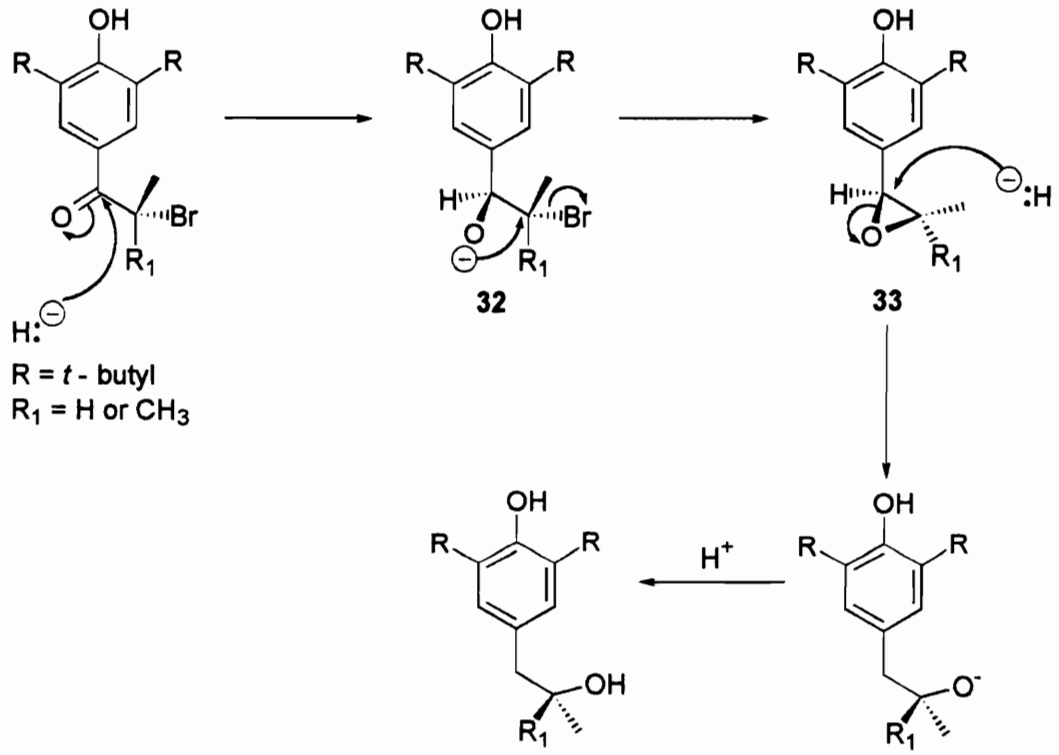


**Scheme 13**

The initial step in this mechanism is hydride addition to the carbonyl carbon resulting in the formation of alkoxide **32**. Intramolecular attack by the alkoxide oxygen results in formation of epoxide **33** and the expulsion of $Br^-$. Hydride addition to the least hindered carbon of the epoxide results in ring opening to the 2° and 3° alcohols after acidification. However, a later investigation discounts the production of these products.[53]

The LAH reduction of **25** or **26** was instead shown to result in 1° alcohols **27** and **28**. The proposed mechanism for production of the 1° alcohols is shown in **Scheme 14**.

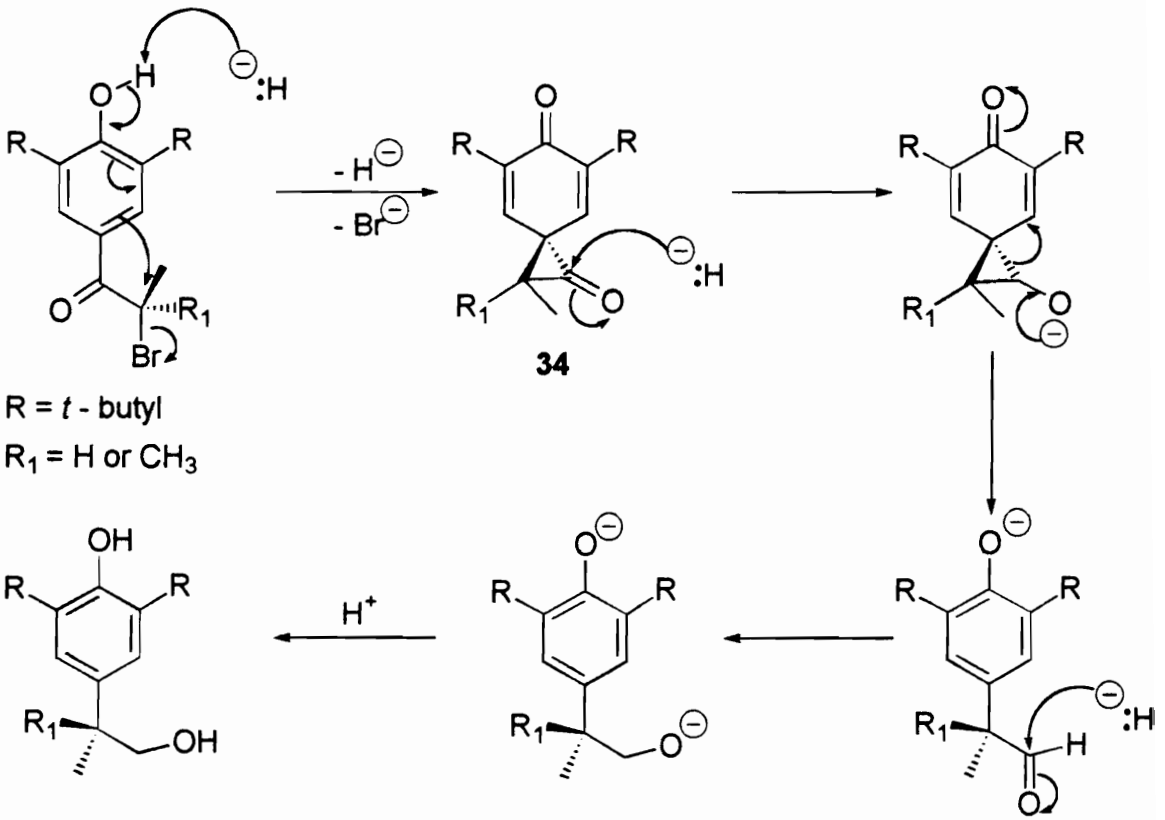


**Scheme 14**

The first step in this mechanism is the removal of the phenolic proton followed by subsequent ring closure to give spirocyclopropanone, **34**. Further reduction of **34** results in cyclopropyl ring opening to the intermediate aldehyde which is then immediately reduced to the alkoxide. Acidic workup affords the primary alcohols.

Characterization of the alcohols produced in this study, via $^1$H NMR, revealed them to be the 1° alcohols, **27** and **28**. Production of these alcohols eliminated the mechanism in **Scheme 13** as the mechanism responsible for the production of products, suggesting that the mechanism in **Scheme 14** was instead the pathway leading to the formation of **27** and **28**.

The primary alcohols **27** and **28** were then converted to tosylates **29** and **30**. Reaction of the tosylates with potassium *tert*-butoxide results in cyclopropane ring closure to give **19** and **20**, **Scheme 15**.

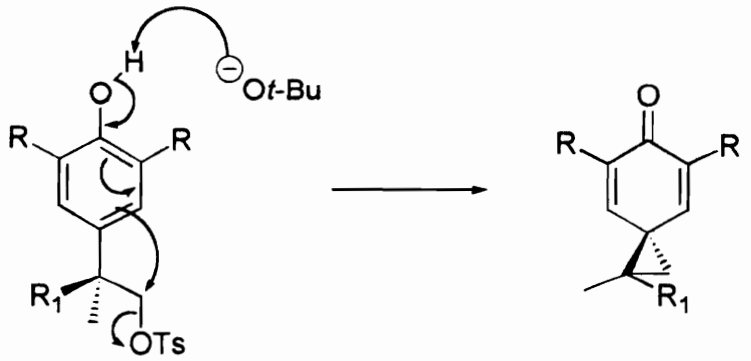


R = *t* -Butyl
$R_1$ = H or $CH_3$

**Scheme 15**

Spirooctadienone **20** has proven itself to be a very reactive substrate. Isolation of this substrate is contingent upon keeping contact with water to a minimum. Optimum yields are obtained when 1% NaOH is used in the place of water in the workup. Atmospheric water is capable of degrading this material; therefore storage with a desiccant is necessary. Isolation via chromatographic methods is not possible due to degradation of the material on the column. Interestingly, **19** has shown none of these problems and can be purified using acetonitrile/water mixtures via high pressure liquid chromatography. Once sufficient materials had been isolated and purified, characterization of their ability to serve as substrates capable of identifying SET was initiated.

## THE ELECTROCHEMICAL REDUCTION OF 1,1-DI-METHYL-5,7-Di-*t*-BUTYLSPIRO[2,5]OCTA-4,7-DIEN-6-ONE (20).

Our investigations into the utilization of **20** as a SET probe were based upon the premises that cyclopropyl ring opening would be fast and irreversible as a result of establishment of aromaticity and relief of cyclopropyl ring strain upon introduction of an electron, **Scheme 16**.

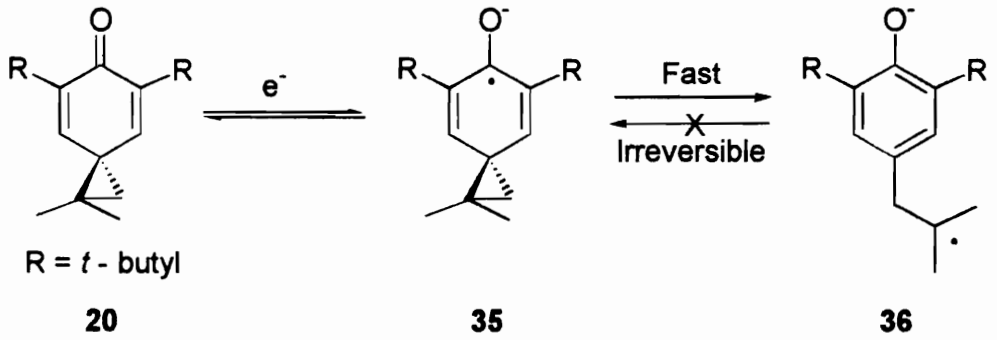


**20** **35** **36**

**Scheme 16**

Based upon the observed ring opening for the radical anion of 1-benzoyl-2,2-dimethylcyclopropane, **9**, in which only the 3° distonic radical anion, **37**, is observed upon cyclopropyl ring opening,[37] **Scheme 17**, and the 7 kcal/mol difference in energy observed between ethyl and *t*-butyl radical,[54] we were confident that in all probability the 3° distonic

radical anion, **36**, would be the major if not the only radical anion produced in the reduction.

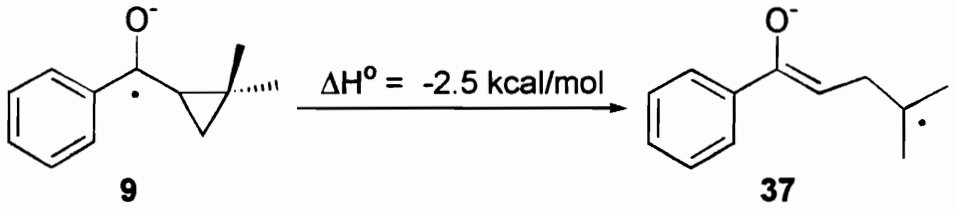


**9** **37**

**Scheme 17**

Further support to this hypothesis was found in the form of molecular orbital calculations.

The calculated $\Delta H^{\circ}$ of radical anions **36** and **38**, AM1 SCF-MO calculations (DOUBLET), from cyclopropyl ring opening of **35** is exothermic by over 16 kcal/mol, **Table 4**.[55]

**Table 4: Standard heats of formation for the 1° and 3° distonic radical anions.**

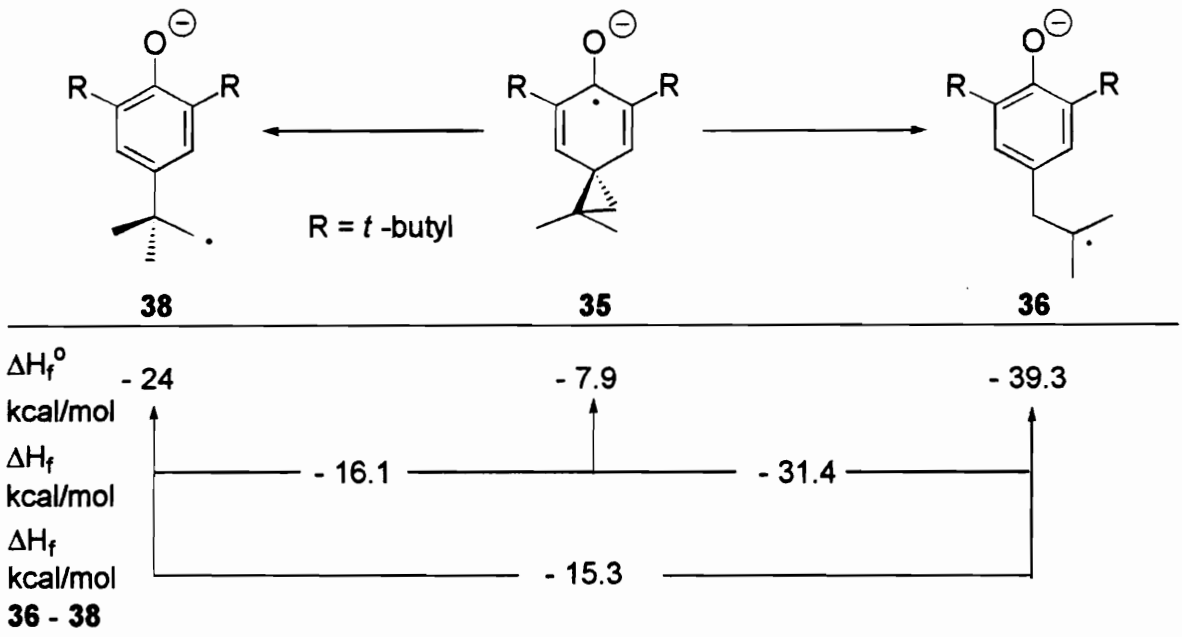


The 3° distonic radical anion, **36**, was determined to have a standard heat of formation, $\Delta H^{\circ}$, 15.4 kcal/mol more negative than the 1° distonic radical anion, **38**. The exothermic nature of the cyclopropyl ring opening of **35** indicates that the ring opening is very facile and that establishment of resonance is a contributing factor to the ease with which the cyclopropyl ring opens. In contrast, fragmentation of the ring opened radical anion derived from 1-benzoyl-2,2-dimethylcyclopropane, **9**, was found to be only slightly exothermic at -2.5 kcal/mol (AM1 SCF-MO calculations, UHF, implemented through MOPAC 6).[37] Electrochemical studies were, therefore, initiated to investigate the one electron reduction of **20** and confirm these hypotheses.

Initial investigations into the cyclic voltammetry of **20** were attempted in anhydrous N,N-dimethylformamide (DMF) employing 0.5 M *n*-$Bu_4NBF_4$ as supporting electrolyte. A gold electrode was utilized as the working electrode. The results obtained in these investigations were extremely erratic. Peak potentials varied by as much as 300 mV. Peak widths ($E_p$-$E_{p/2}$) varied from 59 mV to 125 mV. Adsorption of material on the working electrode surface continually fouled the electrode, making the collection of meaningful data impossible. Changing the solvent to anhydrous dimethyl sulfoxide provided no better results.

Switching the working electrode to a glassy carbon electrode (GCE) resulted in reproducible voltammograms; however, peak widths were broad and remained so regardless of the solvent utilized. Reproducibility was achieved in anhydrous DMF through the following procedure. The electrode was polished between acquisitions to remove any adsorbed material from the gold surface. The auxiliary electrode was isolated to preclude interference from material oxidized at it's surface. The solution was stirred and purged with argon between acquisitions.

The cyclic voltammetry of **20** at 1 V/s was characterized by a broad irreversible reduction wave at -2.35 V vs. 0.1 M $Ag/Ag^+$. A reversible oxidation wave is observed at -0.7 V attributed to oxidation of the phenolate anion produced in the reduction, **Figure 18**.

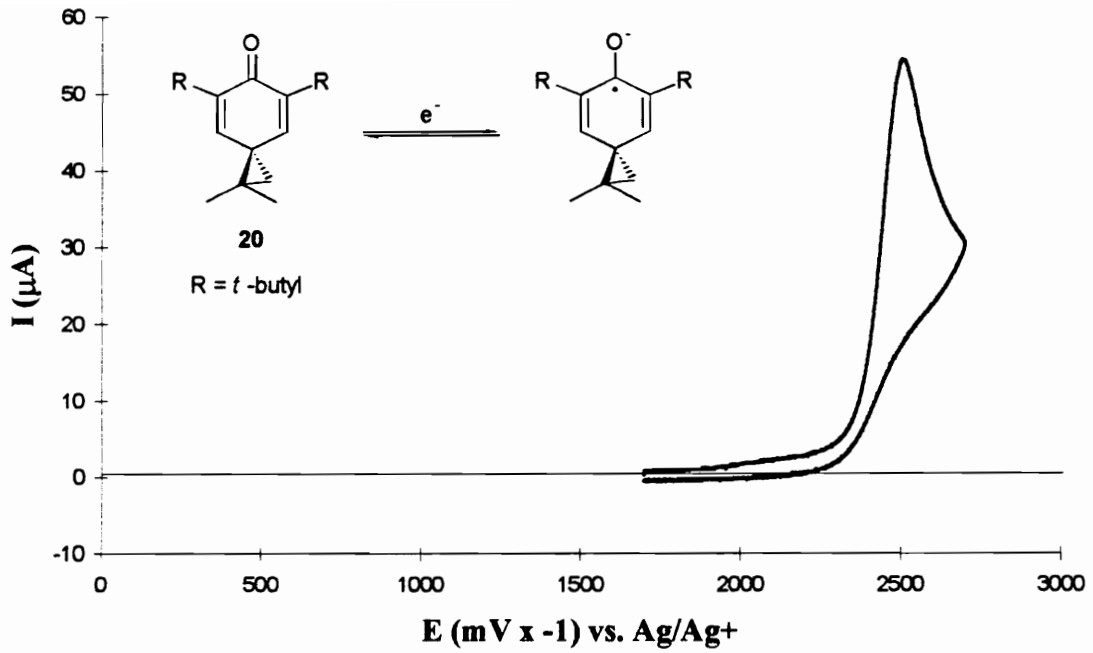


**Figure 18: Cyclic voltammogram of 20 at 1 V/s utilizing a gold working electrode in a 0.1 M solution of *n*-$Bu_4NClO_4$ in anhydrous N,N-dimethylformamide.**

The irreversibility of the reduction wave exhibited in the voltammograms was consistent with what would be observed in an EC mechanism. No oxidation wave was observed in the voltammogram at sweep rates to 8000 mV/S, indicating that the follow-up chemical step proceeded at rates in excess $8 \times 10^3$ $s^{-1}$.

The reduction peak obtained in the voltammograms of **20** was extremely broad. Peak analysis revealed that $E_p - E_{p2} = 105 \pm 8$ mV. Moreover, the peak width of the reduction peak exhibited no dependence on sweep rate. However, the reduction peak was noted to shift to more negative potentials with increasing sweep rate. Analysis of the

dependency of the shift of $E_p$ an the sweep rate revealed that $\delta E_p/\delta \log v = -56 \pm 5$ mV, **Figure 19**.

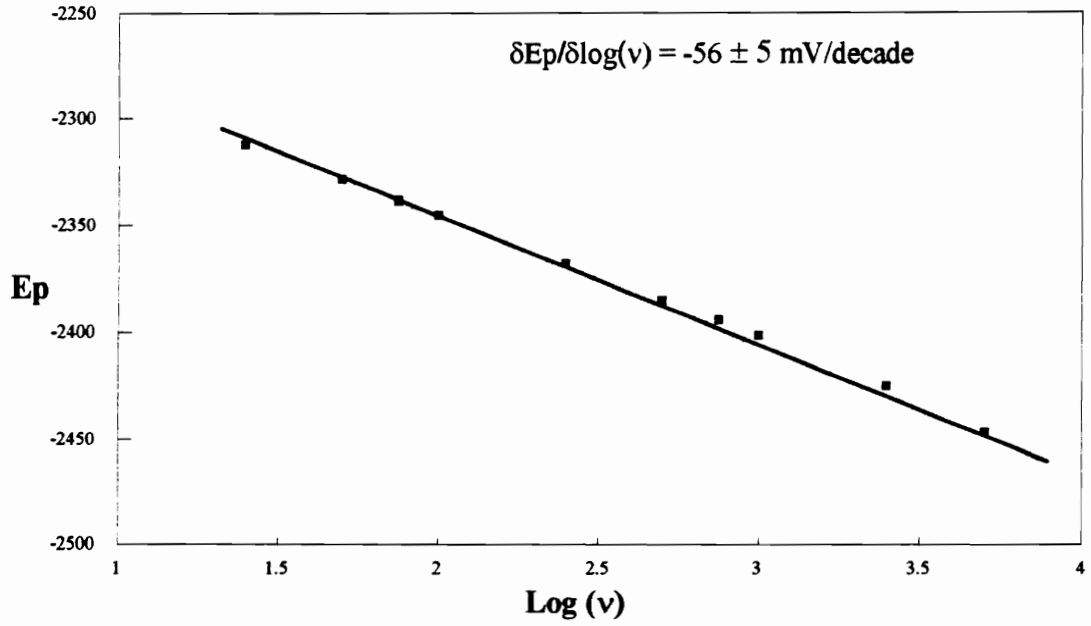


**Figure 19: Plot of $E_p$ vs. log sweep rate for the cyclic voltammetry of 20.**

The broadness of the reduction peak coupled with the magnitude of the shift exhibited by $E_P$ was consistent with what is expected for an EC mechanism exhibiting rate limiting heterogeneous electron transfer. However, confirmation of this hypothesis could only occur, once the value of the transfer coefficient, $\alpha$, had been determined. Determination of $\alpha$ enabled us to ascertain the theoretical peak broadness and peak shift that should be present in voltammograms of **20** in which rate limiting heterogeneous

electron transfer was occurring. Moreover, comparison of the transfer coefficient exhibited by **20** to those observed in the dissociative electron transfer of arylmethyl halides could allow us to determine whether the electron transfer was concerted with the formation of **36** and **39** or proceeded through a discrete radical anion intermediate such as **35**.

Determination of the transfer coefficient using **Eqns. 15** and **16** produced within experimental error the same values for $\alpha$, $0.52 \pm 0.04$ and $0.45 \pm 0.04$ respectively. The value of the transfer coefficient (0.49, median value) indicated that the transition state involved in the heterogeneous electron transfer resided almost exactly between products and reactants. Comparison of the transfer coefficient observed for **20** to those observed in the dissociative electron transfer to arylmethyl halides suggested that the electron transfer was proceeding through a discrete radical anion intermediate (**35** in **Scheme 16**).[49]

Determination of the theoretical peak widths and shift in $E_p$ that should be observed with rate limiting heterogeneous electron transfer was possible through **Equations 17** and **18**.[47]

**Eqn. 17**

$$E_p - E_{p/2} = \frac{47.7}{\alpha n} = \frac{47.7}{(0.49)(1.0)} = 97.3 \text{ mV}$$

**Eqn. 18**

$$\frac{\delta E_p}{\delta \text{Log}v} = \frac{-30}{(0.49)(1.0)} = -61 \text{ mv/decade}$$

The theoretical and experimental values obtained are shown in **Table 5**.

**Table 5: Comparison of theoretical and experimental values for peak widths and for variance of $E_p$ as a function of sweep rate.**

| | $E_{p/2} - E_p$ (mV) | $\delta E_p/\delta \log v$ (mV/decade) |
|---|---|---|
| Experimental | $105 \pm 8$ | $56 \pm 5$ |
| Theoretical | 97.3 | 61.2 |

The similarity of the theoretical values to the experimental values inferred that heterogeneous electron transfer was the rate limiting step in the EC mechanism. As a result, direct determination of $E^\circ$ and $k_c$ were prevented. However, indirect methods existed that allowed estimation of these values from the available data.[56]

In an EC mechanism the competition between the heterogeneous electron transfer, $k_s$, and the chemical step, $k_c$, for kinetic control depends on the parameter, p. In systems exhibiting rate limiting $k_s$, $p \leq 0.1$, **Equation 19**.

**Eqn. 19**

$$p = \left[\frac{\alpha n F v}{RT}\right]^{(\alpha-1)/2\alpha}\left[\frac{k_s^{1/\alpha}}{k^{1/2}}\right] D^{-1/2\alpha}$$

For a given value of $k_s$, kinetic control of an EC mechanism can be transferred from the chemical step to the electron transfer step by increasing the sweep rate or by increasing the rate of the chemical step. Therefore, assuming a typical value for the rate of electron transfer will allow determination of a lower limit for the chemical step. Rearranging **Eqn. 19** affords a method for the determination of the rate of the chemical step, $k_c$, **Equation 20**.

**Eqn. 20**

$$k_c = \left[\frac{\left[\frac{\alpha n F v}{RT}\right]^{(\alpha-1)/2\alpha} k_s^{1/\alpha} D^{-1/2\alpha}}{p}\right]^2$$

Using the upper limit of p established for rate limiting electron transfer, $p = 0.1$, typical values for D and $k_s$ ($1 \times 10^{-5}$ $cm^2/s$ and 1.0 cm/s respectively),[48] and the previously determined value for the transfer coefficient (0.49), we estimated that $k_c \geq 10^7$ $s^{-1}$. This rate constant is similar to that observed for the cyclopropyl ring opening of the 1,1-

dimethylcyclopropylcarbinyl radical which cyclopropyl ring opens to the 3° and 1° homoallylic radicals in a 7:1 ratio respectively( $k_c \cong 10^9\ s^{-1}$ at 60° C), **Scheme 18**.[31]

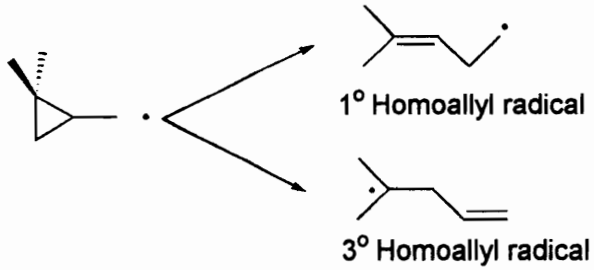


**Scheme 18**

Comparison of the rate of cyclopropyl ring opening of **35** to the rate of cyclopropyl ring opening observed for the radical anion derived from cyclopropyl phenyl ketone, $k \leq 2\ s^{-1}$, indicates that the establishment of aromaticity combined with the cyclopropyl ring opening of **35** plays a major role in the observed rate.

For processes exhibiting rate limiting heterogeneous electron transfer, $E^o$ is related to $E_p$ by **Equation 21**.[57]

**Eqn. 21**

$$E_p = E^o - \left[\frac{RT}{\alpha nF}\right]\left(0.78 - \ln k_s \left(\frac{\alpha nFD\nu}{RT}\right)\right)^{-1/2}$$

At 100 mV/S, $E_p$ of **20** is -2.35 V vs. 0.1 M $Ag^+/Ag$. Again assuming typical values for D and $k_s$ (1 x $10^{-5}$ $cm^2/s$ and 1.0 cm/s respectively) and 0.49 for the transfer coefficient, $E^o$ was estimated to be in the order of -2.5 V vs. 0.1 M $Ag^+/Ag$.

Upon completion of the voltammetry investigation, we were in a position to undertake a modeling study to investigate the theoretical response a voltammogram would display utilizing the experimental values we obtained.[58] Theoretical voltammograms were produced utilizing the previously determined values for $E^o$, $k_c$, and $\alpha$. The reverse rate constant of the chemical step was assumed to be 0.0 $s^{-1}$ and the rate of heterogeneous electron transfer was assumed to be 0.1 cm $s^{-1}$, $k_s$ = 0.1 cm $s^{-1}$. Comparison of the theoretical and experimental results are shown in **Figure 20**.

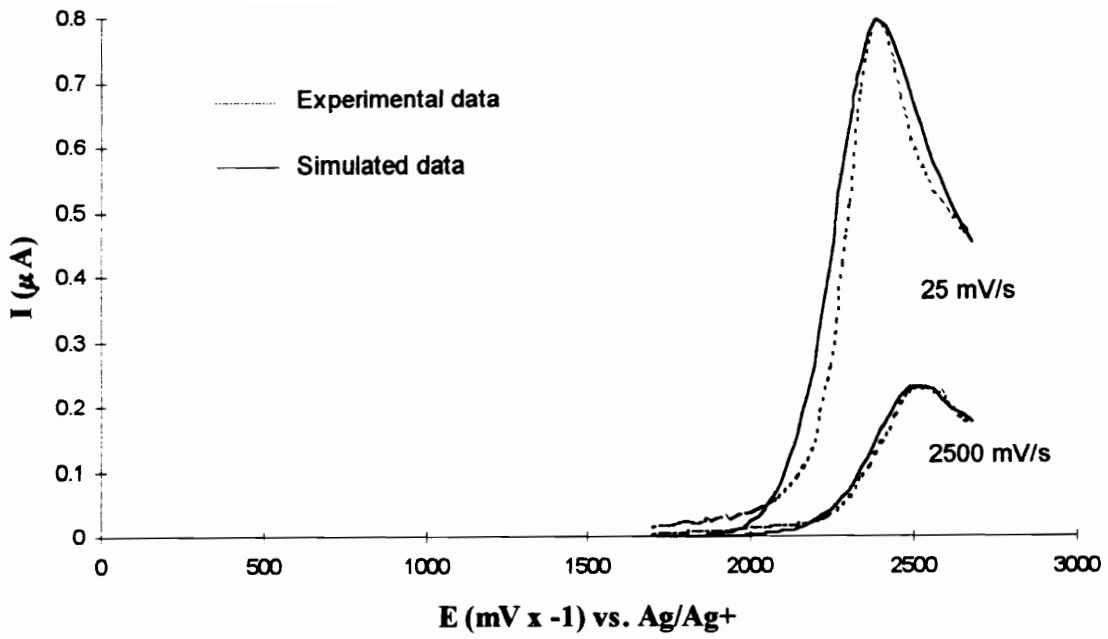


**Figure 20: Comparison of theoretical voltammogram response to the experimental voltammogram of 20.**

The theoretical voltammograms exhibited behavior similar to that observed in the experimental voltammograms. The similarity in the voltammograms suggest that the experimental estimates obtained for $E^{\circ}$, $k_c$, and $\alpha$ are consistent for a system exhibiting rate limiting heterogeneous electron transfer.

Cyclic voltammetry proved itself a powerful tool in the characterization of the behavior exhibited by **20** upon one electron reduction. However, the nature of the chemical step is still speculative. While cyclopropane ring opening could be responsible for the irreversible voltammogram displayed, the amounts of material generated in a cyclic

voltammetry experiment do not permit the isolation of the electrochemically generated species. Thus, electrolytic techniques were employed for generation of sufficient material to allow characterization of the products from the one electron reduction of **20** and subsequent identification of the mechanism involved in the reduction.

## ELECTROLYSIS OF 1,1-DIMETHYL-5,7-DI-*t*-BUTYLSPIRO[2,5]OCTA-4,7-DIEN-6-ONE (20).

Electrolysis of **20** was accomplished by Manuel Hervas employing constant current electrolysis.[59] In a constant current electrolysis current is supplied to a solution containing the material to be electrolyzed over a predetermined period of time. The time duration of the electrolysis was determined through the use of **Equation 22**.

**Eqn. 22**

$$T = nFM / I$$

Where: T = time in seconds
n = number of electrons
F = Faraday's constant
M = equivalents of substrate
I = current in Amperes

Constant current electrolysis of **20** was performed in anhydrous DMF employing *n*-$Bu_4NBF_4$ as supporting electrolyte. Gold foil was employed as the working electrode and a platinum coil as the auxiliary electrode.

Constant current electrolysis of **20** (0.98 $e^-$/ molecule) resulted in three major products in a 78% overall yield, **Scheme 19**.

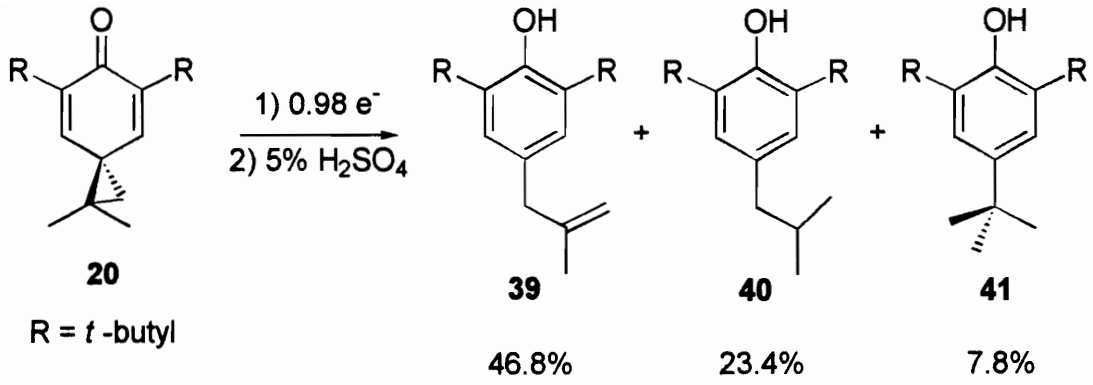


**Scheme 19**

A mechanism consistent with the observed products is shown in **Scheme 20**.

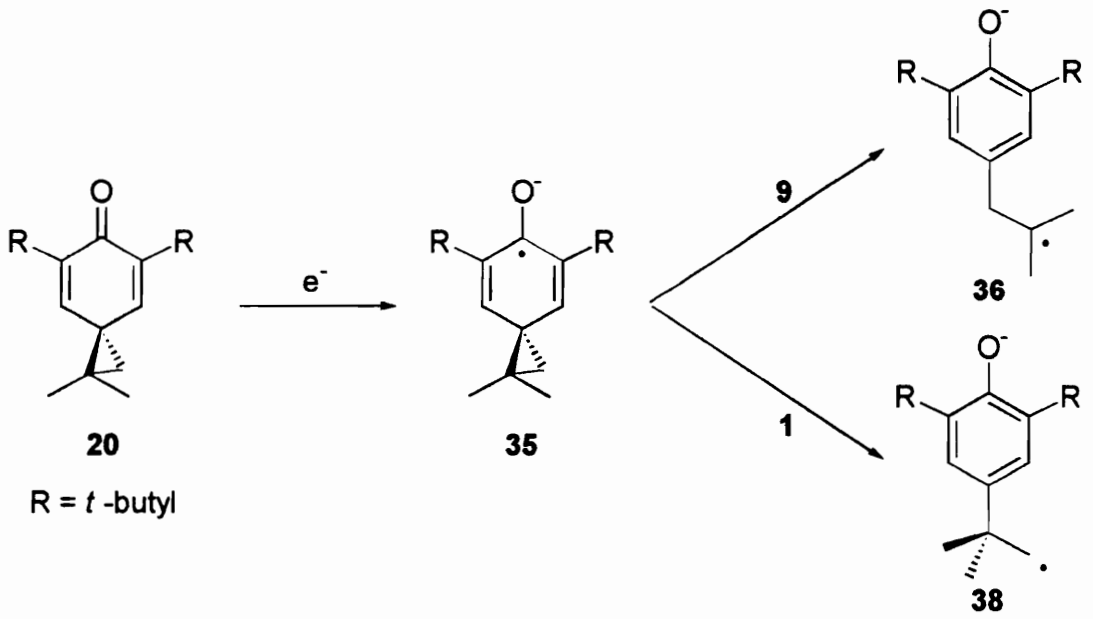


**Scheme 20**

One electron reduction of **20** results in the cyclopropyl ring closed radical anion **35**. The ring closed radical anion undergoes cyclopropyl ring opening in a 9:1 ratio to the 3° and 1° distonic radical anions, **36** and **38** respectively, **Scheme 20**. Formation of phenolates **42**, **43**, and **44** are a result of disproportionation reactions between the 1° and 3° distonic radical anions, **Scheme 21**.

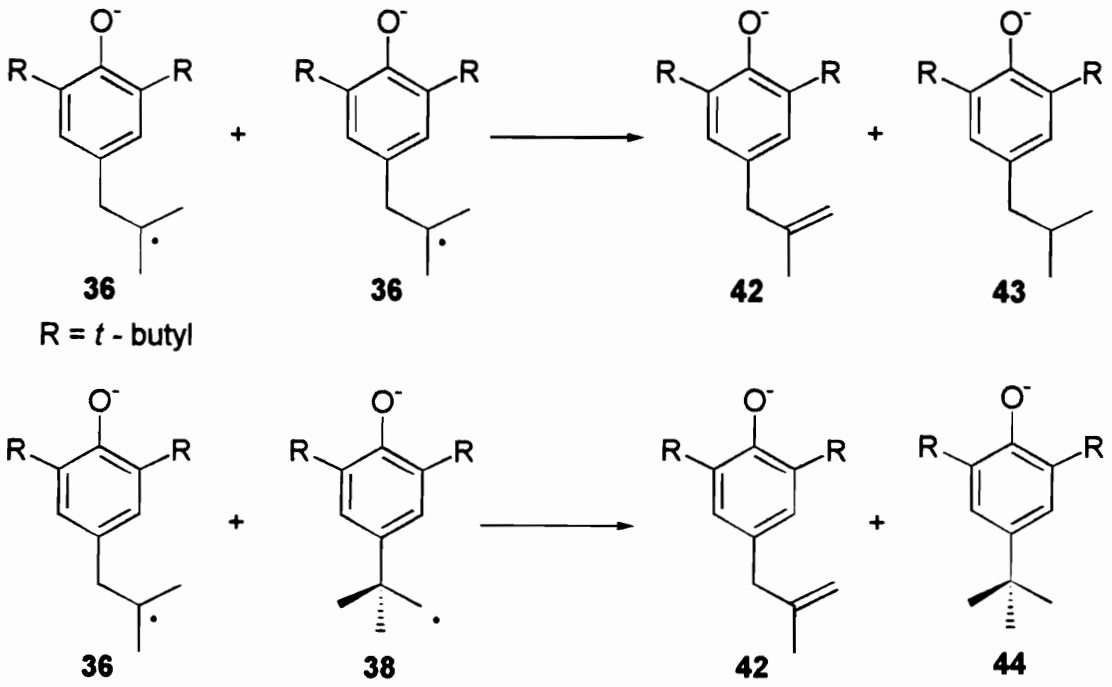


**Scheme 21**

It was interesting that only the terminal alkene **39** derived from phenolate **42** was produced from the disproportionation of the 3° distonic radical anion since an alternative disproportionation pathway exists that would result in formation of a more substituted internal alkene, **45**, **Scheme 22**.

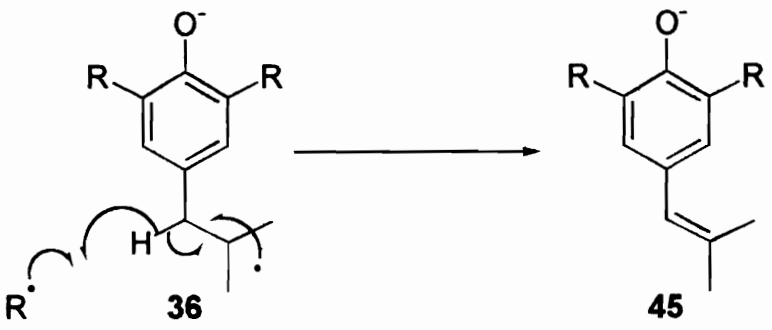


R = *t* -butyl

**Scheme 22**

Semi-empirical molecular orbital calculations (AM1 SCF-MO (RHF), implemented through MOPAC 6.0) have shown **45** to be 7.5 kcal/mol more stable than **39**. Based on heats of formation alone, one would expect the presence of the conjugated alkene in the product distribution. However, these calculations do not account for the geometry of the molecule during the hydrogen atom abstraction or the steric hindrance involved in the abstraction.

Semi-empirical molecular orbital calculations (AM1 SCF-MO (DOUBLET)) of the geometry of radical anion **36** have shown that the most stable form of the 3° distonic

radical anion places the radical p-orbital perpendicular to the π–system of the aromatic ring, **Figure 21**.[55]

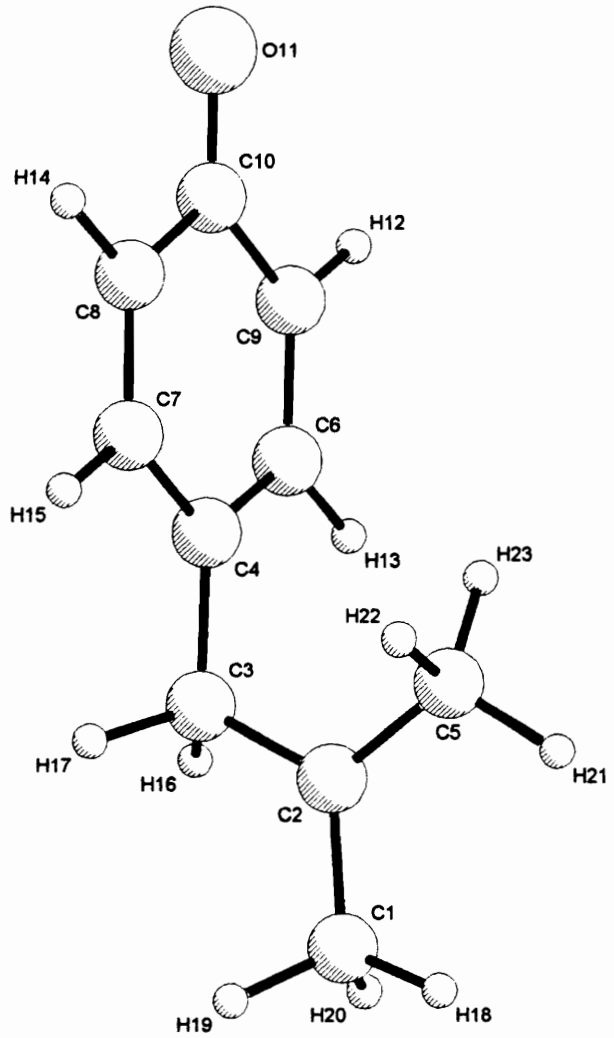


**Figure 21: Geometry of the 3° distonic radical anion, 36.**

As a consequence of this geometry, abstraction of a benzylic hydrogen is unfavorable due to stereoelectronic factors. Therefore, the developing π–system of the alkene can not benefit from stabilization from the aromatic ring. The steric hindrance associated with hydrogen abstraction at the benzylic position is also much greater than steric hindrance associated with hydrogen abstraction from one of the methyl groups. The absence of aromatic stabilization during formation of trisubstituted alkene **45** combined with the steric hindrance associated with hydrogen abstraction at the benzylic position, therefore, makes the hydrogen abstraction from a methyl group a kinetically faster process. As a result only alkene **40** is produced.

A more intriguing result from the electrolysis of **20** was the appearance of products attributable to the 1° distonic radical anion, **38**. Based on the results obtained from the electrolysis of 1-benzoyl-2,2-dimethylcyclopropane which resulted in exclusive formation of the 3° distonic radical anion, **37**, the appearance of **38** was unexpected, **Scheme 23**.[36,37]

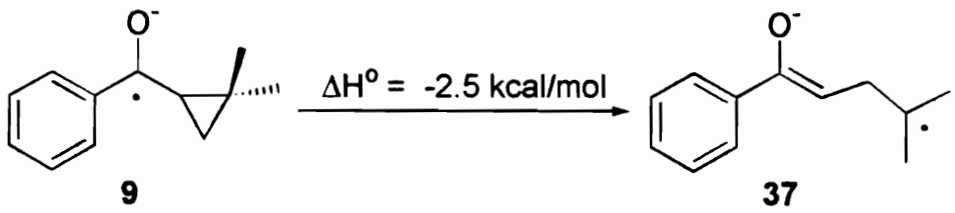


**9** **37**

**Scheme 23**

However, the Hammond postulate can be utilized to forward an explanation for the appearance of **38**.

The Hammond postulate implies that the transition state of a highly exothermic reaction will resemble reactants (an early transition state). As the exothermicity of the reaction is reduced the location of the transition state will change accordingly until the transition state resembles products (a late transition state in the case of an endothermic process). In a reactant-like transition state, the stability of products will have little impact on the kinetics of the reactions occurring. In contrast, in a product-like transition state the stability of the products will directly influence the kinetics involved in their production.

The enthalpy for ring opening to the 3° distonic radical anion, **37**, from **9** is slightly exothermic at -2.5 kcal/mol.[36,37] We can, therefore, infer that product formation occurs through an early (reactant-like) transition state. However, the enthalpy of cyclopropyl ring opening resulting in **37** is much less exothermic than the enthalpy of cyclopropyl ring opening involved in the formation of radical anions **36** and **38**, -31.4 kcal/mol and -16.0 kcal/mol respectively. As a result, the transition state involved in the ring opening of **35** to **36** and **38** is much more reactant-like than the transition state involved in the formation of **37**, **Scheme 23**. Therefore, product stability will not play as large a role in the formation of **36** and **38** as it will in the formation of **37**. A direct result of the much earlier transition state in the cyclopropyl ring opening of **35** is formation of both the 1° and 3° distonic radical anions. Whereas, the much later transition transition state involved in the cyclopropyl ring opening of **9**, as compared to **35**, results in ring opening to the more stable tertiary distonic radical anion.

From the 9:1 ratio observed for the formation of **36** relative to **39**, it is clear that the placement of geminal dimethyl groups on the cyclopropyl ring provide an intermediate allowing a distinction between products as a result of a radical or nucleophilic pathway. Identification of the mechanism through which addition has occurred should be readily apparent based upon the regiochemistry of cyclopropyl ring opening, **Figure 22**.

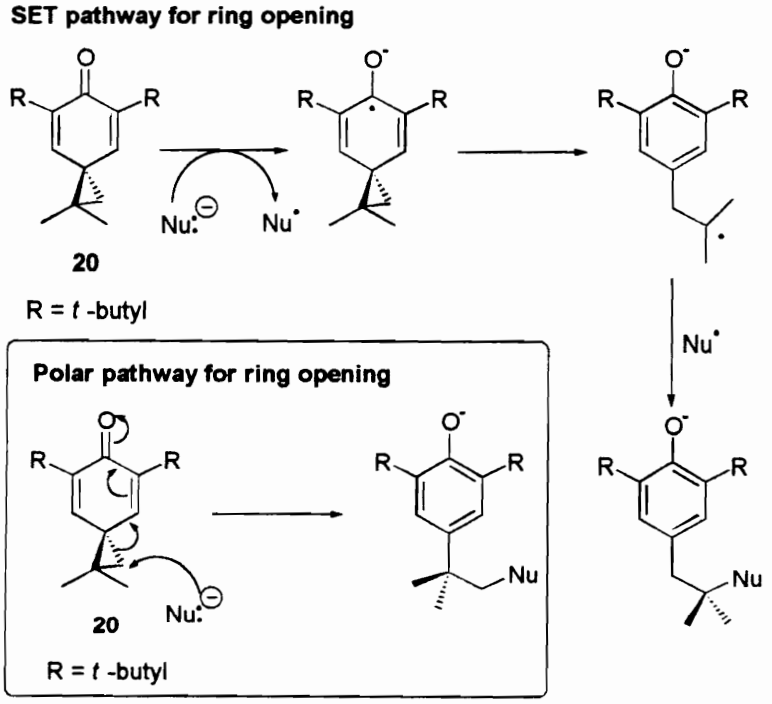


**Figure 22: Identification of SET based upon the regiochemistry of cyclopropyl ring opening of 20.**

# CONCLUSIONS

The one electron reduction of **20** proceeds through an EC mechanism in which the kinetics is governed by the electron transfer. The standard reduction potential of **20** has been estimated at -2.5 V vs. 0.1 m $Ag^+/Ag$, similar to that observed for other aromatic ketones and enones.[7,37,60] Cyclopropyl ring opening is a very facile process, $k_c \geq 10^7\ s^{-1}$, driven by both establishment of aromaticity and relief of cyclopropyl ring strain. A 9:1 ratio of the 3° vs. 1° distonic radical anion is observed in the cyclopropyl ring opening of radical anion **35**. Differentiation between radical and polar processes can therefore be determined based upon the regiochemistry of cyclopropyl ring opening.

## THE ELECTROCHEMICAL REDUCTION OF 1-METHYL-5,7-Di-*t*-BUTYLSPIRO[2,5]OCTA-4,7-DIEN-6-ONE (19).

The cyclic voltammetry of **19** was hampered by the same irreproducibility that was initially observed in the cyclic voltammetry of **20**. Unlike **20,** the experimental complications observed in the cyclic voltammetry of **19** have yet to be resolved. Initial investigations have indicated that the reduction potential of **19** is similar to that estimated for **20**. The peak widths are very broad, which could indicate rate limiting electron transfer, but the erratic nature of the voltammograms prevents any conclusions to be drawn.[59] However, mechanistic information concerning the decay of the radical anion generated from **19** was obtained from constant current electrolysis.

## ELECTROLYSIS OF 1-METHYL-5,7-Di-*t*-BUTYLSPIRO[2,5]OCTA-4,7-DIEN-6-ONE (19).

The electrolysis of **19** was expected to proceed in the same manner as that observed for the electrolysis of **20**. However, the energy difference between a 2° (*iso*-propyl radical) and a primary radical (ethyl radical) is ≅ 4.5 kcal/mol; therefore, the ratio of the 2° to 1° distonic radical anion is not expected to be as great as the 9:1 ratio observed for the 3° and 1° radical anions **36** and **38**, respectively.[54] Through the use of molecular orbital calculations (AM1 SCF-MO (DOUBLET)) the difference in the enthalpies for cyclopropyl ring opening resulting in the 2° and 1° distonic radical anions, was found to be ca -7 kcal/mol, whereas, the difference calculated for the enthalpies of cyclopropyl ring opening leading to **36** and **38** was found to be -15.4 kcal/mol. This suggests that the ratio of 2° to 1° distonic radical anions produced in the reduction of **19** will not be as great as the ratio of the 3° and 1° distonic radical anions produced in the reduction of **20**.

Constant current electrolysis of **19** was performed in anhydrous DMF employing 0.1 M *n*-$Bu_4NClO_4$ as the supporting electrolyte. The constant current electrolysis of **19** (1.5 $e^-$) resulted in the formation of three products, **46**, **47**, and **48** in an overall yield of 73%, **Scheme 24**.

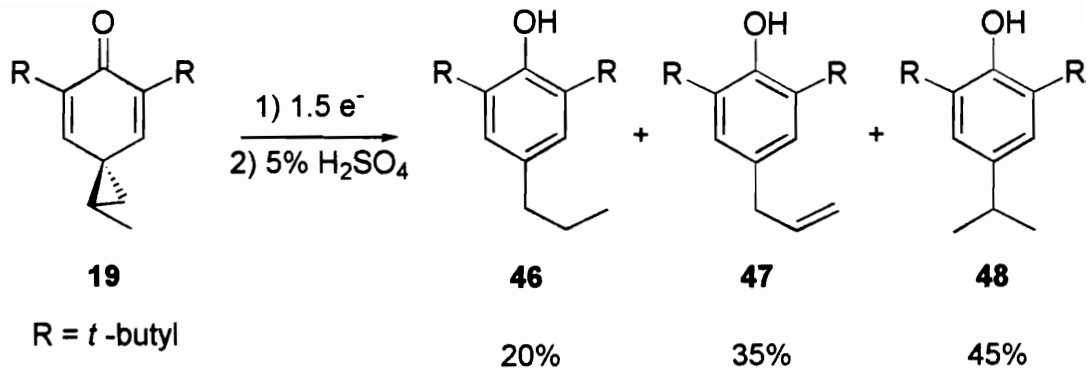


**Scheme 24**

A mechanism consistent with the formation of these products is shown in **Scheme 25**.

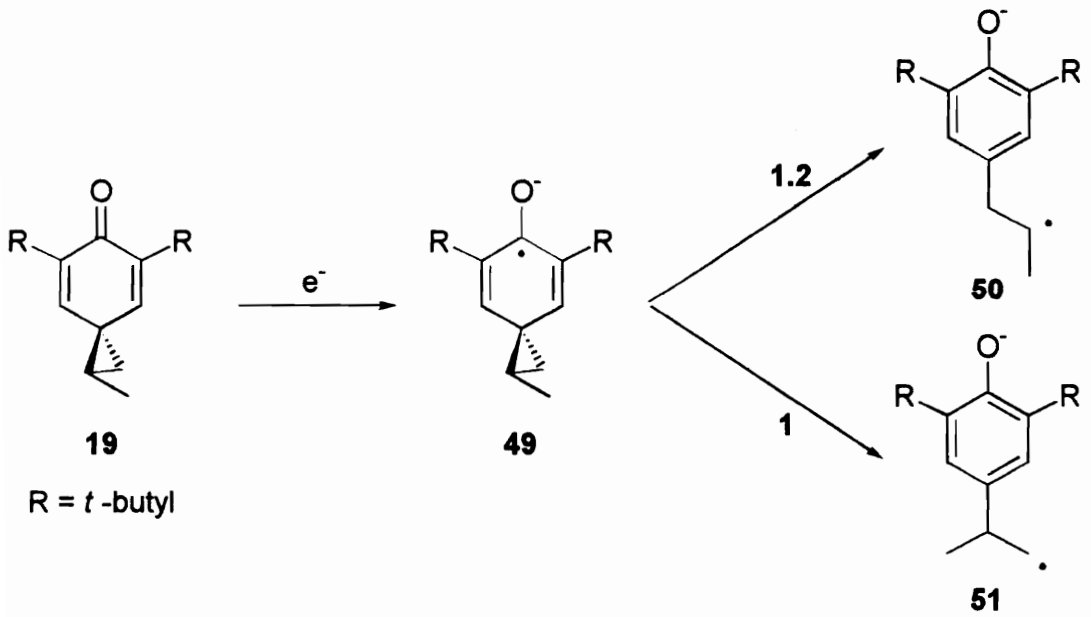


**Scheme 25**

One electron reduction of **19** results in the ring closed radical anion, **49**. The cyclopropyl ring closed radical anion of **19** ring opens in a 1.2:1 ratio to form the 2° distonic radical anion, **50**, and the 1° distonic radical anion, **51**. Product formation occurs via disproportionation reactions involving the ring opened radical anions resulting in the terminal alkene, **47**, **Scheme 26**.

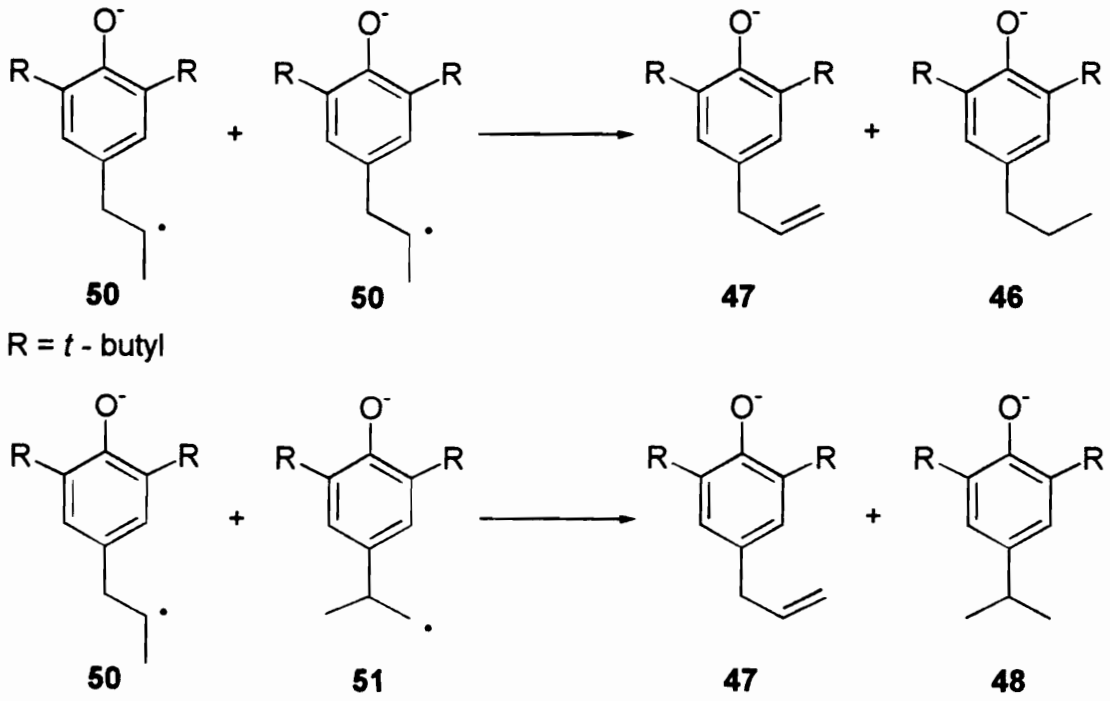


**Scheme 26**

Higher molecular weight products were obtained in the electrolysis. Their presence was initially observed using gas chromatography and high pressure liquid chromatography by their long retention times. These products were tentatively identified by $^1$H NMR as dimeric products derived from the radical anions produced during electrolysis. The concentration of the dimeric products increased as the concentration of **19** undergoing electrolysis was increased.

The exclusive formation of the terminal alkene in the electrolysis products was not surprising based on the behavior exhibited by **20**. The trans internal alkene was found to be 8.5 kcal/mol lower in energy than the terminal alkene. However, as in the radical anions generated from **20**, the geometry of the radical p-orbital is perpendicular to the $\pi$-system of the aromatic ring. Therefore, it is kinetically faster for the hydrogen abstraction to occur from the less hindered methyl substituent than hydrogen abstraction from the benzylic hydrogen, **Figure 23**.

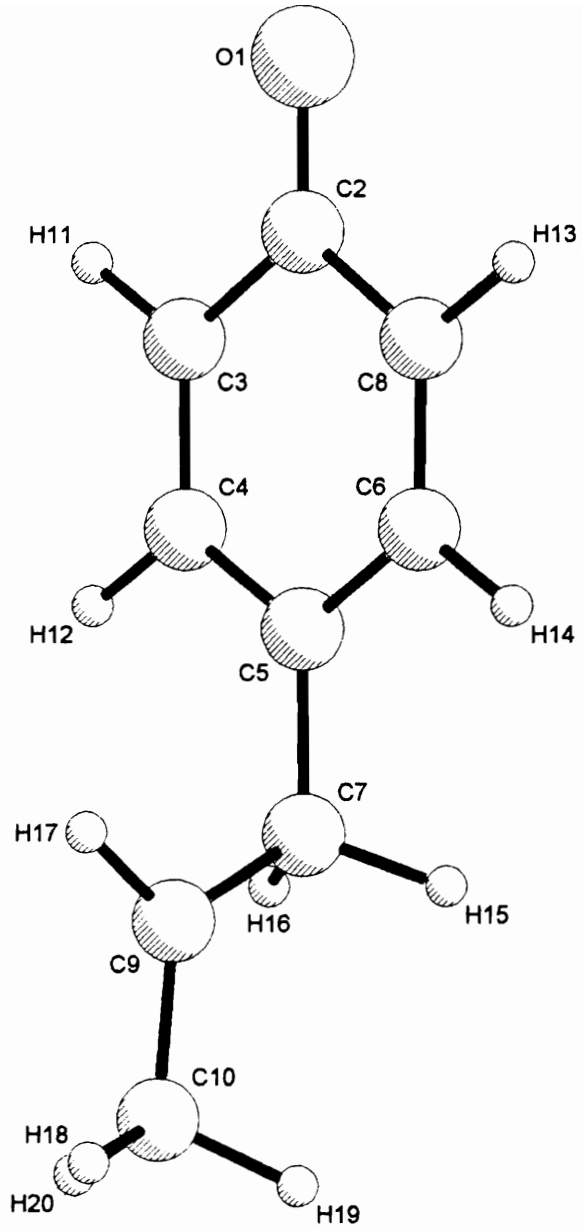


**Figure 23: Geometry of the 2° distonic radical anion, 50.**

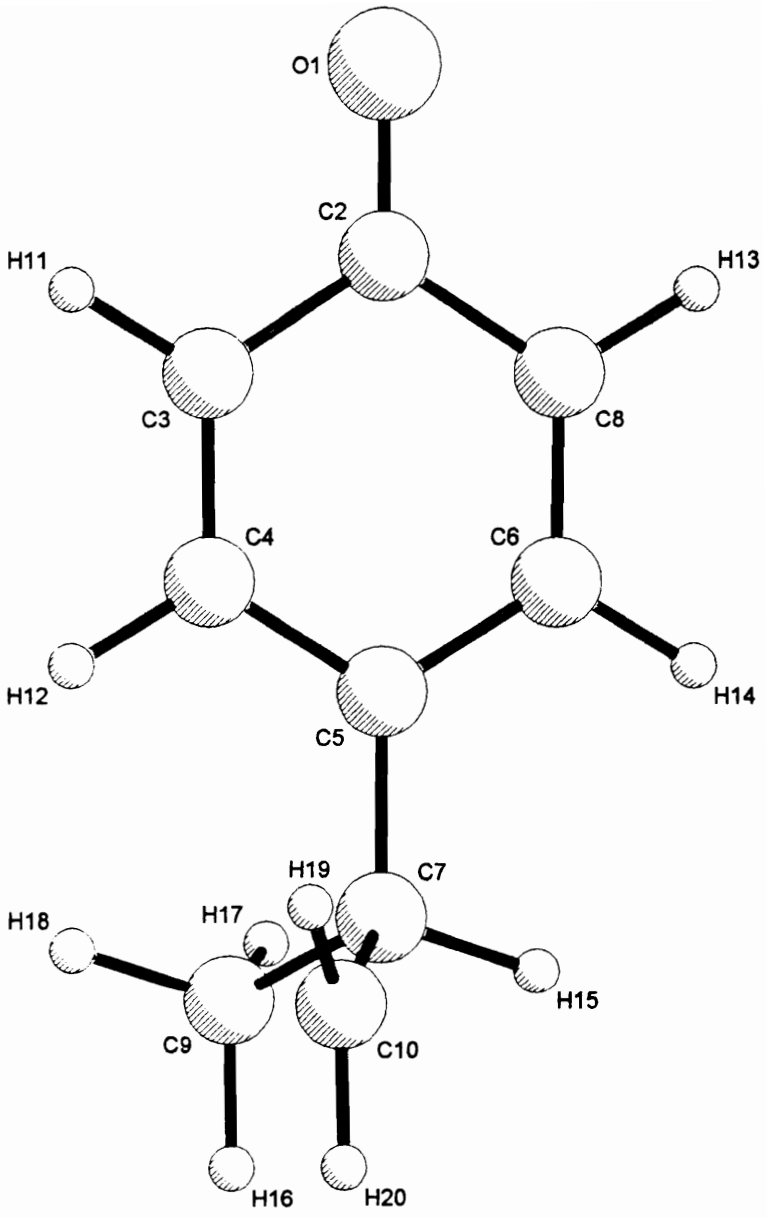


**Figure 24: Geometry of the 1° distonic radical ion, 52.**

The 1.2:1 ratio of radical anions **50** to **51**, **Figure 25**, which is much less than what was expected from molecular orbital calculations, is possibly due to the occurrence of an early transition state as observed in **20**. However, once the nature of the dimeric products become known, the ratio could increase.

While the ratio of radical anions generated from **19**, **Figure 25**, is not as large as that observed for radical anions generated from **20**, identification of SET is still possible based on the formation of the 2° radical anion, **50**. If a polar pathway were in operation, one would expect preferential addition of the nucleophile at the least hindered position of the cyclopropyl ring. As a result, the ratio of products from substitution at the 2° to 1° positions would be opposite to what would be observed in a radical process.

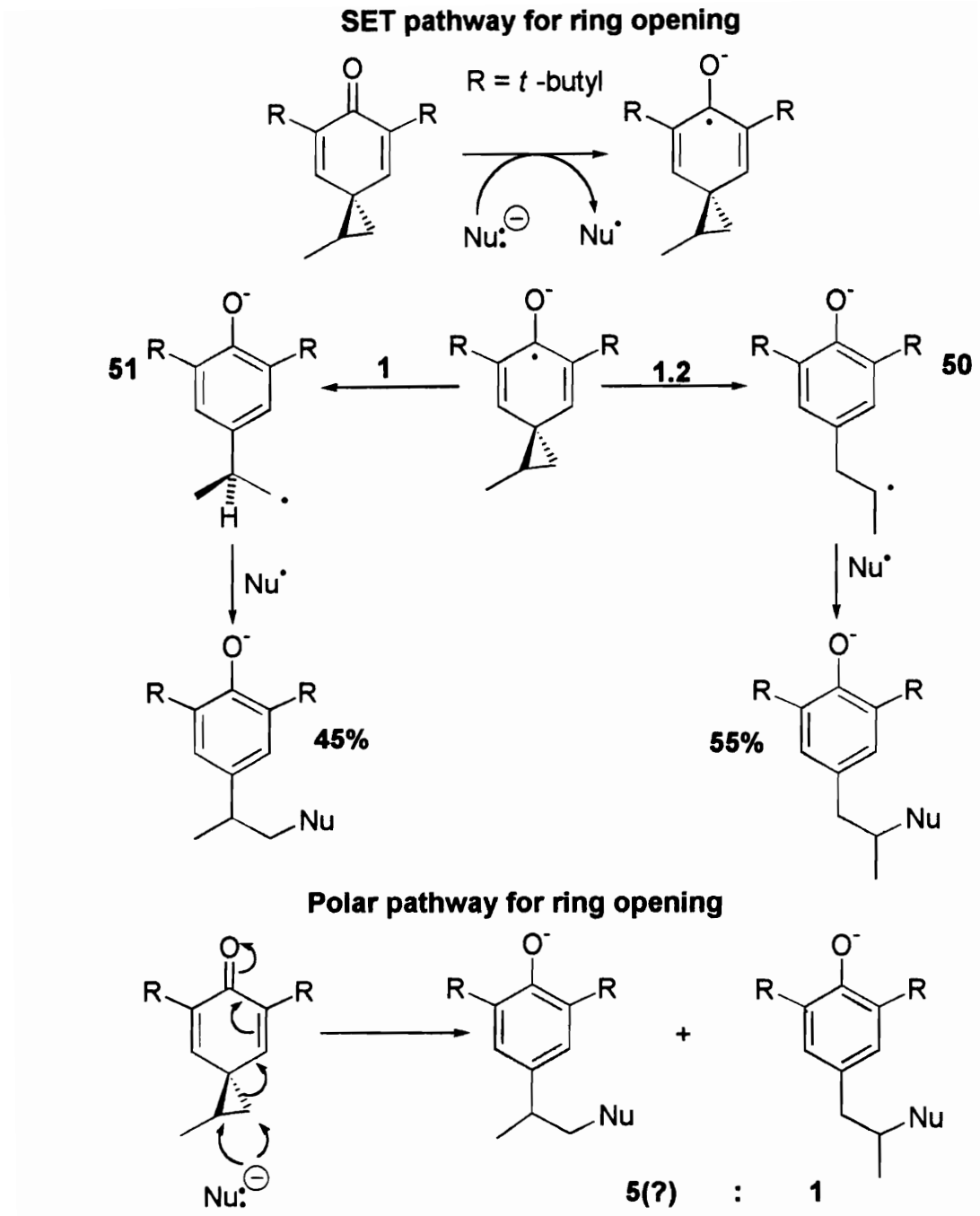


**Figure 25: Identification of SET based upon the regiochemistry of cyclopropyl ring opening of 19.**

The chiral nature of substrate **19** should also allow identification of SET derived products based upon the stereochemistry of such products obtained from an enantiomerically pure substrate, **Figure 26**.

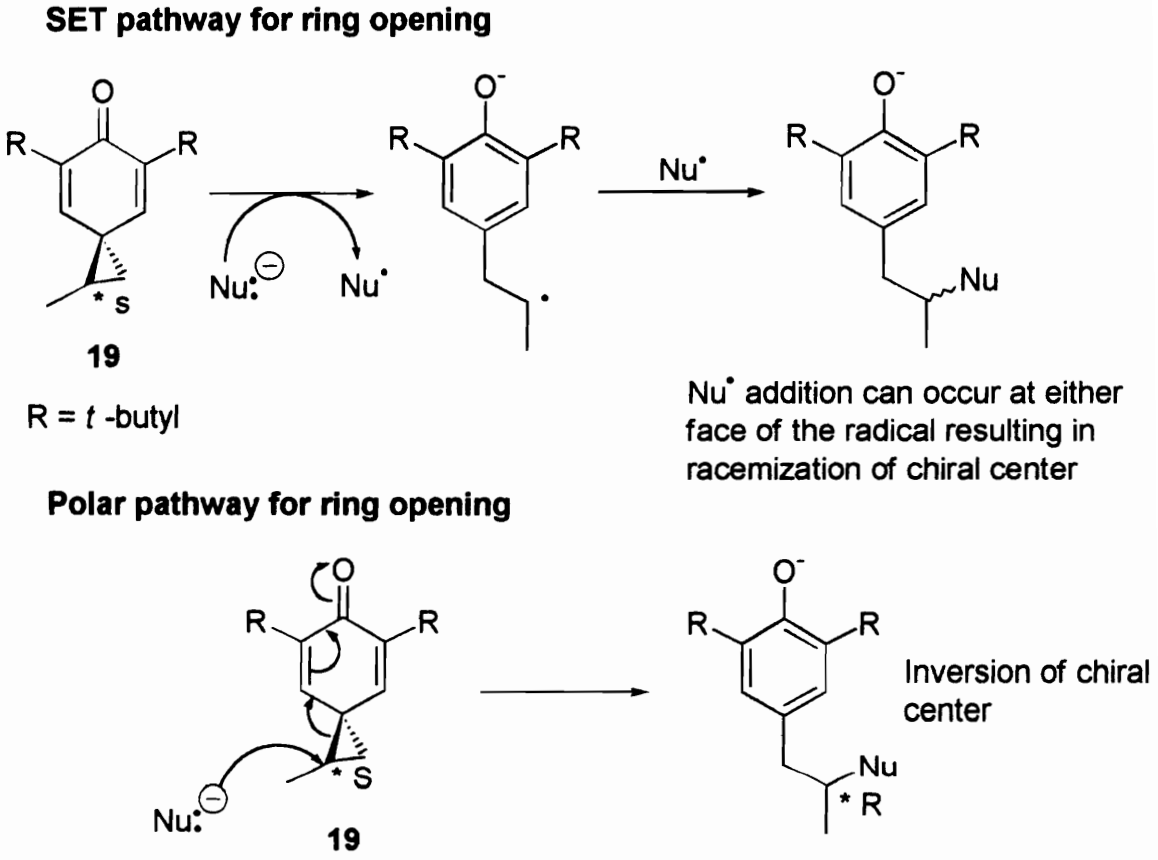


**Figure 26: Identification of SET based upon the stereochemistry of the reaction products.**

Reaction between enantiomerically pure **19** and reagents that proceed through a polar pathway for nucleophilic addition would result in an inversion of configuration at the

chiral center. Whereas, a radical process would result in scrambling of the stereochemistry. Therefore, **19** provides a means for identification of SET based upon the stereochemistry of the products ultimately produced.

# ELECTROCHEMICAL ANALYSIS OF EXO-METHYLENE CYCLOPROPYL KETONE

The cyclic voltammetry of exo-methylene cyclopropyl ketone, **52**, was much more straight forward than what was observed for the preceding substrates.

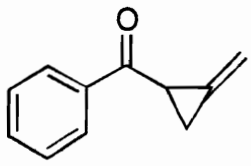

**52**

The experimental procedure utilized to obtain a voltammogram of **20** was utilized in the acquisition of the voltammetry data of **52**. Analyses were performed in anhydrous DMF employing 0.1 M *n*-$Bu_4NBF_4$ as the supporting electrolyte. A gold button was utilized as the working electrode. Electrode potentials were referenced to 0.1 M $Ag^+/Ag$.

The cyclic voltammetry of **52** was characterized by an irreversible reduction peak at -2.3 V and an irreversible oxidation peak at -0.8 V, **Figure 27**.

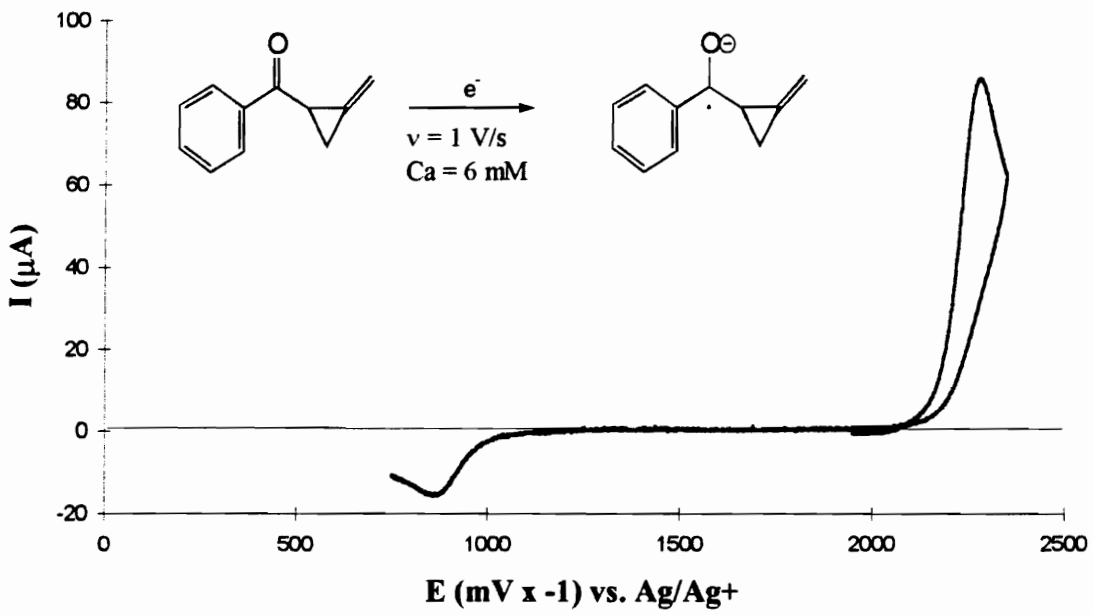


**Figure 27: Cyclic voltammogram of 52 at 1 V/s utilizing a gold working electrode in a 0.1 M solution of *n*-$Bu_4NBF_4$ in N,N-dimethylformamide.**

The peak width ($E_p$- $E_{p/2}$) was found to be 65 ± 3.5 mV. The peak width did not vary significantly with sweep rate. However, $E_{p,c}$ varied linearly with the sweep rate as shown by **Figure 28**.

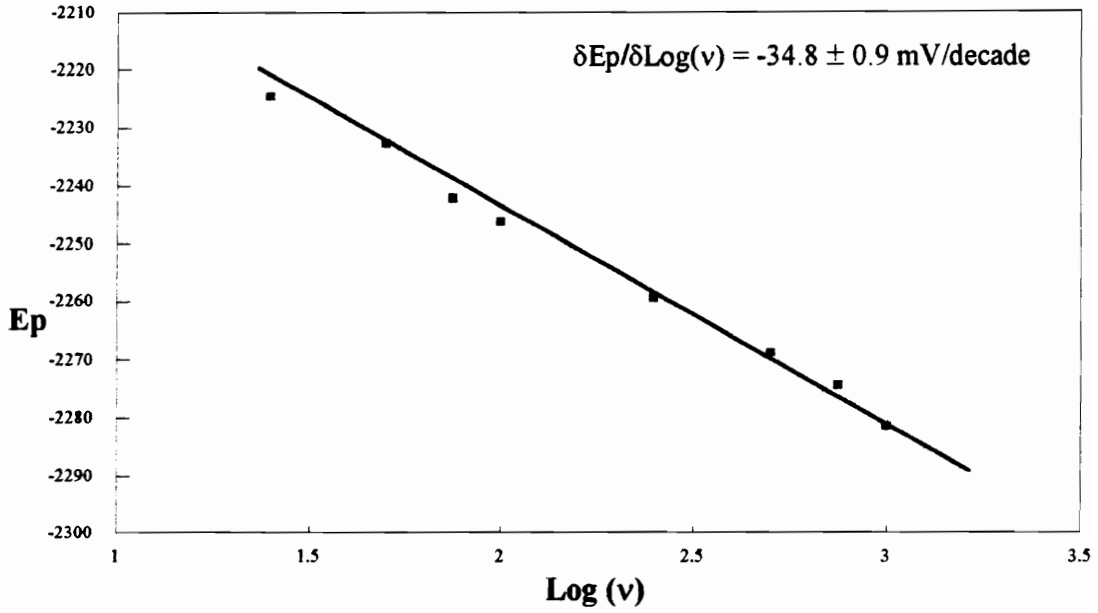


**Figure 28: Plot of $E_p$ vs. log(ν) for the reduction of 52.**

Similarity in the values from the theoretical response expected for an EC mechanism exhibiting a rate limiting chemical step and the experimental response exhibited by **52**, (**Table 5**), indicates that the decay of radical anion **52** is proceeding through an EC mechanism.

**Table 5: Comparison of voltammogram diagnostics for an EC mechanism exhibiting rate limiting $k_c$ to the experimental values obtained for 52.**

| | $E_{p/2} - E_p$ (mV) | $\delta E_p/\delta \log(\nu)$ (mV/decade) |
|---|---|---|
| Diagnostic Values | 59.2 | -29.5 |
| Experimental Values | 65 ± 3.5 | -34.8 ± 0.9 |

As a result, LSV could be utilized to determine the rate law for radical anion decay.

Having previously determined the slope from a plot of $\delta E_p/\delta \log v$, only the slope from a plot of $E_p$ vs. $\log(C_X)$ (where $C_x$ is the concentration of the substrate to be reduced) was needed in order to determine the rate law for the decay of the radical anion generated from **52**, **Figure 29**.

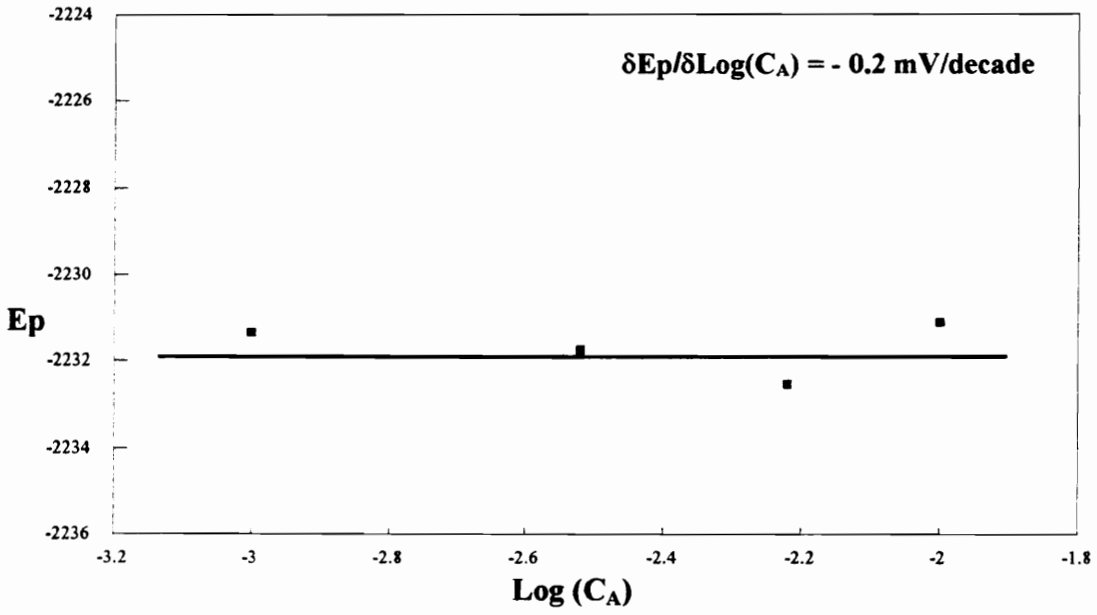


**Figure 29: Plot of $E_p$ vs. Log $C_A$.**

Once the slopes of $\delta E_p/\delta \log(C_X)$ and $\delta E_p/\delta \log v$ were determined, the reaction order of A and B was determined using **Equations 23** and **24** respectively.

**Eqn. 23**

$$R_B = \frac{\left(59.2\ \text{mV/decade}\right)}{\left(\frac{\delta E_p}{\delta \log v}\right)} + 1 = \frac{\left(59.2\ \text{mV/decade}\right)}{\left(-33.5\ \text{mV/decade}\right)} + 1 = -1.767 + 1 = -0.767$$

**Eqn. 24**

$$\left(\left(\left(\frac{\left(\frac{\delta E_p}{\delta \log(C_A)}\right)(b+1)}{59.2\ \text{mV}}\right) + 1\right)\right) - R_B = R_A = \left(\left(\frac{-0.2\,(0.8+1)}{59.2\ \text{mV}}\right) + 1\right) + 0.8 = -0.2$$

A comparison of the experimental values observed to the first and second order rate laws available for decay of the radical anion generated from **52**, indicates that the rate of decay of the radical anion generated shows a first order dependence only on the concentration of the radical anion, **Table 6**, rate = $k_{obs}[B]$.

**Table 6: Comparison of experimental values to the theoretical response exhibited for first and second order rate laws.**

| Rate Law | $\delta E_p/\delta \log v$ (mV/decade) | $\delta E_p/\delta \log C_A$ (mV/decade) | Reaction order in B | Reaction order in A |
|---|---|---|---|---|
| k[B] | -29.5 | 0 | 1 | 0 |
| $k[B]^2$ | -19.7 | 19.7 | 2 | 0 |
| k[A][B] | -29.5 | 29.5 | 1 | 1 |
| Experimental | -34.8 | -0.2 | 0.8 | 0.2 |

Therefore, radical anion decay is likely the result of cyclopropyl ring opening. Confirmation of this hypothesis was afforded through electrolysis of **52**.

The constant current electrolysis (1e$^-$) of **52** was performed by Yonghui Wang in anhydrous DMF employing 0.1 M *n*-$Bu_4NClO_4$ as supporting electrolyte and utilizing a gold electrode as the working electrode.[61] The electrolysis resulted in two major products, **53** and **54**, in 49% and 18% yields, respectively, **Scheme 27**.

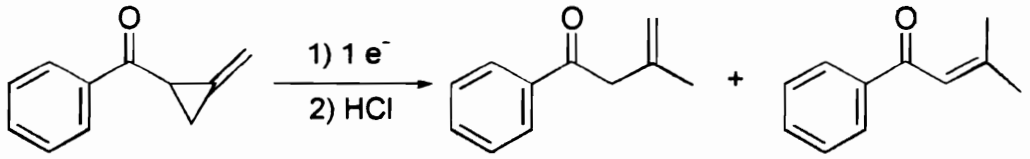


**52** **53** 49% **54** 18%

**Scheme 27**

A mechanism consistent with the formation of these products is shown in **Scheme 28**.

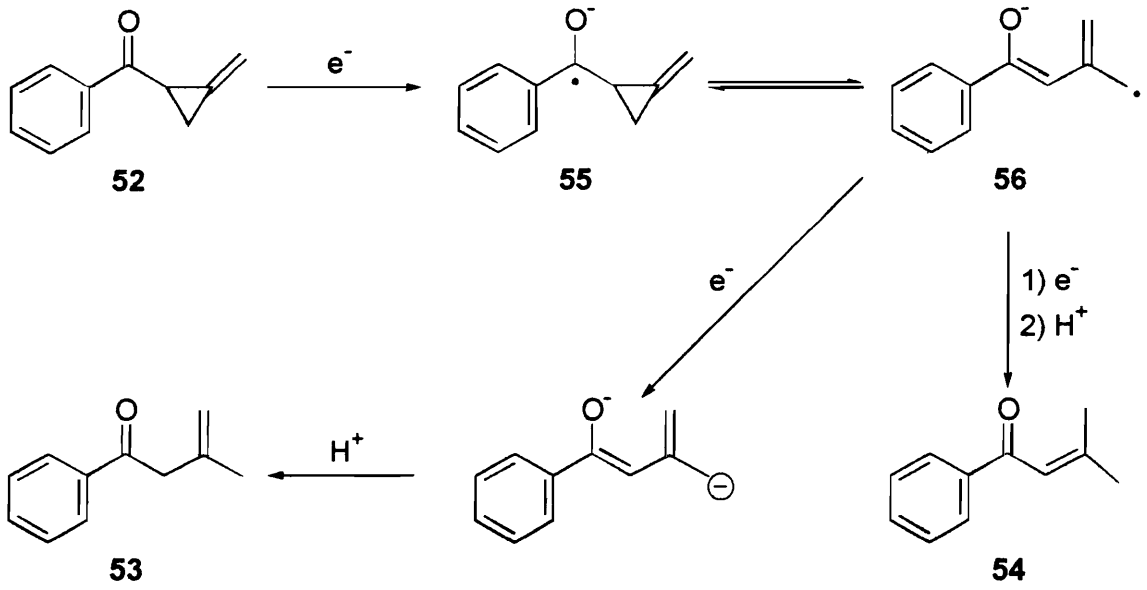


**Scheme 28**

The one-electron reduction of **52** results in formation of intermediate radical anion **55**. Radical anion **55** then undergoes cyclopropyl ring opening to the allylic distonic radical anion, **56**. Further one-electron reduction of **56** to the dianion leads to **53** and **54** after acidification. Product formation is solely dependent upon the rate of cyclopropyl ring opening, consistent with the rate law observed in the LSV investigation.

# CONCLUSIONS

The cyclic voltammetry of **52** is characterized by an irreversible reduction wave at -2.3 V and an irreversible oxidation wave at -0.8 V vs. 0.1 M $Ag^+/Ag$. The one electron reduction of **52** proceeds through an EC mechanism exhibiting rate limiting $k_c$. Reaction order evaluation of the voltammograms indicated that the rate of radical anion decay exhibited a first order dependence on the concentration of the radical anion, rate = $k_{obs}[B]$. Confirmation of this rate law was afforded through electrolysis of **52**.

# CHAPTER 3. THE UTILIZATION OF 1,1-DIMETHYL-5,7-DI-*t*-BUTYLSPIRO[2,5]OCTA-4,7-DIEN-6-ONE AS A PROBE FOR THE DETECTION OF SINGLE ELECTRON TRANSFER IN REACTIONS WITH ORGANOMETALLIC REAGENTS.

## INTRODUCTION

Of the substrates analyzed electrochemically, **20** emerged as the strongest candidate for the detection of SET in the reactions of carbonyl compounds with nucleophiles. The cyclopropyl ring opening of the radical anion derived from **20** is facilitated by the establishment of resonance upon relief of cyclopropyl ring strain. As a result, the cyclopropyl ring opening of **20** is very facile and is estimated to occur at $k \geq 10^7$ $s^{-1}$, several orders of magnitude faster than the rate constants observed for cyclopropyl ring opening of aryl cyclopropyl ketones.[36,37] Moreover, because the radical anion rearranges preferentially to the 3° rather than the 1° distonic radical anion (in a 9:1 ratio), we believed that the identification of SET might be achieved based upon the regiochemistry of cyclopropyl ring opening. Based on the electrochemical data, we felt that **20** was a much better probe for the detection of SET than any of the previous substrates described in the literature. In order to test this hypothesis we began a study to investigate the reactivity of **20** with nucleophiles which have been shown to undergo SET with carbonyl compounds.

A large amount of literature exists providing evidence that some component of SET is responsible for the addition of Grignard reagents and alkyllithium reagents to aryl ketones and enones. The reduction potential of **20** is estimated at -2.5 V vs. 0.1 M $Ag^+/Ag$, similar to the reduction potential observed for aryl ketones and enones. If electron transfer is occurring, **20** should exhibit behavior similar to that observed in the reactions of aryl ketones with these reagents.[7,36,37,38] Therefore, the effectiveness of **20** in detecting SET will be established through reactivity studies involving Grignard reagents and alkyllithium.

Little doubt exists to the ability of Grignard reagents and alkyllithiums to undergo SET with carbonyl compounds. However, the occurrence of SET in the reactions of l lithium dialkylcuprates with carbonyl compounds has not been fully established. Therefore, we felt that once we had determined the effectiveness of **20** in differentiating between polar and SET processes, we could use **20** to establish the nature of the process involved in the nucleophilic addition of cuprates to carbonyl compounds

Initial indication of radical intermediates in the reaction of organolithiums and Grignard reagents with ketones and enones resulted from the identification of reaction products that could only be a result of a radical intermediate (e.g. radical coupling and reduction products).[62] Direct observation of the paramagnetic intermediates present in the reactions of organometallic reagents with carbonyl compounds has been provided through ESR spectroscopy.[63] ESR spectroscopy has been used extensively to verify the presence of radical intermediates in the reactions of Grignard reagents with carbonyl compounds, and to provide a means for determination of their structure. Through the use of ESR

spectroscopy and UV-VIS spectrophotometry the rate of decay for a number of paramagnetic intermediates involved in the reactions of Grignard reagents to carbonyl compounds has been determined.[63] Although ESR provides a means of observing and characterizing a paramagnetic intermediate generated during the reaction of a organometallic reagent with a carbonyl compound, verification that the pathway involving the paramagnetic intermediate, as opposed to a polar pathway, is responsible for the observed products can not be accomplished.

A number of other methods have been employed in an attempt to demonstrate the radical intermediates present in reactions of organometallic reagents with carbonyl compounds are responsible for the observed products. The more successful of these methods include kinetic isotope effect studies,[64] radical trapping,[65] isomerization probes,[66] fragmentation probes,[67] and rearrangement probes.[68] Each of these methods have been able to provide some evidence for SET in the reaction of organometallic reagents with ketones. However, the most intensive work in the investigation of SET in the reactions of organometallic reagents to ketones has occurred through the use of rearrangement probes based on the $\Delta^5$-hexenyl $\rightarrow$ cyclopentylcarbinyl radical rearrangement.

SET probes based upon the $\Delta^5$-hexenyl radical rearrangement have provided a plethora of information pertaining to the mechanism of nucleophilic addition of Grignard reagents to carbonyl compounds. Through the use of $\Delta^5$-hexenyl radical rearrangement probes, the SET mechanism of Grignard reagent addition to carbonyl compounds has been

thoroughly characterized. Moreover, Ashby and coworkers have shown that primary Grignard reagents are capable of undergoing SET reactions with aryl ketones.[22,23]

Formation of products can occur by two pathways in the SET mechanism of nucleophilic addition to carbonyl compounds: (1) coupling of the geminate radical/ radical anion pair in the solvent cage immediately after electron transfer or (2) coupling of the intermediates after they have diffused from the solvent cage (via a diffusive radical/radical anion pair), **Scheme 29**.[23]

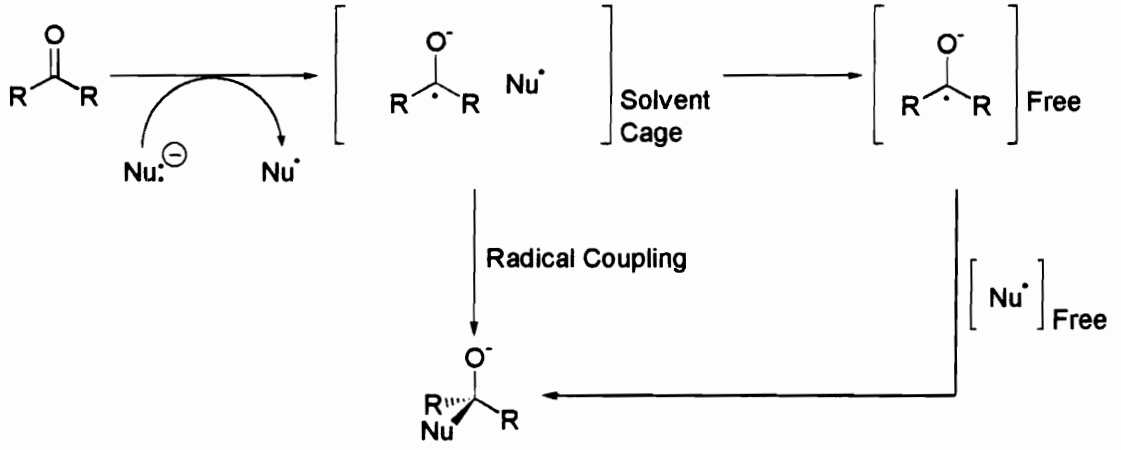


**Scheme 29**

In the reaction of 1,1-dimethyl-5-hexenyl magnesium chloride with benzil, Holm was able to differentiate between those products resulting from addition in the solvent cage to those resulting from diffusion from the solvent cage.[24] Moreover, the rate of rearrangement of the $\Delta^5$-hexenyl radical allowed an estimate of $10^{-9}$ s for the lifetime of the solvent cage in

the reactions of 2,2-dimethyl-5-hexenyl magnesium chloride with benzophenone.[26] The use of the $\Delta^5$-hexenyl radical rearrangement has provided key mechanistic information into the reactions of Grignard reagents with carbonyl compounds.

Aryl cyclopropyl ketones have been utilized extensively for the detection of SET in the reaction of organometallic reagents with carbonyl compounds. However previous studies have indicated that aryl cyclopropyl ketones substituted with only H or alkyl groups are ineffective in identifying SET.[36,37] Reactions of cyclopropyl phenyl ketone with organolithium and Grignard reagents resulted in only 1,2 addition products.[69,70] Similar reactions involving lithium dialkylcuprates resulted in a small quantity of cyclopropyl ring opened products, however, results from this study indicated that lithium dimethylcuprate was adding via a polar process, **Figure 30**.[7]

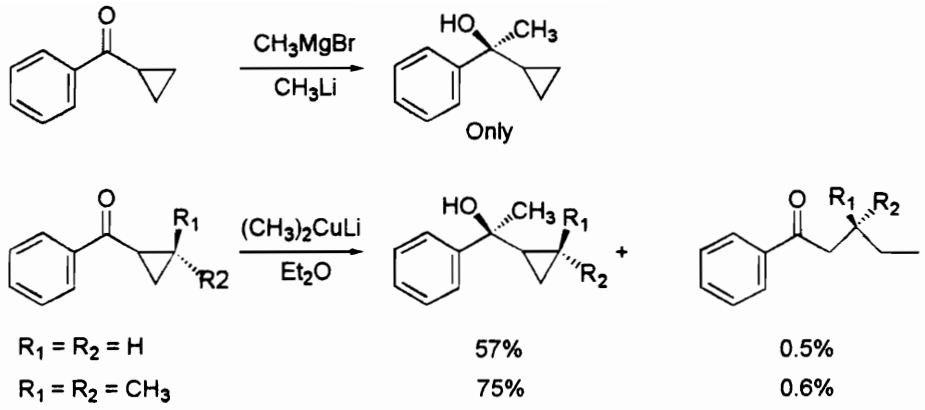


**Figure 30: Reactions of Grignard reagents, organolithiums, and lithium dimethylcuprate with cyclopropyl phenyl ketone.**

While the reaction of lithium dimethylcuprate results in cyclopropyl ring opening with 1-benzoyl-2-vinylcyclopropane, nucleophilic addition occurs across the double bond. As a result, this substrate can not differentiate between a polar and a SET process.[71] The reversibility of the ring opening of 1-benzoyl-2-phenylcyclopropane prohibits its utilization as a SET probe.[39]

Based upon the available literature supporting SET in the reactions of Grignard reagents and alkyllithiums with carbonyl compounds, we felt that the reaction of **20** with these reagents would provide a direct measure of it's ability to detect SET. Therefore, we decided to react **20** with methylmagnesium bromide and methyllithium to determine it's effectiveness in the identification of SET in these reactions. Once we had established the effectiveness of **20** to detect SET, we would then react **20** with lithium dimethylcuprate to determine if nucleophilic addition was occurring through a SET mechanism.

## REACTION OF 1,1-DIMETHYL-5,7-DI-*t*-BUTYLSPIRO[2,5]OCTA-4,7-DIEN-6-ONE (20) WITH METHYLMAGNESIUM BROMIDE

The reaction of **20** with MeMgBr was performed in anhydrous THF at 0° C. After a 2 hour reaction time all of the starting material was consumed. In all 7 products were obtained, two of which obtained in a 39% yield can be ascribed to hydrolysis of unreacted starting material to the corresponding 1° and 3° alcohols. However, products were obtained as a result of nucleophilic addition to **20** in an overall yield of 61%. The relative yields and structures of these products are shown in **Scheme 30**.

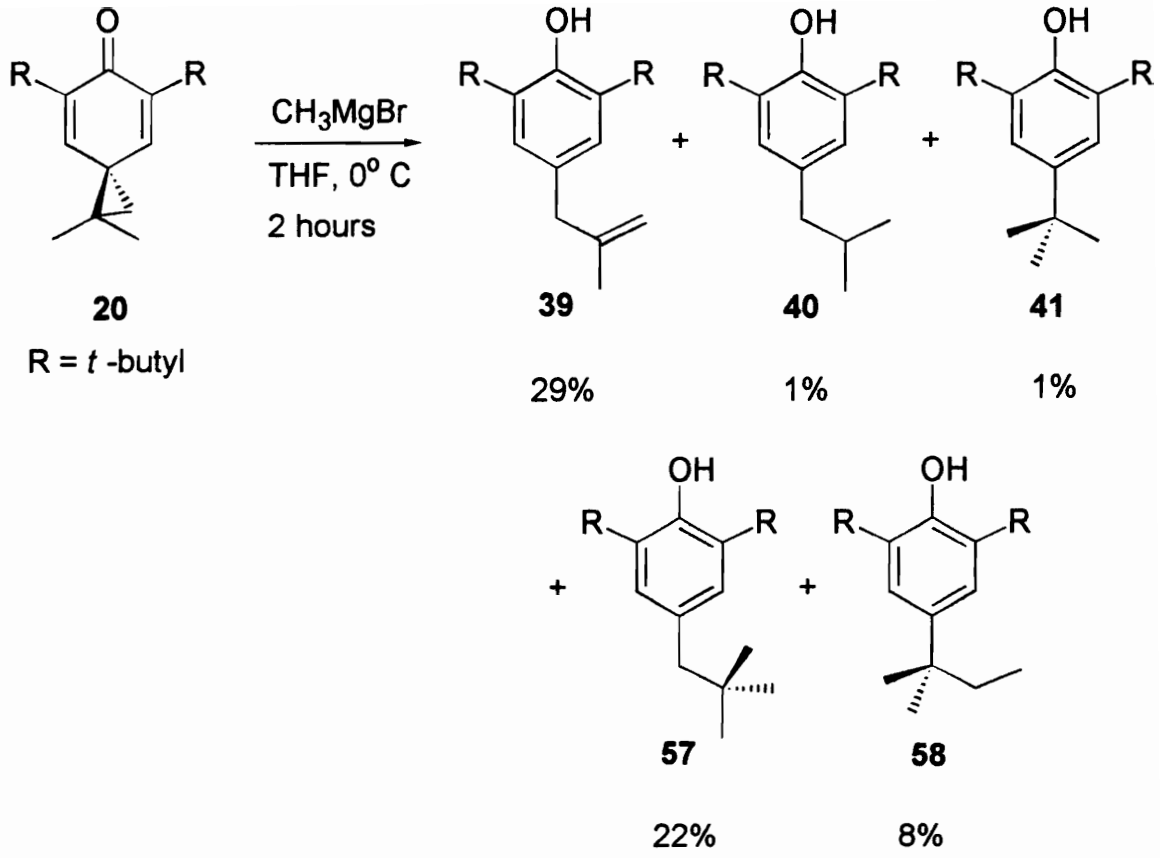


**Scheme 30**

Products resulting from a 1,2 addition to the carbonyl carbon were notably absent. Three of the observed products **40**, **41**, and **57**, formed in a combined yield of 39% are unequivocally the result of a SET mechanism, **Scheme 31**.

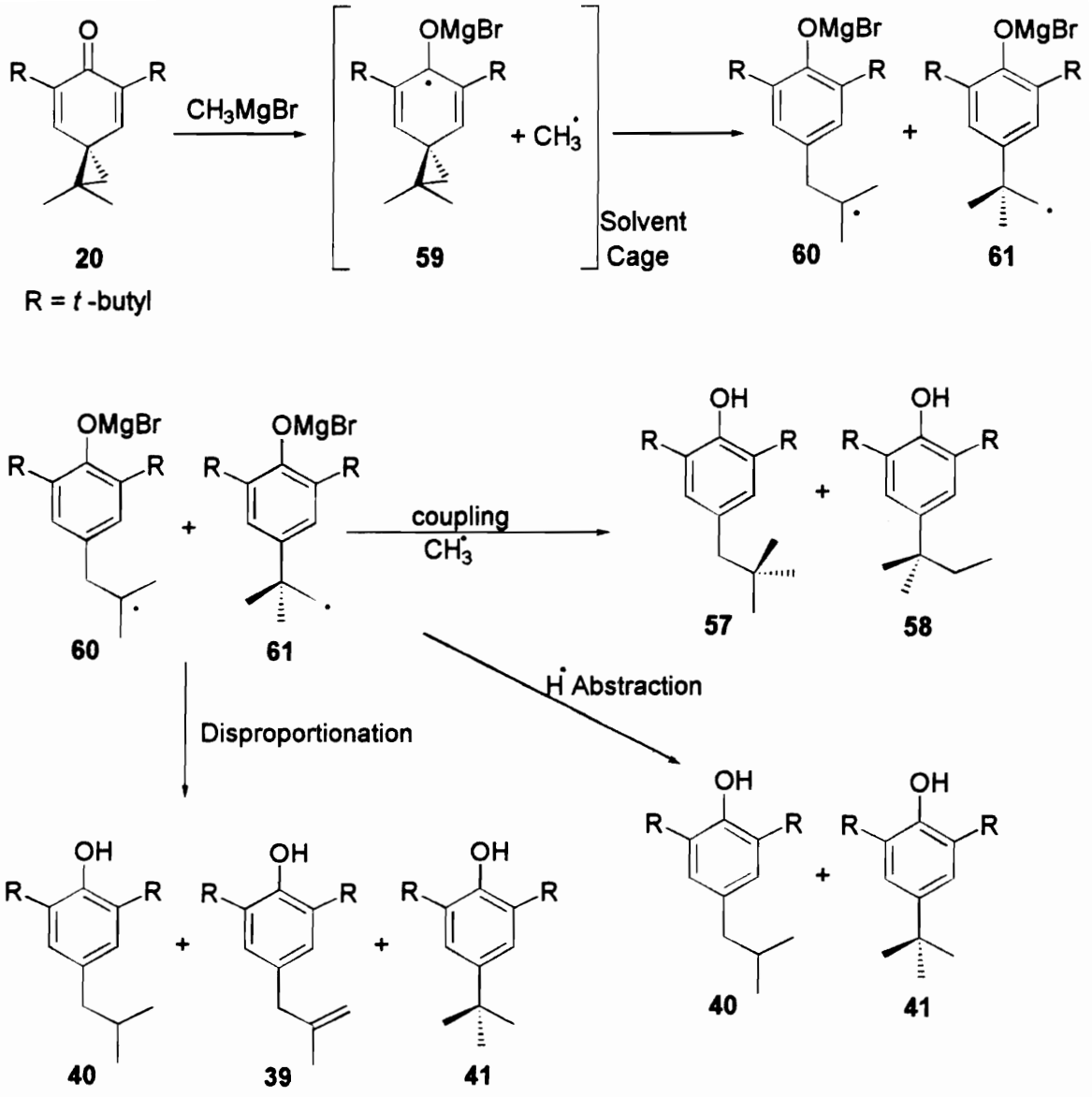
O
R
R
CH3MgBr
OMgBr
+ CH3
Solvent
Cage
20
R = t -butyl
59
60
61
coupling
CH3
57
58
H Abstraction
Disproportionation
40
39
41

**Scheme 31**

Electron transfer from MeMgBr to **20** results in the magnesium ketyl radical, **59**, which then undergoes ring opening to the 1° and 3° distonic radicals, **61** and **60** respectively. Radical coupling can then occur between $CH_3$· and **60** and **61** to give **57** and **59** respectively. This process can either occur in the solvent cage or after diffusion from the solvent cage. The appearance of reduction products **40** and **41** was interesting and somewhat unexpected because a study by Holm has suggested that C-C bonding occurs during electron transfer in the reactions between methylmagnesium bromide and benzophenone.[72] If partial C-C bonding occurs during electron transfer in the reaction of **20** with methylmagnesium bromide, then only **57** and **58** should be formed. The appearance of **40** and **41** in the product mixture suggests that C-C bonding is not occurring in the transition state. As a result, **60** and **61** are able to dispropotionate and/or abstract hydrogen atoms from solvent before radical coupling can occur, **Figure 31**.

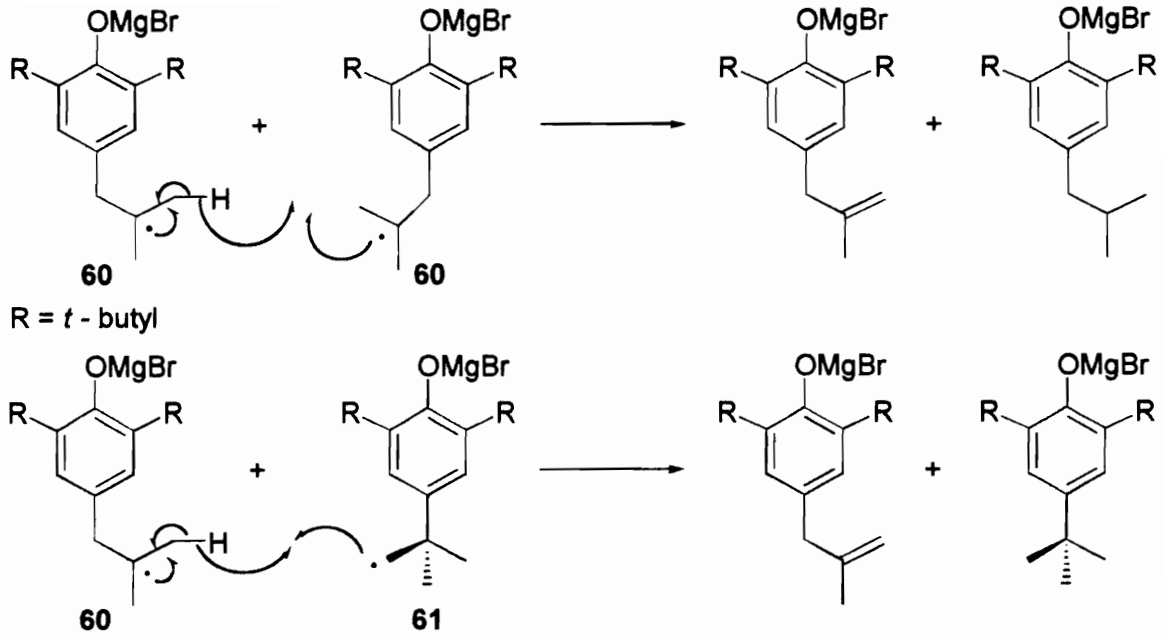


**Figure 31: Disproportionation reactions of 60 and 61.**

The formation of **39** can be ascribed to disproportionation reactions, however, an $E_2$ elimination reaction can not be discounted as an alternative mechanism. The viability of the $E_2$ pathway was established by showing that reaction of **20** with sodium hydride resulted in a quantitative yield of **39**, **Figure 32**.

**$E_2$ elimination with $CH_3MgBr$**

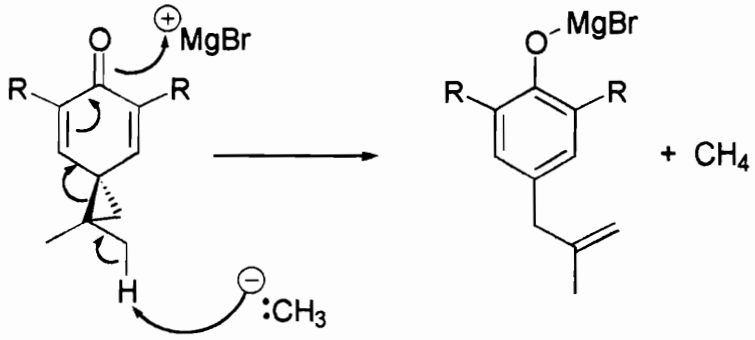


**$E_2$ elimination with NaH**

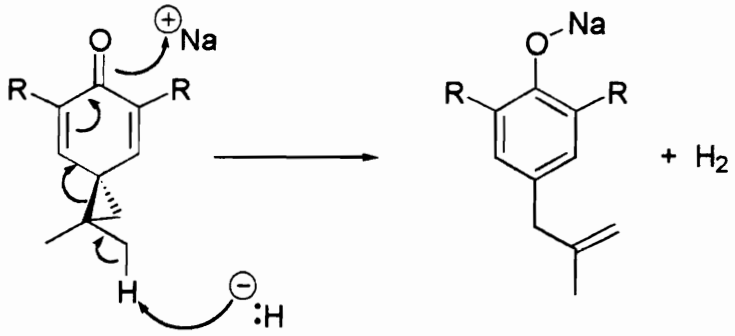


**Figure 32: $E_2$ elimination reaction of 20 with NaH and MeMgBr.**

On the basis of the electrochemical data, a 9:1 ratio of the 3° to 1° distonic radical anions was expected; however, a 6:1 ratio was produced. Since it is not known how the coordination of the counterion might affect the selectivity of ring opening, it is possible that **58** is produced as a result of SET. However, a direct $S_N2$ substitution reaction can not be discounted as an alternative mechanism for the production of **58**, **Scheme 32**.

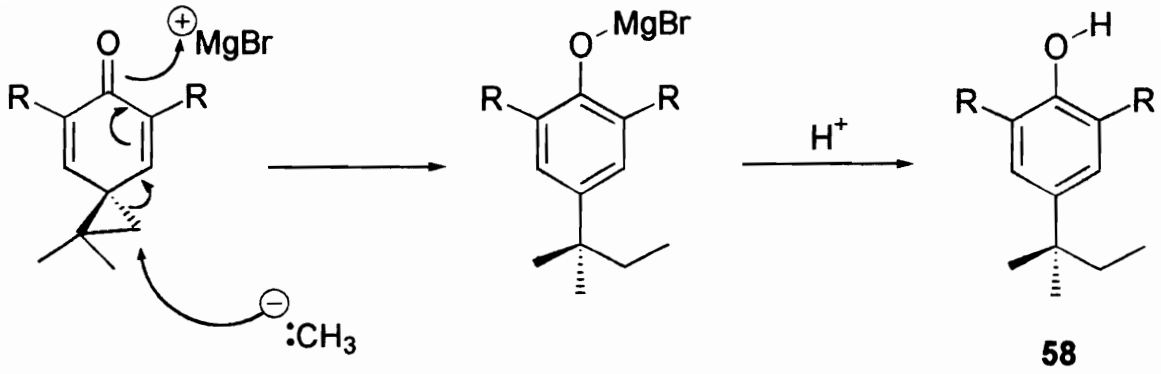


**Scheme 32**

These results confirm the importance of SET in the reaction of MeMgBr with **20**. In addition, the propensity for $CH_3\cdot$ radical coupling to the most-hindered carbon, support the hypothesis that the occurrence of SET in the reactions of **20** can be ascertained based upon the regiochemistry of cyclopropyl ring opening.

## REACTION OF 1,1-DIMETHYL-5,7-DI-*t*-BUTYLSPIRO[2,5]OCTA-4,7-DIEN-6-ONE WITH METHYLLITHIUM

The reaction of **20** with methyllithium in anhydrous THF at 0° C for 20 hours resulted in a 74% recovery of starting material based on the appearance of the 1° and 3° alcohols, and two nucleophilic addition products in an overall combined yield of 26%, **Scheme 33**.

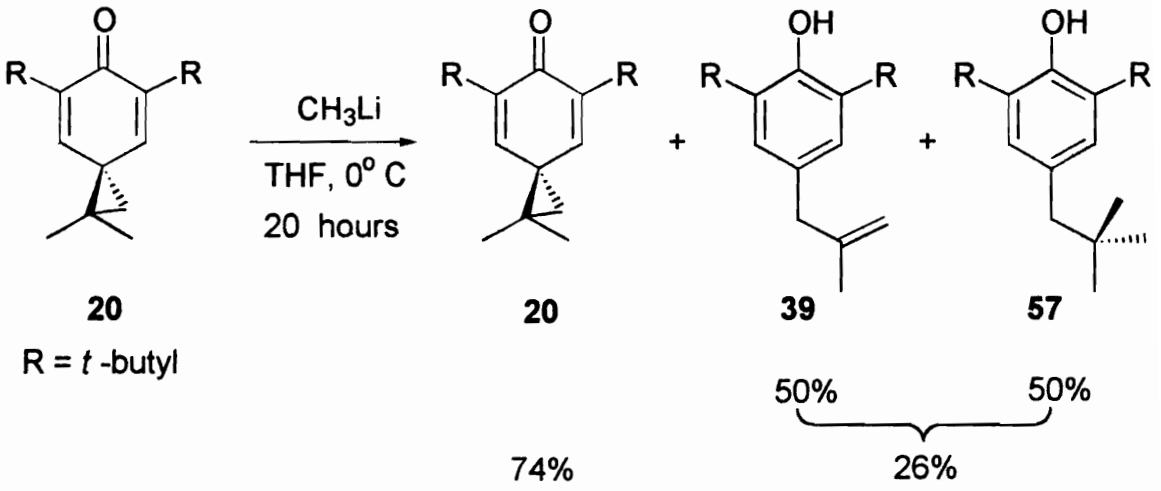


**Scheme 33**

Again, 1,2 addition products were not observed in the reaction. The appearance of **57** is clearly the result of SET between methyllithium and **20**. The absence of products resulting from disproportionation reactions, **40** and **41**, strongly suggests that the formation of **39** is the result of an $E_2$ elimination reaction between **20** and methyllithium,

**Figure 33**. However, **39** could be a result of disproportionation between $CH_3^{\cdot}$ and **60**, **Figure 34**.

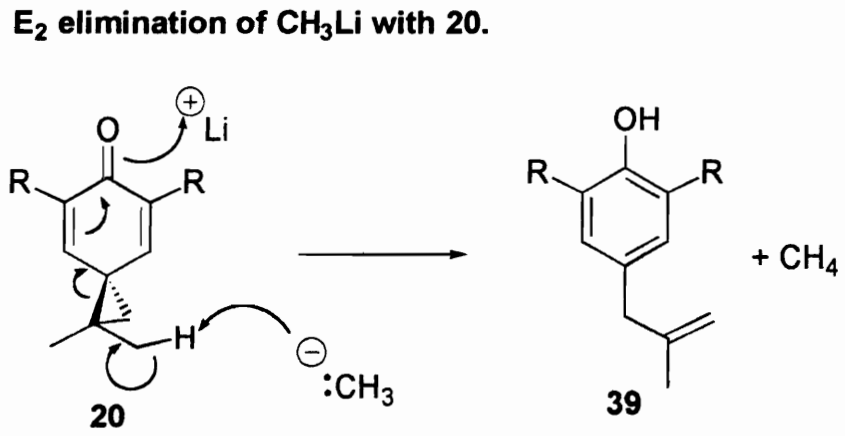


**Figure 33: $E_2$ elimination reaction of 20 with methyllithium.**

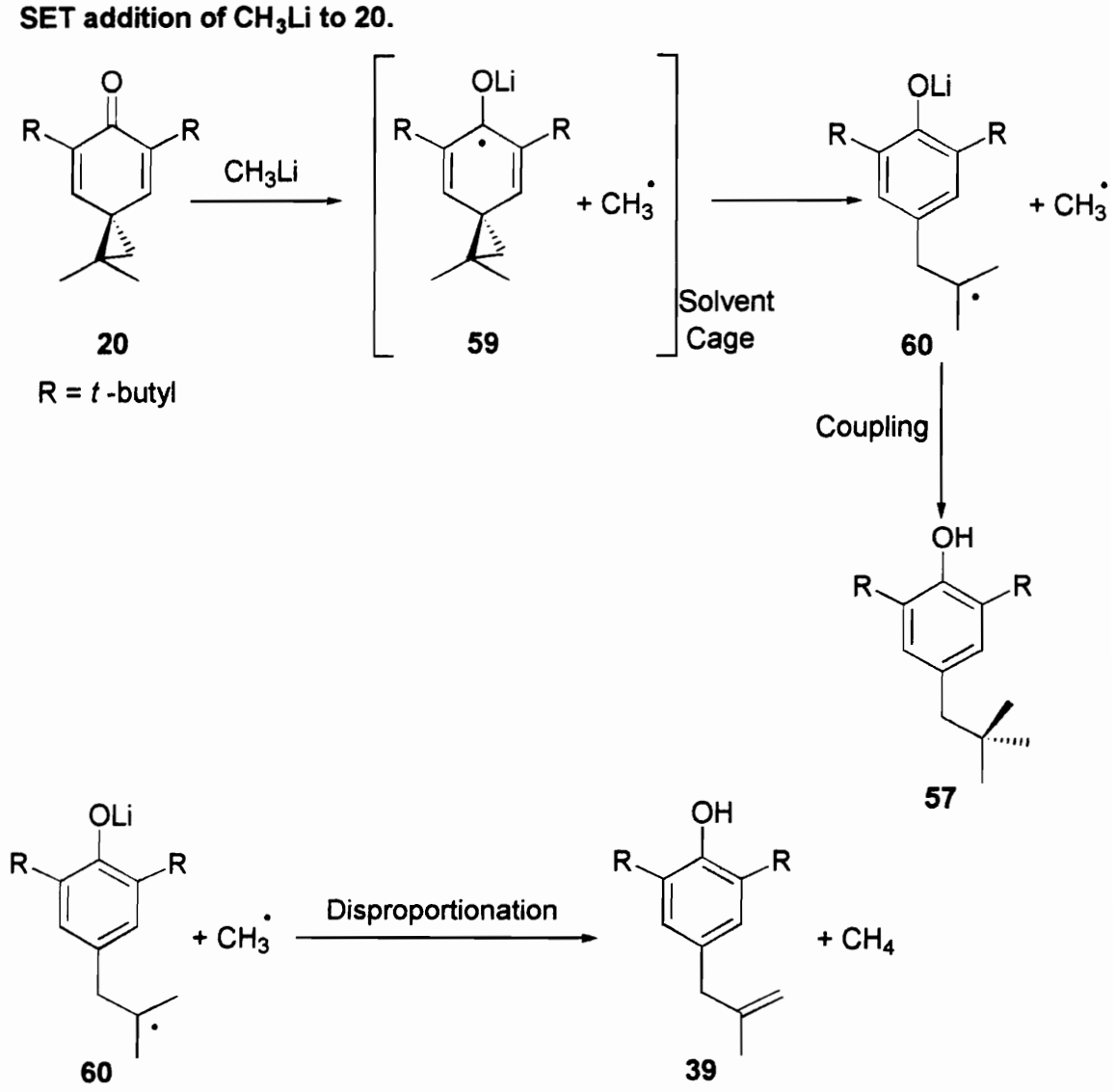


**Figure 34: SET addition of MeLi to 20.**

Interestingly, **40** and **41** were not present in the products. However, based on $^{14}C$ kinetic isotope effect (KIE) studies between methyllithium and benzophenone, their absence is not unexpected.[73] The rate limiting step in the reaction between benzophenone and methyllithium is believed to be the electron transfer. If the reaction between **20** and methyllithium occurs with rate limiting ET, then radical coupling may occur at a rate sufficient to prevent the occurrence of disproportionation reactions. Regardless, the appearance of **57** indicates that SET was occurring in the nucleophilic addition of methyllithium to **20**.

# REACTION OF 1,1-DIMETHYL-5,7-DI-*t*-BUTYLSPIRO[2,5]OCTA-4,7-DIEN-6-ONE (20) WITH LITHIUM DIMETHYLCUPRATE

House has suggested that substrates with reduction potentials ≤ -2.35 V vs. SCE should react via SET with lithium dimethylcuprate.[7] The reduction potential of **20** has been estimated at -2.2 V vs. SCE. We, therefore, expected the reaction between **20** and lithium dimethylcuprate to proceed via SET. The reaction of **20** with lithium dimethylcuprate in anhydrous THF at -10° C resulted in the exclusive production of **58** in a 73% yield, **Scheme 34**.

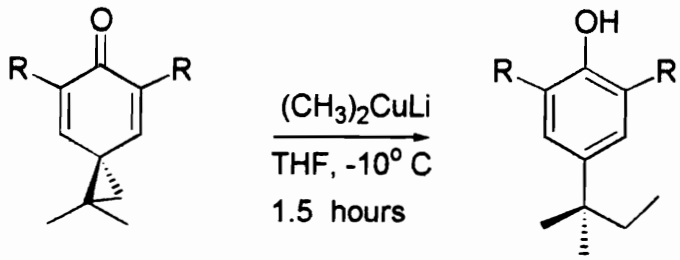


**20**
R = *t* -butyl

**58**
73%

**Scheme 34**

Two mechanisms may account for the exclusive appearance of **58**: (1) A direct nucleophilic displacement ($S_N2$), **Figure 35** or (2) a copper assisted cyclopropylcarbinyl → homoallyl rearrangement, **Figure 35A**.[74]

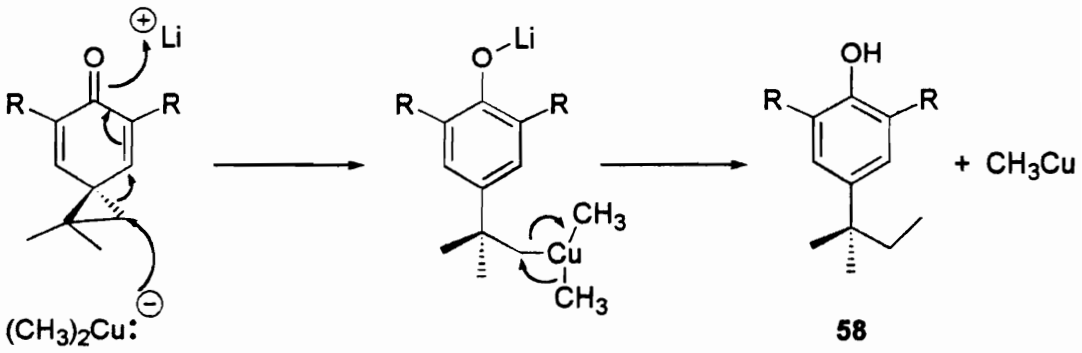


**Figure 35: Polar mechanism for production of 58 in the reaction of lithium dimethylcuprate with 20.**

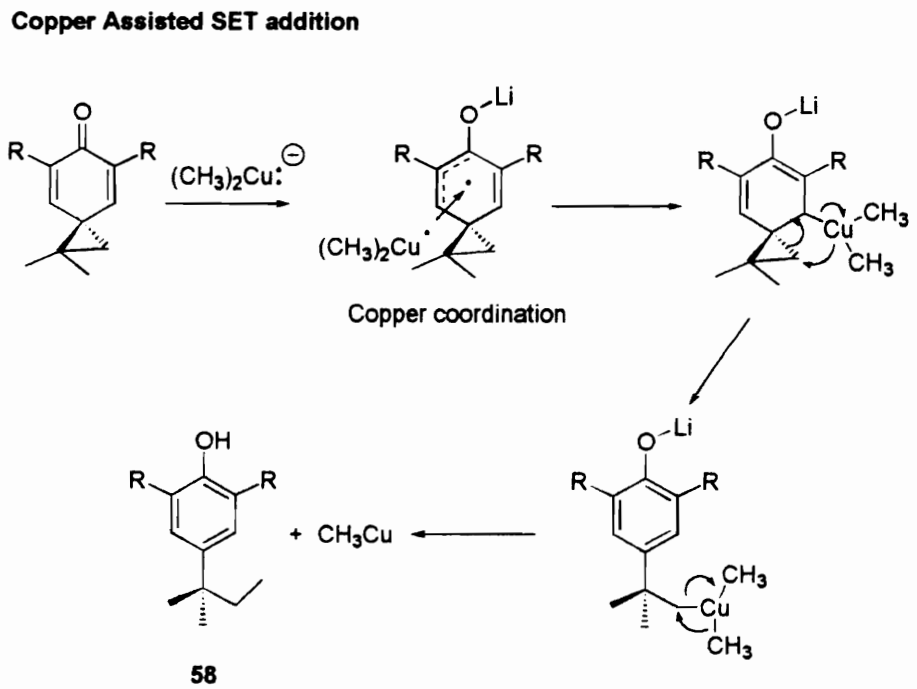


**Figure 35A: SET mechanism for production of 58 in the reaction of lithium dimethylcuprate with 20.**

The dominant mechanism of addition is dependent upon the substitution on the cyclopropane ring and upon the reaction conditions. Doubly activated cyclopropanes (i.e., cyclopropanes with two electron withdrawing groups at the same position of the cyclopropane ring), such as **20**, are capable of undergoing direct nucleophilic substitution at the cyclopropane ring carbon. Therefore, we feel the results are consistent with a polar nucleophilic attack at the least hindered cyclopropane carbon. However, Bertz and coworkers have forwarded an alternative explanation involving single electron transfer, involving a copper assisted cyclopropylcarbinyl → homoallyl rearrangement, **Figure 35A**.[74]

In this mechanism, cyclopropyl ring scission occurs immediately following electron transfer from the cuprate to **20**. Due to the steric hindrance associated with the gem-dimethyl groups, cyclopropyl ring scission occurs at the least hindered side of the cyclopropane ring, resulting in the production of **58**. This mechanism requires coordination of the cuprate to the enone system to prevent cyclopropane ring opening, resulting in a $Cu^{III}$ intermediate.[75] The steric hindrance between the substituents on the cyclohexadienone ring and the dimeric copper species would probably preclude this from occurring. Therefore, the results are better explained by a direct nucleophilic attack by the cuprate on the cyclopropane ring followed by a reductive elimination resulting in substitution of a methyl group at the least hindered carbon.

# CONCLUSIONS

Utilizing reagents recognized for proceeding through some component of SET in their addition to carbonyl compounds, **20** has shown itself to be an effective probe for the identification of SET. In addition to detecting radical ketyl anions generated in a SET pathway, **20** is effective in trapping the radical intermediate derived from the nucleophile. The steric hindrance provided by the *t*-butyl groups eliminates the ambiguity surrounding 1,2 addition products by eliminating their occurrence. Moreover, the geminal dimethyl groups on the cyclopropane ring provide clear distinction between ring opened products as the result of SET and those observed in a nucleophilic process. Based on the previously described reactivity studies, **20** emerges as the premier substrate for the detection of SET to carbonyl compounds.

# CHAPTER 4. REACTION OF SPIRO[2,5]OCTADIENONES WITH POTASSIUM THIOPHENOXIDE.

## INTRODUCTION

We became interested in the possibility that thiolate ions undergo SET in reactions with **20** based on a report that reaction of lithium thiophenoxide with benzophenone generated an EPR active species.[76] The observed EPR signal was assigned to that of the benzophenone ketyl radical anion. However, only benzophenone was recovered upon quenching the reaction mixture. Reduction and radical coupling products consistent with the formation of a radical anion intermediate were absent, **Scheme 35**.

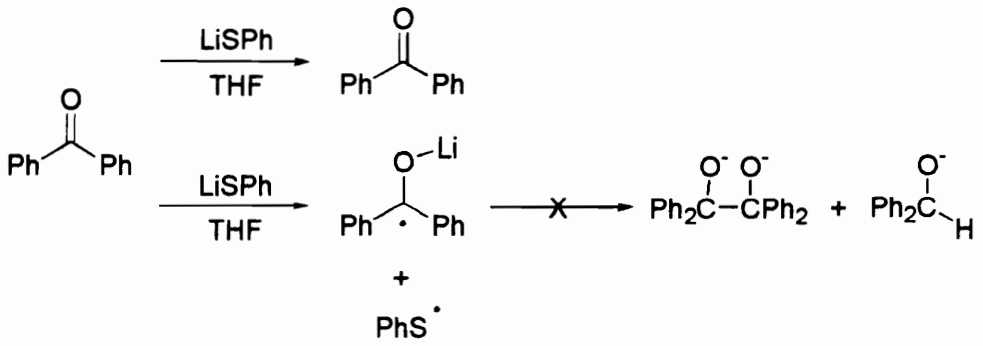


**Scheme 35**

The appearance of a paramagnetic intermediate in the reaction indicated that SET was occurring; however, the absence of products resulting from a radical anion

intermediate cast doubt on the validity of SET being responsible for the addition of thiophenoxide to benzophenone.

The reduction potential of benzophenone (-2.2 V vs. 0.1 M $Ag^+/Ag$) is similar to that observed for **20** (-2.5 V vs. 0.1 M $Ag^+/Ag$). Therefore, **20** should react with thiophenoxide in a manner similar to benzophenone. Based on the previous utility that **20** exhibited in the identification of SET in the reactions with organometallic reagents, we felt that reaction of **20** with thiophenoxide would allow determination as to the occurrence of SET.

Due to the monomeric and dimeric nature of organometallic reagents, controversy exists as to the actual structure of the nucleophile responsible for reduction of carbonyl compounds.[77] The uncertainty surrounding the structure of the reactive species as well as the presence of monomeric and dimeric species complicate the mechanistic and kinetic analyses of reactions of carbonyl compounds with organometallic reagents. These complications are not observed in reactions involving thiophenoxide.[78] Thus, mechanistic and kinetic analyses of the reaction between **20** and thiophenoxide should be straightforward. By employing a crown ether as a chelating reagent for the counter ion, we should be able to diminish the capability of the counter ion to behave as a Lewis acid catalyst, insuring that the counter ion does not facilitate a charge separated species in solution.

Cyclopropane ring opening of **20** with thiophenoxide should occur with the regiospecificity dependent upon the mechanism in operation. Addition of thiophenoxide to **20** should result in one of two products, either the 1° sulfide (**62**) from nucleophilic attack

at the least hindered carbon of the cyclopropane ring, or the 3° sulfide (**63**) from Nu·/radical coupling in a SET reaction, **Figure 36**.

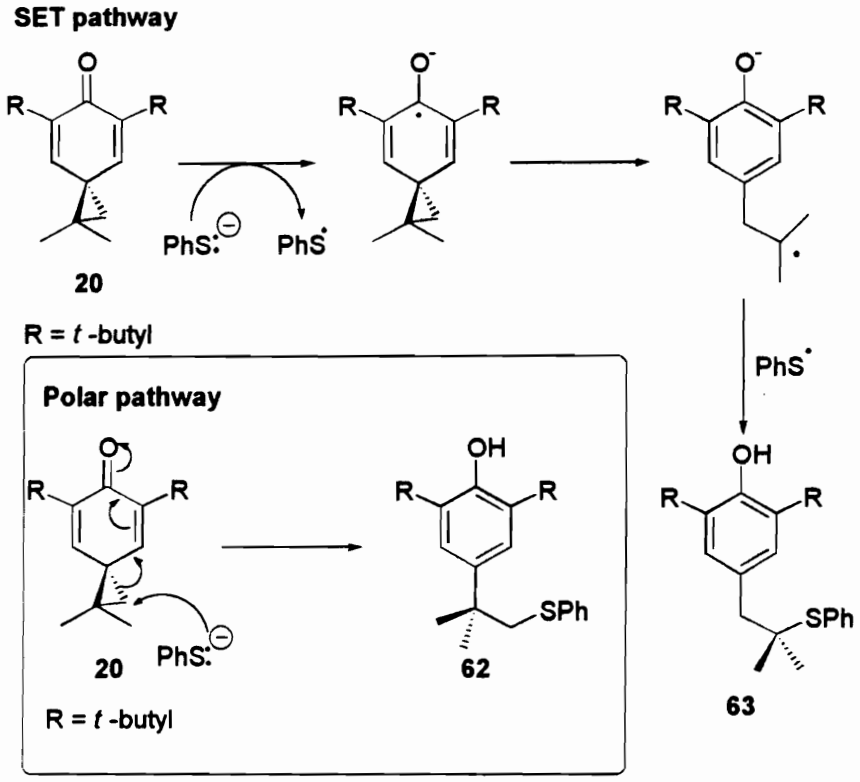


**Figure 36: Proposed SET and polar addition of thiophenoxide to 20.**

It was hypothesized that product analysis should afford an accurate account of the ability of **20** to undergo SET with thiophenoxide.

# MECHANISTIC ANALYSIS OF THE REACTION OF THIOPHENOXIDE WITH SPIRO[2,5]OCTADIENONES

## A. Preliminary Results and Initial Conclusions.

Studies of the reactivity of **20** with thiophenoxide were conducted utilizing potassium thiophenoxide, dimethyl sulfoxide (DMSO), and 18-crown-6. Potassium thiophenoxide was prepared by reaction of potassium *t*-butoxide with benzenethiol. The crude reaction material was extracted with anhydrous ether until no impurities were observed in the $^1$H NMR spectrum and HPLC chromatogram of the salt. DMSO was chosen as solvent based upon its well known ability to solvate cations and minimize ion-pairing effects. This solvation produces an essentially "naked" anion in solution, thereby increasing its reactivity. Furthermore, the use of 18-crown-6 to chelate $K^+$ should further remove any influence by the counter ion in these reactions.

Upon reaction of potassium thiophenoxide with **20** under the conditions described above, a 3.6:1 ratio of **62** versus **63** was obtained, **Table 7**.

**Table 7: Reaction of potassium thiophenoxide with 20.**

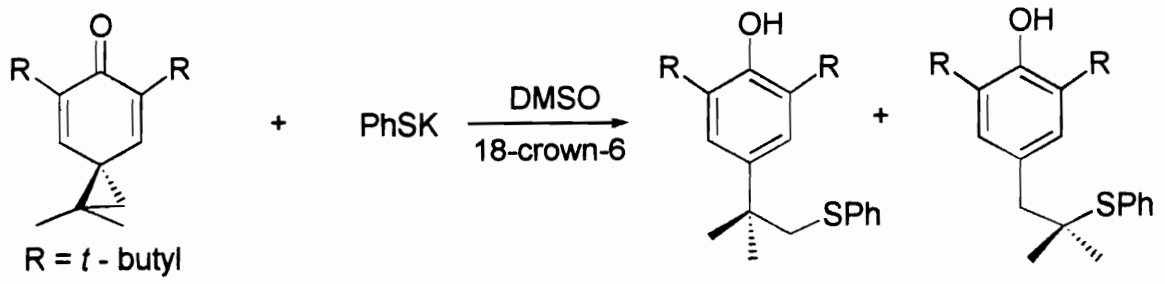


| **20** | | **62** | **63** |
|---|---|---|---|
| 0.02 M | 0.02 M | 3.6 | 1.0 |
| 0.02 M | 0.2 M | 3.6 | 1.0 |

A 10 fold increase in concentration of thiophenoxide had no effect upon the ratio of **62** to **63**. This observation suggests that both **62** and **63** are formed by processes having the same reaction orders with respect to thiophenoxide (presumably first order). The rate of $S_N2$ and SET processes should be dependent on both the concentration of **20** and thiophenoxide; therefore, an increase in thiophenoxide would not affect the product ratios. Thus, it was initially believed that **62** was formed as a result of a $S_N2$ substitution reaction, while **63** was presumed to result from a SET reaction, **Scheme 36**.

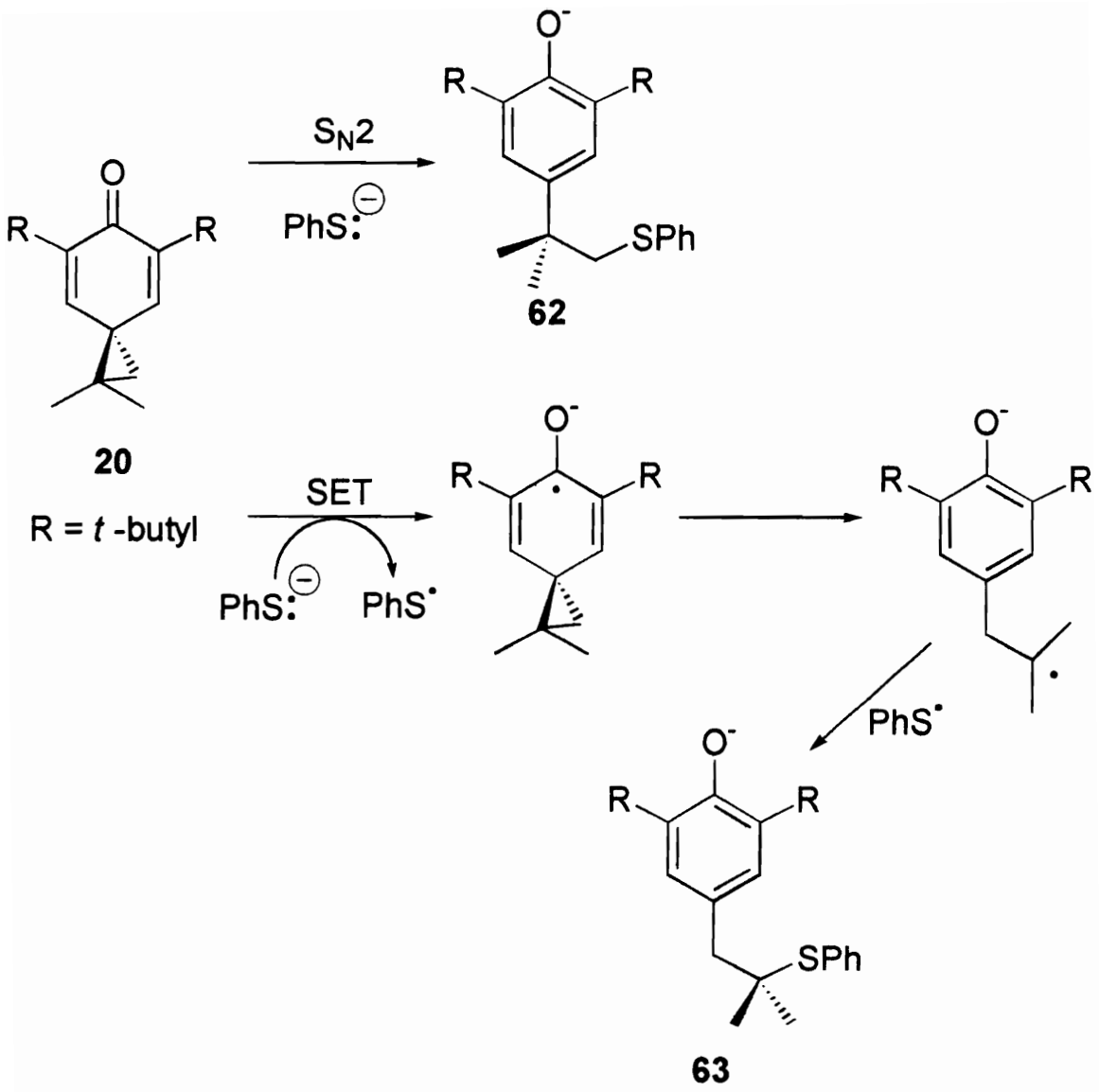
O
R
R
20
R = t -butyl
S_N2
PhS:⊖
O⁻
R
R
SPh
62
SET
PhS:⊖
PhS•
O⁻
R
R
O⁻
R
R
PhS•
O⁻
R
R
SPh
63

**Scheme 36**

Similarly it was found that the reaction of **19** under the conditions described above resulted in a 3.8:1 ratio of the primary (**64**) versus the secondary sulfide (**65**), **Table 8**.

**Table 8: Ratios obtained from reaction of 19 with thiophenoxide.**

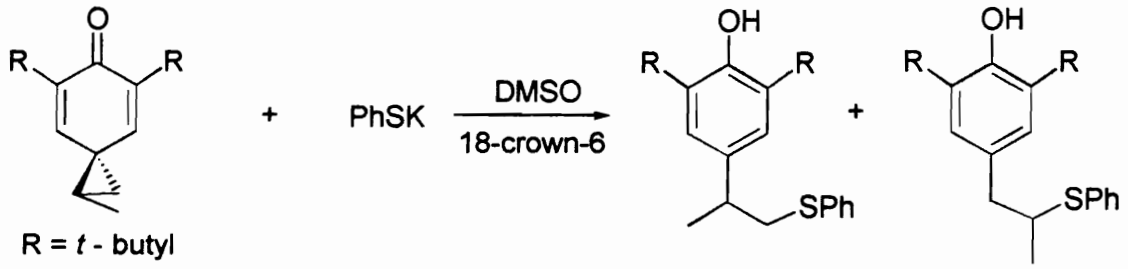


| **19** | | **64** | **65** |
|---|---|---|---|
| 0.02 M | 0.02 M | 3.8 | 1.0 |

These observations seemed to rule out a competing $S_N2/S_N1$ processes, **Scheme 37**.

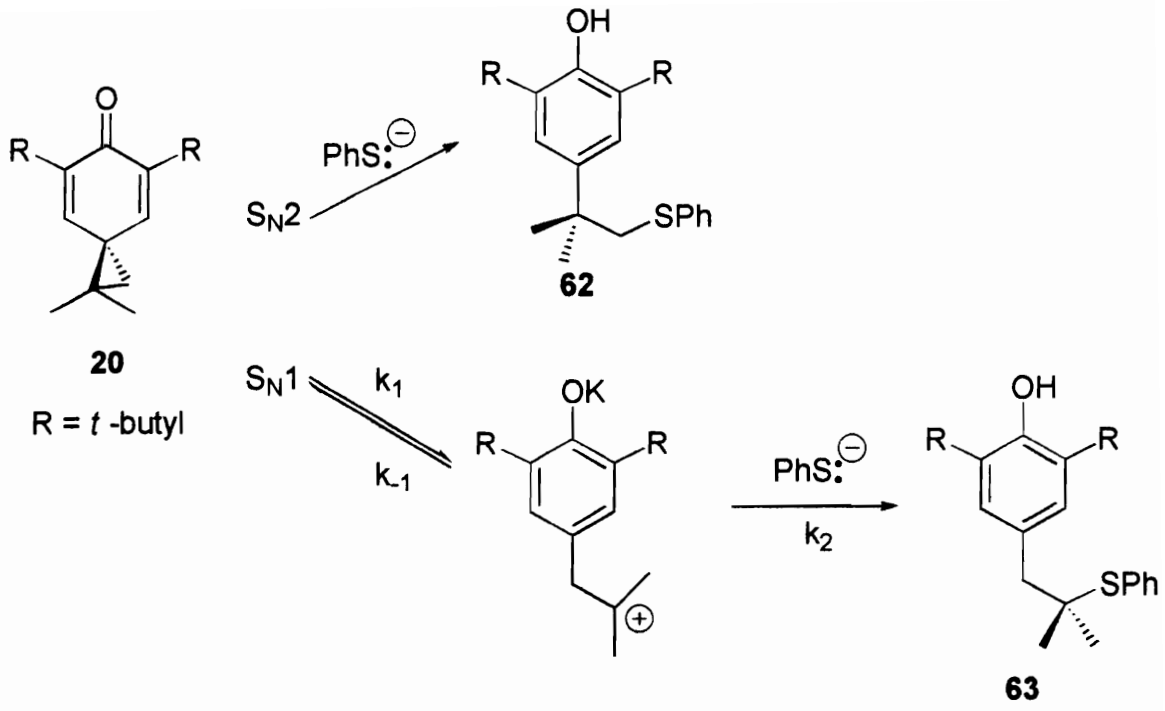


**Scheme 37**

The difference in energy between a secondary and tertiary carbocation is ca. 17 kcal/mol.[79] As a consequence, it was assumed that if competing $S_N2/S_N1$ processes were involved, the ratio of 3°/1° sulfides produced via the reaction of **20** with thiophenoxide would be vastly greater than the ratio of 2°/1° sulfides produced from the reaction of **19** with thiophenoxide. A 10% difference between the product ratios obtained from the reaction of **19** and **20** with thiophenoxide was not felt to be large enough to account for the difference in energies of the intermediate carbocations, so the classic $S_N1$ mechanism was discounted as a mechanistic possibility through which **63** was produced.

## B. Why Single Electron Transfer is Not Involved In The Reaction of Thiophenoxide With 20.

During the course of this investigation a reliable value for the oxidation potential of thiophenoxide was published. The oxidation potentials of the previous nucleophiles have only been provisionally determined; therefore, the exact oxidation potentials of these substrates are not known. The oxidation potential of thiophenoxide has been electrochemically determined and is now known precisely.[80]

The reduction potential of **19** has yet to be determined; however, through the use of voltammetric techniques, we have estimated the reduction potential of **20** to be -2.2V vs. SCE. The oxidation potential of thiophenoxide was found to be -0.1 V vs. SCE.[80] Since both potentials are known, the free energy ($\Delta G$) of electron transfer can be calculated using the equation shown in **Figure 37**.

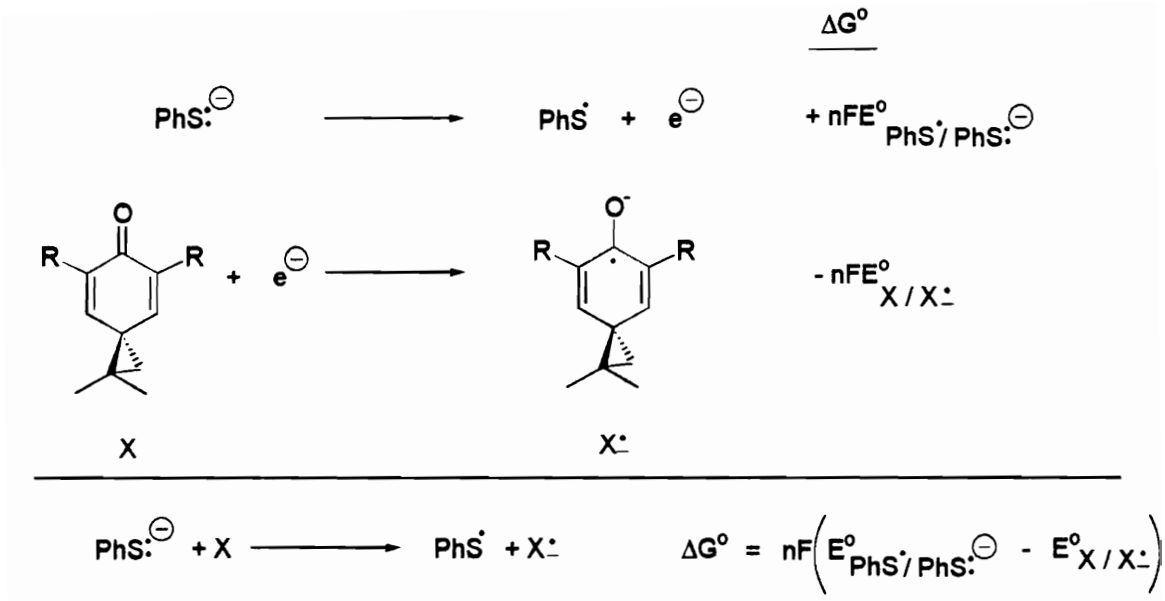


**Figure 37: Determination of the free energy for electron transfer between thiophenoxide and 20.**

On the basis of this analysis, electron transfer was found to **be endothermic** by 50 kcal/mol. Assuming that the activation free energy for electron transfer ($\Delta G^{\neq}$) is $\geq$ 50 kcal/mol, the rate constant for this process at room temperature would be prohibitively slow (the reaction of thiophenoxide with **20** is complete in 5 minutes at room temperature). Consequently a possible direct electron transfer mechanism can be unambiguously excluded on both thermodynamic and kinetic grounds.

## C. Electron Transfer Proceeding Through A Radical Chain Mechanism: The $S_{RN}1$ Mechanism.

An alternative electron transfer pathway which might explain the production of **64** is the $S_{RN}1$ mechanism, **Scheme 38**.

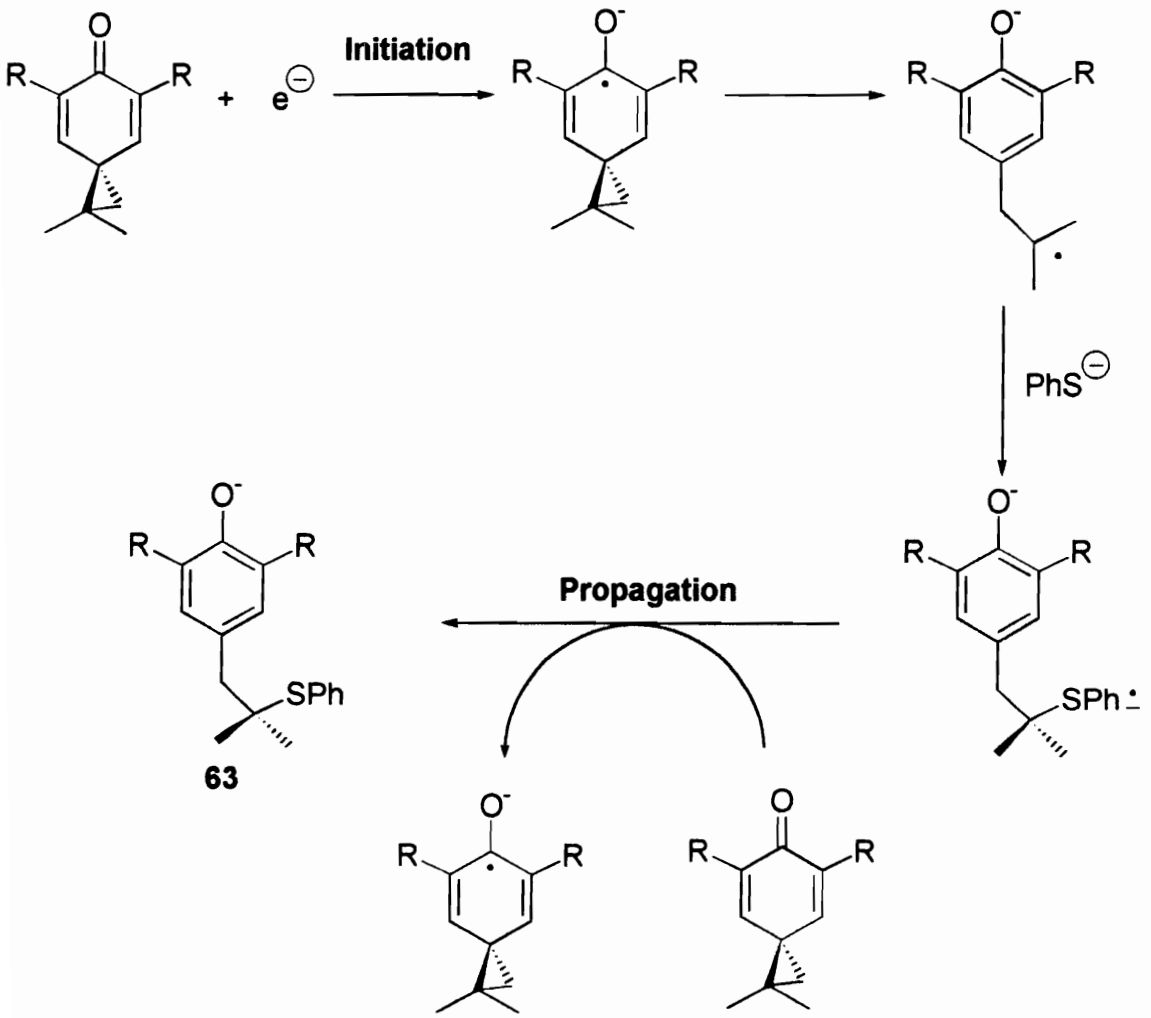


**Scheme 38**

This type of reaction proceeds through a chain mechanism and as a result there are three discrete steps involved: initiation, propagation, and termination.[54,81] Generally this reaction is initiated photochemically, or via addition of a catalytic quantity of a one-electron reducing agent. A few instances involving "spontaneous" initiation are known.[81] After ring opening the resulting radical anion can then react with the nucleophile resulting in the radical anion of the product. Chain transfer (propagation) occurs when the electron from the radical anion of the product is transferred back to the starting material. Termination of the chain may occur through either radical coupling or through disproportionation reactions of the radicals, **Figure 38**. However, radical anion coupling has not been observed in this system and probably will not occur.

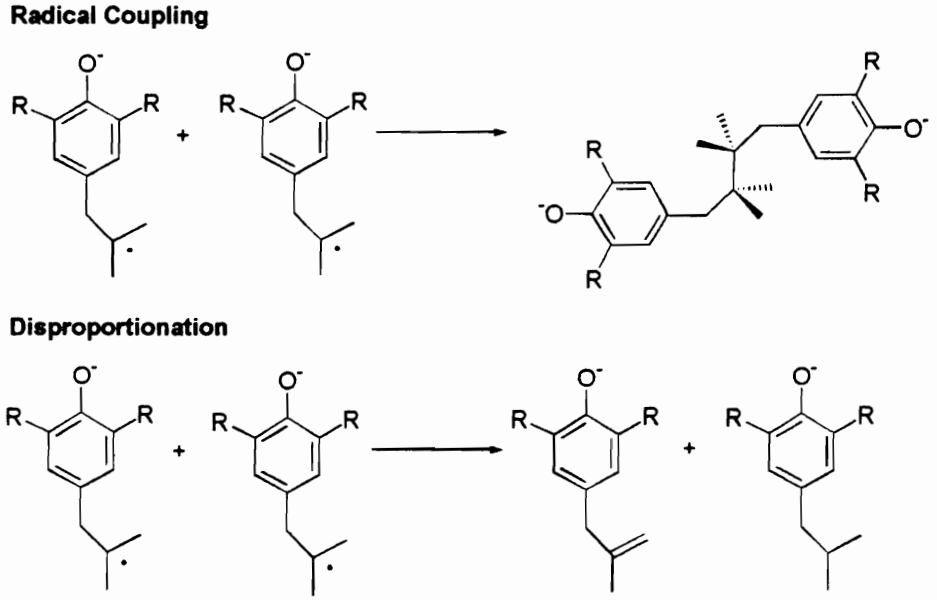


**Figure 38: Termination reactions possible in the $S_{RN}1$ reaction.**

To ascertain whether the reaction of **20** with potassium thiophenoxide in DMSO was photoinduced, the reaction was conducted in the absence of light. This reaction was conducted at night to minimize stray light entering the flask. The reagents were mixed after the room lights had been extinguished. Gas chromatographic analyses were conducted in the dark to insure the reaction did not occur between the time the aliquots were removed and subsequently injected. The reaction between **20** and thiophenoxide in complete darkness was essentially complete in 5 minutes in a 3.2:1 ratio of **62** to **63** in an overall yield of 63%, **Table 9**.

**Table 9: Reaction of 20 with thiophenoxide in the absence of light.**

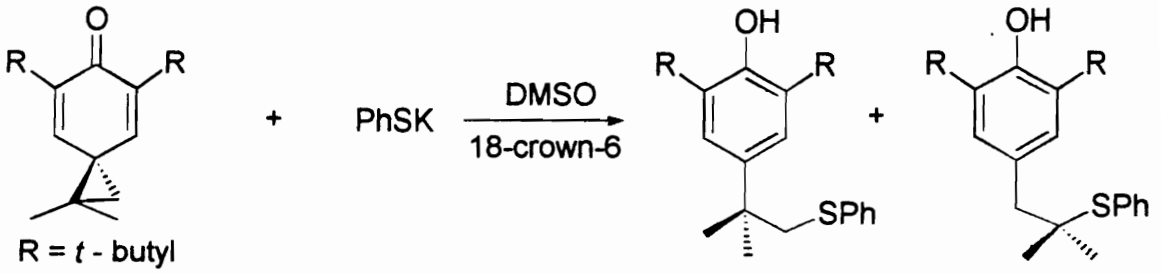


| **20** | | **62** | **63** |
|---|---|---|---|
| 0.02 M | 0.02 M | 3.2 | 1.0 |

Upon workup and gas chromatographic quantitation of the reaction mixture, no discernible difference in the ratio of **62** to **63** was observed relative to that in light. If the reaction were proceeding through a light initiated $S_{RN}1$ reaction, the absence of light should have diminished the product yields. The similarity between the results in the

presence and absence of light indicate that the reaction was not photo-induced and suggested that the $S_{RN}1$ reaction may not be occurring.

A second test for the $S_{RN}1$ reaction is to examine the affect of added inhibitors. Three substrates were chosen as inhibitors: oxygen, thiophenol, and diphenyl disulfide. These reagents were chosen based on their availability and on their well documented ability to trap radical intermediates. Oxygen reacts with alkyl radicals at rates $k > 10^9$ $M^{-1}$ $s^{-1}$, whereas, thiophenol and diphenyl disulfide react with alkyl radicals at rates ranging from $k = 10^4 - 10^8$ $M^{-1}$ $s^{-1}$.[54, 82] The reaction rates of the inhibitors should be competitive with the other radical processes occurring, therefore, allowing inhibition of a radical chain process. The effect on product ratio as a result of adding these reagents is shown in **Table 10**.

**Table 10: Added inhibitor effect upon product ratios in the reaction of 20 with thiophenoxide.**

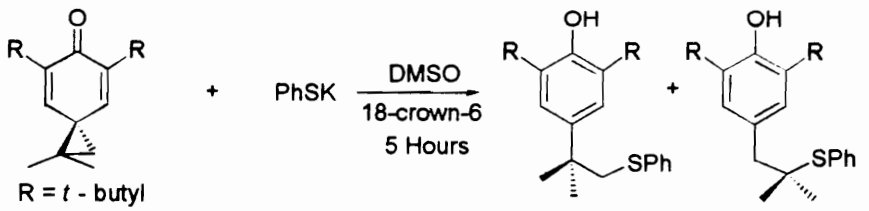


| Inhibitor | 20 | | Inhibitor | 62 | 63 | Overall Yield |
|---|---|---|---|---|---|---|
| $O_2$ | 0.02 M | 0.02 M | | 3.2 | 1.0 | 23.3% |
| PhSSPh | 0.02 M | 0.02 M | 0.04 M | 3.7 | 1.0 | 72.5% |
| PhSH | 0.02 M | 0.02 M | 0.06 M | 3.6 | 1.0 | 73.8% |

The similarity in the product ratio **62**:**63** in the presence and absence of inhibitors strongly suggests that the $S_{RN}1$ mechanism is not the pathway through which **63** is produced. Product yields were similar except in the reaction in which air was constantly bubbled in the reaction mixture. The reduced product yield in this reaction was ascribed to oxidation of potassium thiophenoxide. Elimination of the $S_{RN}1$ mechanism excluded pathways proceeding through a radical chain mechanism for formation of **63**. Therefore, we began to investigate the possibility of competing polar processes as the processes responsible for the production of **62** and **63**.

## D. Competing $S_N2$/Carbocationic Pathways.

### 1. Reevaluation of previous data.

Elimination of pathways involving radical intermediates suggested that polar reaction mechanisms were responsible for the observed products. In the reaction of potassium thiophenoxide with **20**, **Table 7**, a 10 fold increase in the concentration of the nucleophile produced no difference in the product ratio. The rate equation for formation of **62** and **63** through competing zero and first order reactions is shown in **Equation 26**.

**Eqn. 26**

$$\frac{1^{st}\text{ order rate dependence}}{\text{Zero order rate dependence}} = \frac{k[Nu][\mathbf{20}]}{k[\mathbf{20}]} = \frac{\mathbf{62}}{\mathbf{63}}$$

If competing first order and zero order processes were responsible for formation of **62** and **63**, then an increase in the concentration of thiophenoxide would cause an increase in **62** and affect the product ratios. Since product ratios were unaffected by increasing thiophenoxide concentration, the dependence of the reactions involved in the production of **62** and **63** on thiophenoxide concentration must be the same, either both reactions exhibit a zero order dependence on thiophenoxide or both reactions exhibit a first order dependence on thiophenoxide concentration. Since, DMSO is not generally considered to be a solvent conducive to the formation of carbocationic intermediates, we felt that the $S_N2$ mechanism, which shows a first order dependence on both the concentrations of the nucleophile and substrate, was a better choice for explanation of these results, **Equation 26**.

**Eqn. 26A**

$$A + B \xrightarrow{k} C$$

$$\text{rate} = k[A][B]$$

However, $S_N2$ reactions are generally avoided as explanations for substitutions at 3° centers.

The substitution of nucleophiles at 3° centers is generally associated with a radical or carbocationic intermediate. The elimination of a radical pathway as an explanation for the production of **63**, leaves a mechanism involving a carbocationic intermediate as a likely explanation. However, the rate of a classic $S_N1$ mechanism shows no dependence on the concentration of the nucleophile, **Scheme 39**.

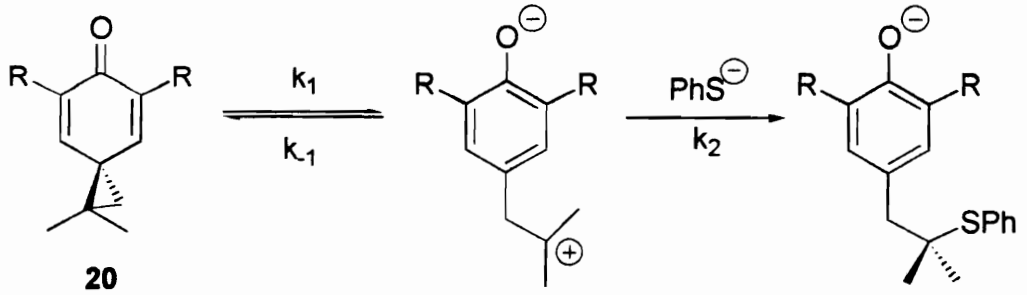


**20**

R = *t* -butyl

**63**

rate = $k_1$[**20**]

**Scheme 39**

In the mechanism for the classic $S_N1$ reaction, ionization of the substrate ($k_1$) to the carbocationic intermediate is rate limiting; thus, a first order dependence is shown only on the concentration of the substrate undergoing substitution. However, if $k_{-1}$ is faster than the rate of nucleophilic attack, $k_2[PhS^-]$, a preequilibrium is established between the unionized substrate and the carbocationic intermediate, thus, the rate of nucleophilic attack becomes rate limiting, resulting in a first order rate dependence on the nucleophile, **Scheme 40**.

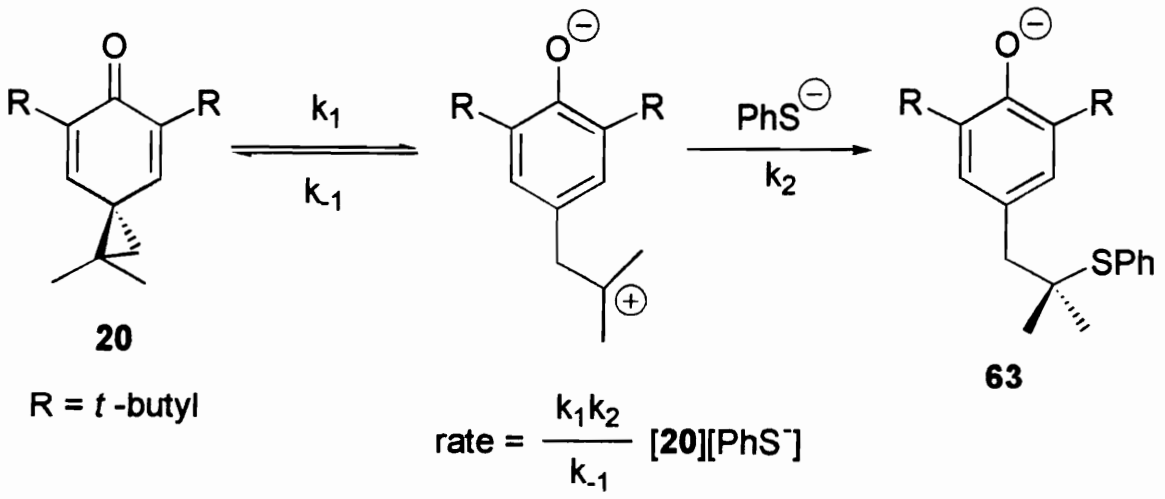


**Scheme 40**

This mechanism was coined as the $S_N2C+$ mechanism.[83] The $S_N2C+$ mechanism has precedence in the literature. However, it has only been observed in highly polar solvents,

under very strong common ion effects, when the carbocation is in conjugation with a phenyl ring, or when the nucleophile is so sterically hindered that the rate of addition is retarded.[84]

A second mechanism proceeding through a carbocationic intermediate that also exhibits a dependence on both the concentration of the nucleophile and the electrophile is the $S_{ET}2$ mechanism, **Scheme 41**.[85,86]

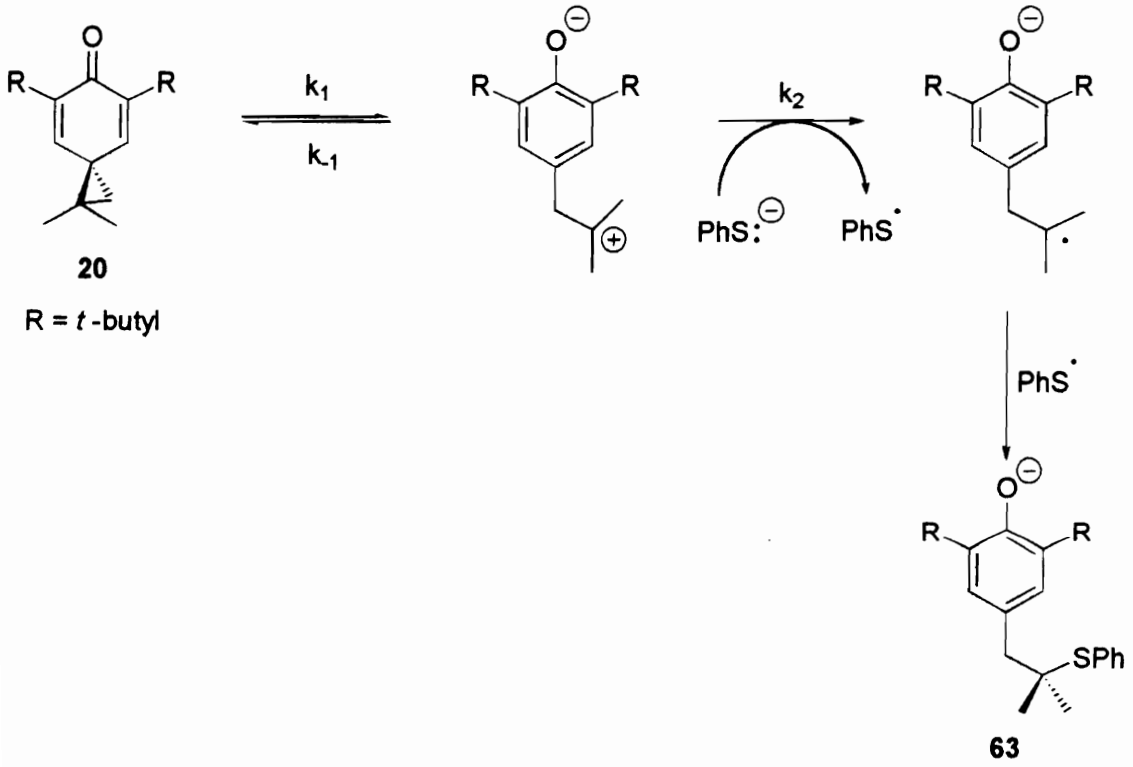


**20**

R = *t*-butyl

**63**

**Scheme 41**

As in the classic $S_N1$ mechanism the first step is ionization of the substrate to the intermediate carbocation. At this point an electron is transferred from the nucleophile to the carbocationic intermediate, resulting in the formation of the radicals derived from the electrophile and the nucleophile. These species then undergo subsequent coupling, resulting in the final products.

Based on the first order dependence on nucleophile concentration exhibited by the $S_{ET}2$ or $S_N2C+$ mechanisms, we began an investigation to determine if these mechanism were responsible for the production of **63** and **65**.

**2. Solvent effects on the ratios of sulfides produced in the reaction of 19 and 20 with potassium thiophenoxide.**

In general the rate of radical reactions is not affected by the solvent in which they are conducted. This is due to the absence of charged intermediates in these reactions. However, the rate at which nucleophilic substitution reactions proceed is very solvent dependent. The manner in which solvent affects the rate of substitution reactions depends on the mechanism of the substitution (i.e., $S_N1$ or $S_N2$) reaction.

The generally accepted mechanism for the $S_N2$ reaction involves the backside addition of a nucleophile to an electrophile in a 5 membered transition state, **Figure 39**.

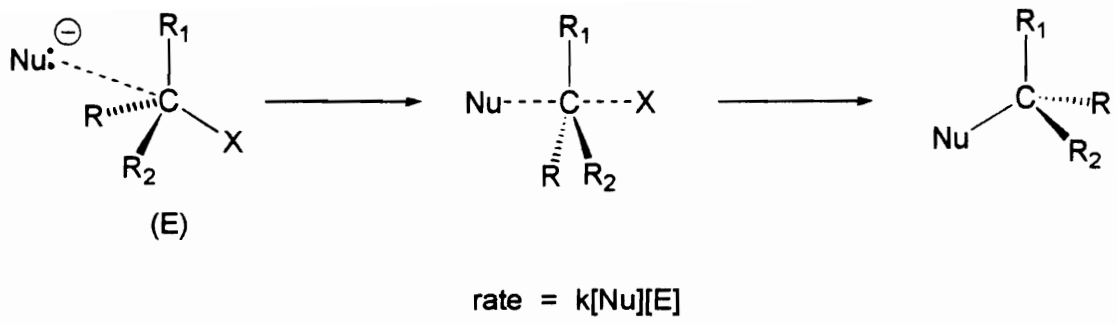


**Figure 39: Transition state associated with $S_N2$ substitution.**

The reaction occurs with an overall inversion of configuration. The rate of this reaction is second order, with a dependency on the concentrations of both the nucleophile and the electrophile. However, the rate is also dependent on the accessibility of the nucleophile for reaction. In protic solvents, the nucleophile is highly solvated. The solvent sphere surrounding the nucleophile shields the nucleophile, thus slowing the rate at which it can react with the electrophile. In contrast, polar aprotic solvents do not behave in this manner. In most cases the reactivity of the nucleophile is increased by solvating the associated counter ion, **Figure 40**.

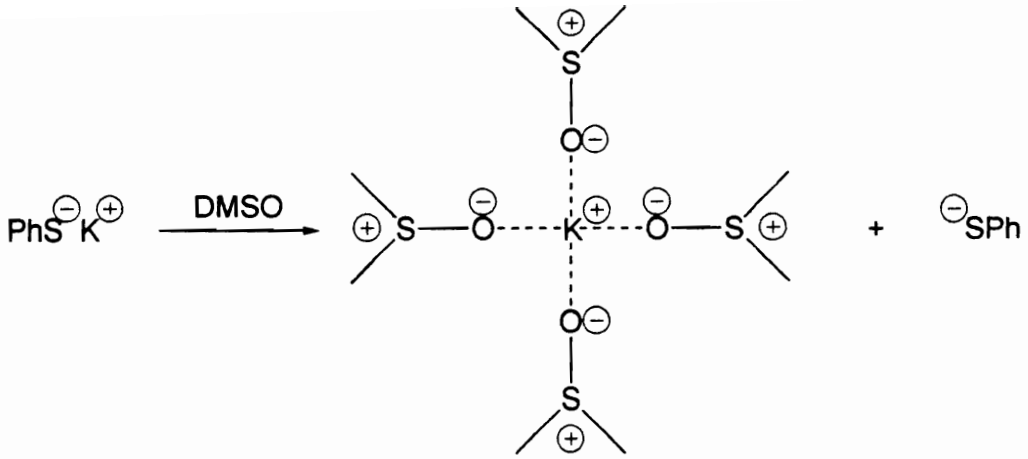


**Figure 40: Solvation of counterion by polar aprotic solvents.**

Therefore, the rates of $S_N2$ reactions in protic solvents are slower than those observed in aprotic solvents.

The solvent dependence of the $S_{ET}2$ and $S_N2C+$ reactions do not stem from solvation of the nucleophile; it instead stems from the solvent's ability to ionize the electrophile to a carbocationic intermediate, and once ionized to stabilize the carbocation/anion pair formed in the transition state, **Figure 41**.

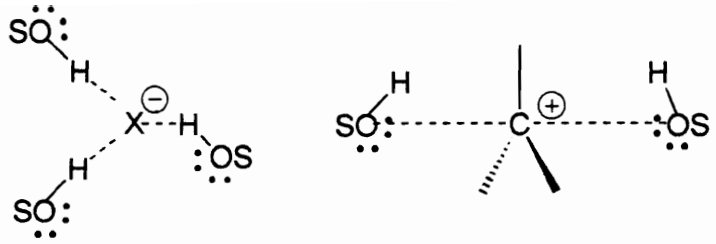

**Figure 41: Solvation of carbocationic intermediates by polar protic solvents.**

Protic solvents are better suited than aprotic solvents to ionize the substrate and stabilize the carbocationic transition through solvation of the ion pair.

The rates of $S_N2$ reactions are generally faster than reactions proceeding through carbocationic intermediates in polar aprotic solvents, while the rate of reactions proceeding through carbocationic intermediates are generally faster than $S_N2$ reactions in protic solvents. If indeed a mechanism proceeding through a carbocationic intermediate were responsible for the production of **63** and **65** then an incremental increase in the ionizing power of the solvent should increase the rates of these reactions relative to the rates of the $S_N2$ reactions through which **62** and **64** are formed. Any change in the rates of the reactions will be readily apparent by a change in the ratio of **64**:**65** in reactions of thiophenoxide with **19** and the ratio of **62**:**63** in the reactions of thiophenoxide with **20**. Therefore, we felt that conducting the reaction of **19** and **20** with potassium thiophenoxide utilizing a number of different solvents would allow us to assess whether our results were explicable on the basis of a competing $S_N2$/carbocationic intermediate.

There are several scales available for correlating the ionizing power of a solvent. Most are based upon the Y scale or a variation of the Y scale, **Equation 27**.[87,88]

**Eqn. 27**

$$\text{Log}\,(k_o/k_a) = mY$$

where: $k_o$ = rate of ionization of *t*-butyl chloride in 80:20 ethanol/water.
$k_a$ = rate of ionization of *t*-butyl chloride in other protic solvents.
m = measure of substrate's sensitivity to ionization.
Y = measure of a solvent's ionizing power.

This scale is based upon the $S_N1$ ionization of *t*-butyl chloride to the *t*-butyl carbocation. This equation is a free energy relationship which relates the solvent's effect on the free energy of activation in the transition state. The slope obtained from a plot of log(k) for the rate of ionization of a particular substrate versus the Y values determined from the ionization of *t*-butyl chloride indicates the susceptibility of a substrate to ionization. Slopes ranging from 0.7 to 1 indicate that the reaction is proceeding through a carbocationic intermediate.[88] While slopes < 0.3 indicate that the reaction is proceeding through an $S_N2$ reaction mechanism.

The ionization of *t*- butyl chloride involves the formation of a tertiary carbocation; therefore, this scale is limited to measuring the ionization of *t*-butyl chloride to the *t*-butyl carbocation in polar protic solvents. A second limitation associated with this scale is its inability to account for a solvent's nucleophilicity. In formation of a carbocationic

intermediate solvents can exert a backside push in an $S_N2$ type interaction, thereby weakening the bond of the leaving group, **Figure 42**.

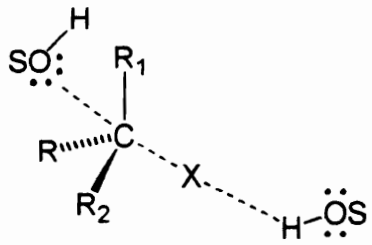


**Figure 42: Nucleophilic solvent assistance in carbocation formation.**

The more nucleophilic a solvent, the greater the push felt. Therefore, solvents with high nucleophilicity could be erroneously identified as better able to ionize a substrate into a carbocationic intermediate than non-nucleophilic solvents. A four parameter solvent system was established to correct the deficiencies of the Y scale due to solvent nucleophilicity, **Equation 28**.[89]

**Eqn. 28**

$$\text{Log } (k_a/k_o) = lN + mY$$

where: N = nucleophilicity of the solvent.
l = substrate susceptibility parameter.

The addition of these parameters is able to correct for solvent nucleophilicity; however, they also complicate the determination of m and investigations are still limited to polar protic solvents.

Since we were interested in the behavior **19** and **20** in both protic and aprotic solvents, correlation of sulfide ratios to Y values would only allow investigation of a part of the solvents necessary. Fortunately, measurement of the rate of ionization of neophyl tosylate (**66**) was able to extend the measure of a solvents ionizing ability to the polar aprotic solvents, **Scheme 42**.[90]

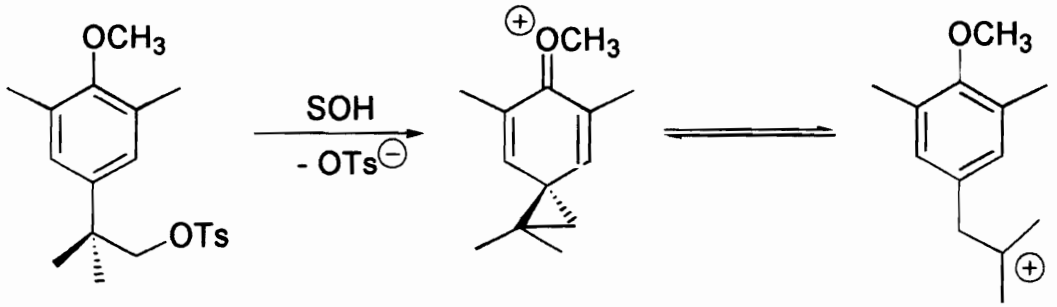


**66** **67**

**Scheme 42**

The ionization of **66** proceeds with anchimeric assistance provided by the aromatic ring resulting in the positively charged spirane intermediate (**67**). This intermediate subsequently rearranges to the 3° carbocation. The nucleophilic nature of the solvent is eliminated in this rearrangement by the anchimeric assistance provided by the aromatic

ring. We felt fortunate in locating this scale due to the similarity in structure of **67** to **19** and **20**. We felt confident that a comparison of the sulfide ratios obtained in the reactions of **19** and **20** in a particular solvent to the rate of ionization exhibited by **67** in that solvent would provide an accurate account of the mechanism through which the sulfides were being formed.

The reactions between **19** and **20** and thiophenoxide were conducted at room temperature. The concentration of **19** and **20** was maintained at $3.4 \times 10^{-3}$ M in all solvents investigated. To enable complete reaction of substrate, thiophenoxide concentrations were maintained at concentrations ranging from $4.5 \times 10^{-3}$ to $6.5 \times 10^{-3}$ M. All solvents were dried prior to use and reactions were conducted under argon. Upon reaction of **19** and **20** with thiophenoxide the following ratios were observed, **Table 11**.

**Table 11: Sulfide ratios in the reaction of 19 and 20 with thiophenoxide.**

| Solvent | Log k Neophyl Tosylate[80] | Ratio 63-64 | Yield | Ratio 65-66 | Yield |
|---|---|---|---|---|---|
| THF | -6.073 | 5.34 ± 0.08 | 84% | 4.81 ± 0.01 | 63% |
| EtOAc | -5.947 | 3.91 ± 0.03 | 84% | 4.77 ± 0.03 | 87% |
| Acetone | -5.067 | 4.68 ± 0.17 | 96% | 4.17 ± 0.1 | 97% |
| Pyridine | -4.670 | 3.93 ± 0.02 | 80% | 4.37 ± 0.02 | 86% |
| DMF | -4.298 | 4.75 ± 0.1 | 86% | 4.70 ± 0.1 | 87% |
| DMSO | -3.738 | 3.05 ± 0.09 | 80% | 3.75 ± 0.01 | 80% |
| *t*-BuOH | -3.59 | 1.35 ± 0.01 | 91% | 2.47 ± 0.03 | 89% |
| *i*-PrOH | -3.41 | 0.96 ± 0.01 | 84% | 2.30 ± 0.16 | 90% |
| EtOH | -3.204 | 0.65 ± 0.01 | 72% | 1.75 ± 0.01 | 97% |
| MeOH | -2.796 | 0.43 ± 0.01 | 56% | 1.46 ± 0.02 | 95% |

Ionization values were not available for 2-propanol and *t*-butanol; therefore, the values were extrapolated from the slope of a graph of the Y values vs. log(k) neophyl tosylate.

In all but two cases the sulfide yields exceeded 80 %. The depressed yields observed in the reaction of **20** with potassium thiophenoxide in methanol and ethanol were due to the formation of a side product identified utilizing $^1$H NMR as the polymeric ether (**68**).

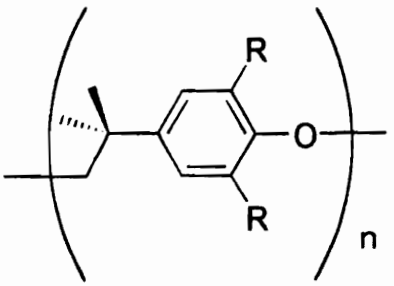


**68**

R = *t*-butyl

Previous studies have shown that 5,7-dimethyl-1-vinylspiro[2,5]octa-4,7-dien-6-one (**68**) was able to undergo anionic polymerization in DMF.[91] In this polymerization a 200 to 1 ratio of substrate to $CN^-$ was used to initiate the reaction. Interestingly attack by $CN^-$ on the cyclopropyl ring occurred at the more hindered position, **Scheme 43**.

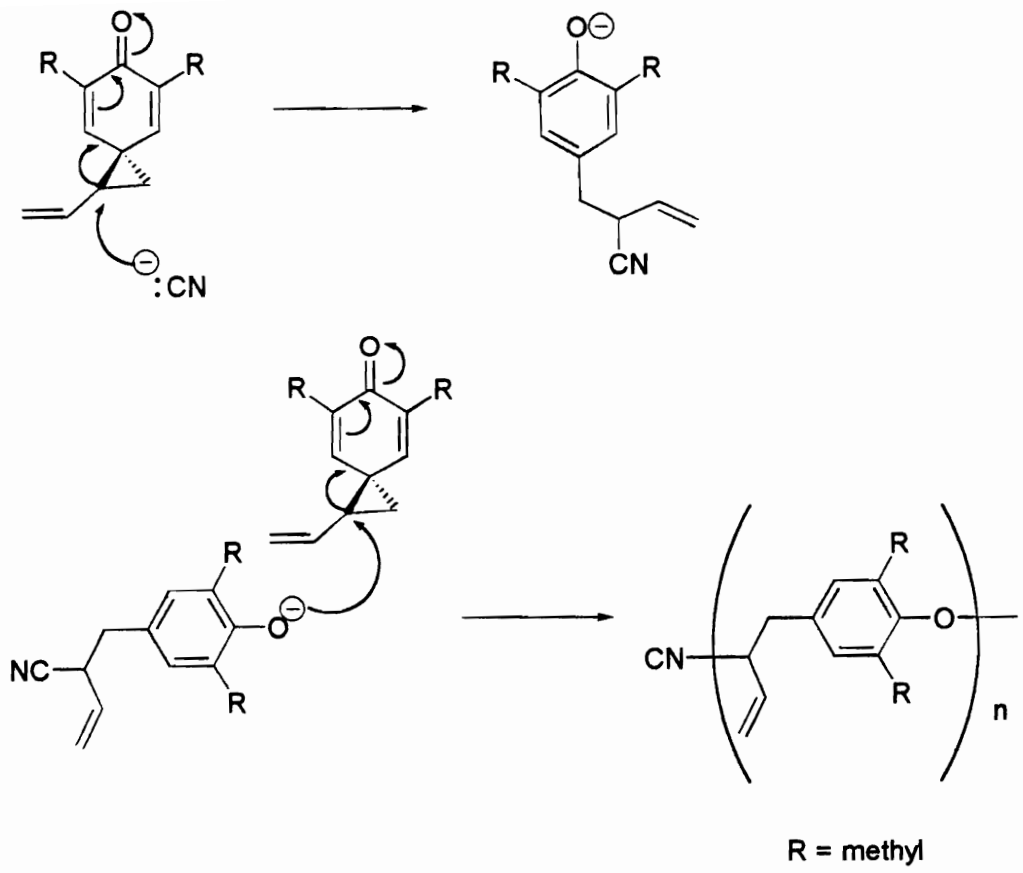


**Scheme 43**

It seems unlikely that the polymer formed in the reaction of **20** with thiophenoxide was formed as a result of an anionic process. In an anionic polymerization, the concentration of the nucleophile used as the initiator is kept at low concentrations in order to maximize the length of the polymer chains. However, the concentration of thiophenoxide in our reactions was in excess relative to the concentration of substrate. Due to the nature of the solvents in which the polymeric product occurred, it is more probable that **68** was formed as a result of a cationic polymerization process.

Even though polymerization has been observed in analogous systems, the appearance of polymeric product in the reaction of **20** was still surprising. There is much more steric hindrance associated with the *t*-butyl groups of the substrates that we are investigating than the methyl groups of **68** in **Scheme 43**. Therefore, it was felt that the steric hindrance of the two *t*-butyl groups would preclude addition of substituents to the phenoxide oxygen. It was also surprising that the polymer formed in the presence of excess thiophenoxide, since the unhindered thiophenoxide would be expected to be much more nucleophilic and thus react at faster rates than the hindered phenoxide of **20**. This seems to indicate that the cyclopropyl ring opening of **20** is very facile in methanol and ethanol or that ethanol and methanol are very efficiently solvating the thiophenoxide, thereby, slowing the addition enough that the polymerization becomes a competing process.

A plot of the sulfide ratios obtained in the reaction of **19** and **20** with potassium thiophenoxide are shown in **Figure 43**.

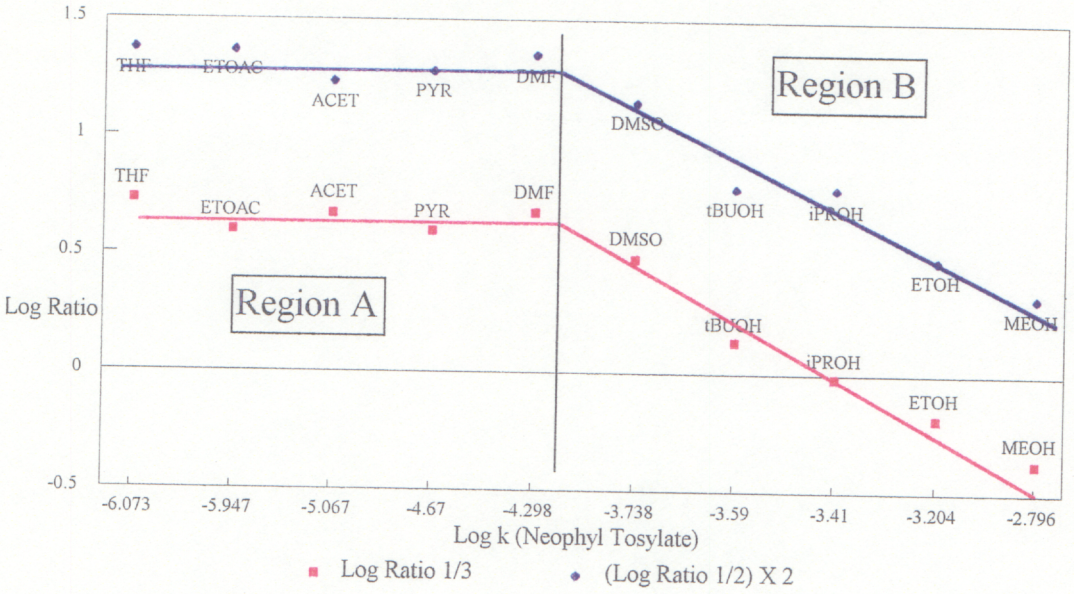


**Figure 43: Plot of sulfide ratios vs. log k neophyl tosylate.**

In **Figure 43**, two distinct regions emerge, a region including all of the polar aprotic solvents ( Region A), except DMSO, with a slope of $-1.1 \times 10^{-2}$ for the 1°/3° sulfide ratio and $-2.0 \times 10^{-2}$ for the 1°/2° sulfide ratio and a region that includes DMSO and the polar protic solvents (Region B) with a slope of -0.84 for the 1°/3° sulfide ratio and a slope of -0.40 for the 1°/2° sulfide ratio.

The slope of zero observed in region A is attributed to product forming processes that either have no dependence on solvent or where solvent affects each process equally. If competing $S_N2$/carbocationic processes were occurring in this region of the graph, solvents better able to stabilize the carbocationic transition state would result in an increase of the more substituted sulfides. The absence of a solvent effect in region A

eliminates the possibility of a process proceeding through a carbocationic intermediate in this region of the graph.

Region B of **Figure 43** exhibits a solvent dependence by both **19** and **20** on the product ratio. As the solvent's ability to ionize the substrate becomes greater, the amount of the more substituted sulfide increases. Therefore, the pathway producing the more substituted sulfide must be proceeding through a mechanism with a charged separated intermediate in the transition state, formation of which is dependent on the ionizing ability of the solvent. This suggests that a $S_N2$ process is responsible for the production of **62** and **64**, whereas, a process involving a carbocationic intermediate is responsible for the production of **63** and **65**.

The solvent study indicated that two dissimilar mechanisms were responsible for the formation of **63** and **65** in regions A and B. In region B the addition of thiophenoxide to **19** and **20** proceeded through a carbocationic intermediate, while the absence of a solvent effect on sulfide ratios in region A suggested that the formation of **62** and **64** was proceeding through a relatively non-polar transition state. Initial concentration studies involving the reaction of thiophenoxide with **20** in DMSO exhibited either first or zero order dependence upon the concentration of thiophenoxide. However, as noted in **Figure 43**, DMSO seems to be the transition between the polar transition states in region B and the non-polar transition states in region A. As a result, the concentration effects upon product ratio can not be extended to either regions of the plot. Therefore concentration studies were initiated to determine what affect changing concentrations of thiophenoxide had upon the reactions of **19** and **20** in regions A and B in **Figure 43**.

**3. Concentration effects on the ratios of sulfides produced in the reaction of 19 and 20 with potassium thiophenoxide.**

To ascertain the reaction orders of the processes responsible for the products formed in all regions of **Figure 43**, the concentration of thiophenoxide was increased incrementally to a concentration 100 fold in excess of the concentration of **19** or **20**. Since the rate of the $S_N2$, $S_N2C+$, and $S_{ET}2$ reactions would be dependent on the concentration of both thiophenoxide and substrate an increase in the concentration of nucleophile should have no influence on the ratio of sulfides produced. Therefore, reaction of **19** and **20** with increasing concentrations of thiophenoxide should produce within experimental error the same ratio of sulfides. If, however, the formation of the more substituted sulfides is occurring via a classic $S_N1$ mechanism in Region B of **Figure 43**, an increase in the concentration of thiophenoxide would increase the ratio of $S_N2$ product relative to **65, Equation 28**.

**Eqn. 28**

$$\frac{S_N2 \text{ rate}}{S_N1 \text{ rate}} = \frac{k[Nu][\mathbf{19}]}{k[\mathbf{19}]} = \frac{\mathbf{64}}{\mathbf{65}}$$

Thus, concentration studies would allow us to ascertain whether the reaction order of thiophenoxide was similar for the production of the sulfides in all regions of **Figure 43**.

The concentration study was conducted utilizing a representative solvent in both regions of **Figure 43** and in DMSO which seemed to be the break point between region A and region B. The experiments were conducted by dissolving the appropriate amount of potassium thiophenoxide and 18-crown-6 in an aliquot of the solvent under investigation. Upon complete dissolution of the salt, a second aliquot of the solvent, in which the appropriate amount of either **19** or **20** was dissolved, was syringed into the reaction mixture. The reaction was allowed to stir for 1 hour at room temperature, at which time the reaction mixture was acidified and analyzed quantitatively utilizing HPLC chromatography. The results of this study are shown in **Table 12**.

**Table 12: Concentration affects upon the sulfide ratios in the reactions of 19 and 20 with thiophenoxide.**

| Solvent | [20] | [KSPh] | Ratio 62-63 | [19] | [KSPh] | Ratio 64-65 |
|---|---|---|---|---|---|---|
| Acetone | 0.02 | 0.002 | 5.1 ± 0.1 | 0.1 | 0.001 | 4.1 ± 0.1 |
| | 0.02 | 0.02 | 4.9 ± 0.1 | 0.1 | 0.005 | 4.2 ± 0.1 |
| | | | | 0.1 | 0.01 | 4.4 ± 0.1 |
| DMSO | 0.02 | 0.02 | 3.6 ± 0.1 | 0.1 | 0.001 | 3.9 ± 0.1 |
| | 0.02 | 0.2 | 3.6 ± 0.1 | 0.1 | 0.005 | 4.1 ± 0.1 |
| | | | | 0.1 | 0.01 | 4.1 ± 0.1 |
| *i*-PrOH (**19**) | | | | 0.1 | 0.001 | 2.1 ± 0.1 |
| | | | | 0.1 | 0.005 | 3.1 ± 0.1 |
| | | | | 0.1 | 0.01 | 3.1 ± 0.1 |
| EtOH (**20**) | 0.02 | 0.02 | 0.60 ± 0.05 | | | |
| | 0.02 | 0.2 | 0.62 ± 0.05 | | | |

The results in **Table 12** show that the product ratios were not affected by increasing the concentration of the nucleophile. Thus, it was ascertained that the reactions were either zero order or first order in potassium thiophenoxide in **all** of the solvents utilized in **Figure 43**. Before we could determine the exact mechanisms occurring, we had to determine the exact reaction order of thiophenoxide addition to **19** and **20**.

**4. Competition reactions for exact determination of the reaction orders involved in the production of products.**

Exact determination of the reaction order through which the sulfides were produced was accomplished through competition reactions comparing the change of ratio of sulfides produced from **19** to ethyl phenyl sulfide (**69**) produced from the reaction of potassium thiophenoxide and ethyl bromide, **Scheme 44**.

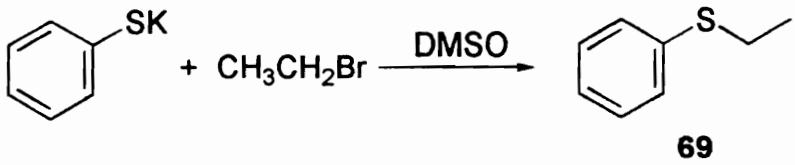


**69**

**Scheme 44**

It was assumed that the reaction of thiophenoxide with ethyl bromide will occur through an $S_N2$ process in all of the solvents investigated. Thus the rate of this reaction will exhibit a first order dependence upon the concentration of thiophenoxide. As a result, a change in the concentration of thiophenoxide should cause no difference between the

ratio of **70:64** and **70:65** if the reaction of **19** is proceeding with a first order dependence on thiophenoxide, **Figure 44**.

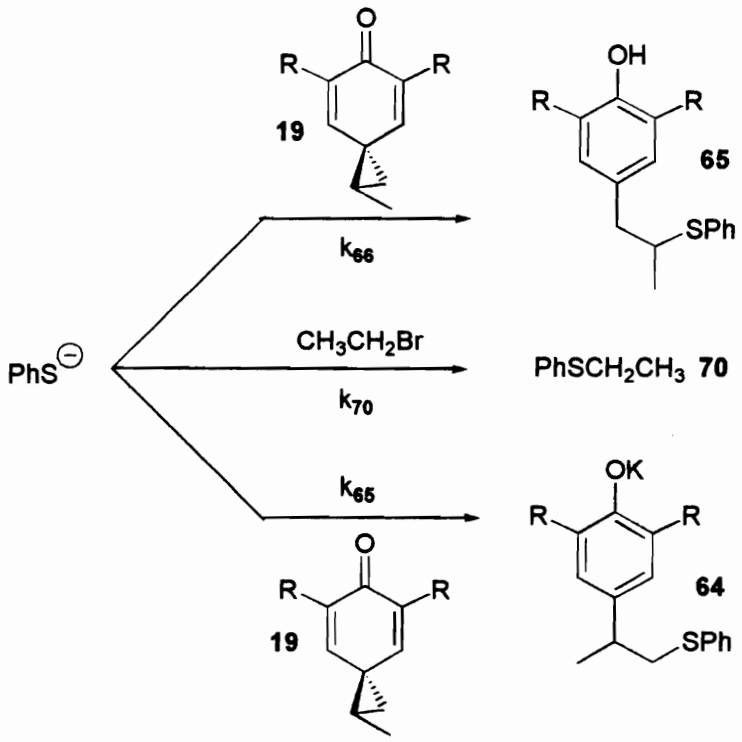


$$\frac{70}{65} = \frac{k_{70}[EtBr]}{k_{66}[19]}$$

$$\frac{70}{64} = \frac{k_{70}[EtBr]}{k_{65}[19]}$$

**Figure 44: Competition kinetics associated with a first order dependence on thiophenoxide concentration.**

If, however, the reaction of **19** and thiophenoxide proceeds with a zero order dependence on thiophenoxide in the production of **65**, then an increase in the thiophenoxide concentration will increase the ratio of **70:65**, **Figure 45**.

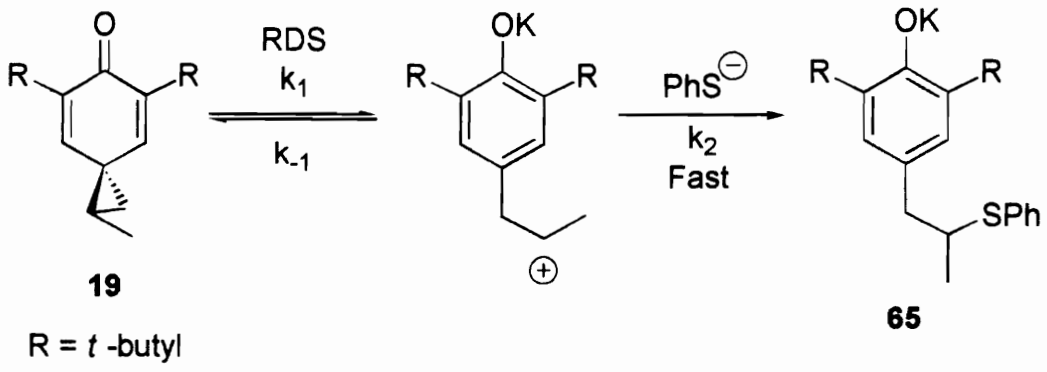


$$PhSK + EtBr \longrightarrow PhSEt + KBr$$

**70**

$$\frac{\mathbf{70}}{\mathbf{65}} = \frac{k_{70}[Phsk][EtBr]}{k_{66}[\mathbf{19}]}$$

**Figure 45: Competition kinetics associated with a zero order dependence on thiophenoxide concentration.**

The competition studies were conducted utilizing the same procedure employed in the concentration studies. Sulfide ratios were determined from HPLC quantitation. The results of this study are shown in **Table 13**.

**Table 13: Observed sulfide ratios from competition studies with ethyl bromide.**

| Solvent | [KSPh] | [19] | [EtBr] | Ratio 70 - 65 | Ratio 70 - 66 | Ratio 65 - 66 |
|---|---|---|---|---|---|---|
| Acetone | 0.001 | 0.1 | 0.1 | 7.4 ± 0.1 | 33 ± 1 | 4.5 ± 0.1 |
| | 0.005 | 0.1 | 0.1 | 7.8 ± 0.1 | 41 ± 1 | 5.2 ± 0.1 |
| | 0.01 | 0.1 | 0.1 | 10.0 ± 0.1 | 52 ± 1 | 5.2 ± 0.1 |
| *i*-PrOH | 0.001 | 0.1 | 0.1 | 0.49 ± 0.01 | 0.94 ± 0.01 | 2.1 ± 0.1 |
| | 0.005 | 0.1 | 0.1 | 0.35 ± 0.01 | 0.75 ± 0.01 | 2.1 ± 0.1 |
| | 0.01 | 0.1 | 0.1 | 0.42 ± 0.01 | 0.88 ± 0.01 | 2.1 ± 0.1 |
| DMSO | 0.001 | 0.1 | 0.1 | 7.1 ± 0.1 | 28 ± 1 | 3.95 ± 0.1 |
| | 0.005 | 0.1 | 0.1 | 6.7 ± 0.1 | 27 ± 1 | 4.1 ± 0.1 |
| | 0.01 | 0.1 | 0.1 | 8.0 ± 0.1 | 36 ± 1 | 4.1 ± 0.1 |

The absence of an effect on the sulfide ratios by increasing the concentration of thiophenoxide suggests that the same dependence on thiophenoxide is being observed in the formation of **64** and **65** as is observed in the formation of **69**. Since the reaction of ethyl bromide with thiophenoxide is assumed to occur with a first order dependence on the concentration of thiophenoxide, the reaction(s) through which **64** and **65** are formed are also assumed to occur with a first order dependence on thiophenoxide. Similar behavior is observed in the reactions of **20** with thiophenoxide as with **19** and thiophenoxide; therefore, the results obtained from the competition reaction between **19** and ethyl bromide will apply to the reactivity of **20**. Therefore, the reactions of **20** with thiophenoxide can be assumed to be first order in thiophenoxide in all of the solvents

studied. These results indicate that the formation of the sulfides in Region A is occurring via competing $S_N2$ processes, while product formation in Region B is the result of competing $S_N2/S_N2C+$ or $S_N2/S_{ET}2$ processes.

**5. Counter-ion and solvent effects on cyclopropyl bond lengths.**

We have hypothesized that the processes responsible for the production of products in region A of **Figure 43** were competing $S_N2$ substitution reactions. The transition from the $S_N2$ to the $S_N1$ mechanism requires greater involvement by the solvent in forming a carbocationic intermediate in the transition state. In the transition from the $S_N2$ to the $S_N1$ mechanism an intermediate substitution mechanism exists, designated the $S_N2$ (intermediate) mechanism. In this mechanism nucleophilic attack occurs through a charge separated ion pair; thus, a first order dependence on nucleophile concentration is exhibited.

Solvent effect studies have ruled out carbocationic intermediacy in the production of the sulfides from **19** in region A of **Figure 43**; however, we needed to ascertain that a significant charge polarization from either solvent or Lewis acid catalysis by $K^+$, **Figure 46**, was not occurring to establish that substitution of thiophenoxide to **63** was proceeding through a classical $S_N2$ process.

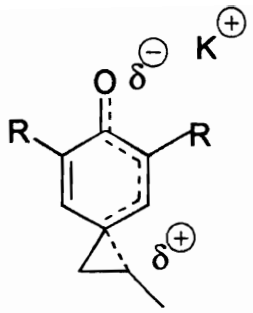


**Figure 46: Lewis acid catalysis of 19 by $K^+$.**

The cyclopropane bond lengths determined for **19** and **20** from semi-empirical molecular orbital calculations (SCF-MO, AM1, RHF) are shown in **Figure 47**.

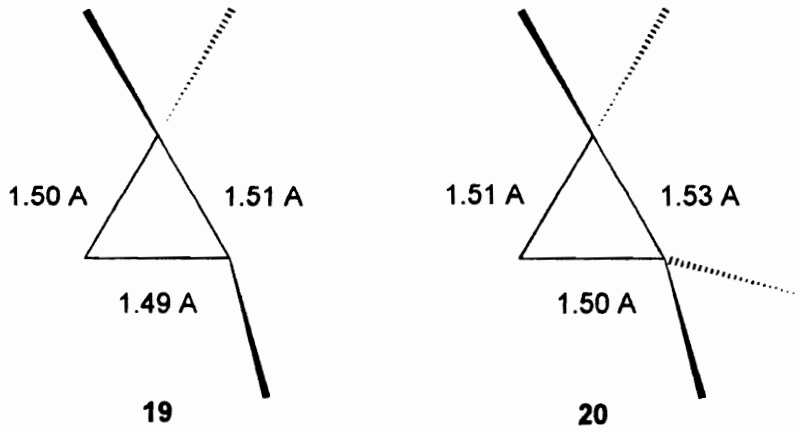


**Figure 47: Calculated cyclopropane bond lengths exhibited in 19 and 20.**

The bond lengths of the cyclopropane adjoining the cyclohexadienone ring are of similar magnitude, suggesting that polarization of electron density away from the more substituted carbon center of the cyclopropane ring is not occurring.

Nuclear magnetic resonance spectroscopy was utilized to further substantiate that cyclopropyl bond lengthening was absent in **19**. The extent of polarization exhibited by **19** in solution can be determined based upon the $^{13}C$ chemical shift of the methine and methylene carbons of the cyclopropyl ring. If charge is being delocalized from these carbons, then an upfield shift in $^{13}C$ resonance will occur. Comparison of the shifts of the cyclopropyl methylene and methine carbons should allow a qualitative assessment of the cyclopropane bond lengths adjacent to the cyclohexadienone ring. Therefore, $^{13}C$ NMR studies were used to determine the extent of polarization of **19** in solution.

Deuterated solvents were chosen in each region of **Figure 43** as well as the break point DMSO. The inclusion of deuterated benzene and deuterated chloroform in this study was based upon their inability to stabilize a carbocationic intermediate and, thus, provide a benchmark for the other solvents. The $^{13}C$ NMR results are shown in **Table 14**.

**Table 14: $^{13}C$ NMR resonances exhibited by the cyclopropyl methine and methylene carbons of 19.**

| Solvent | *C*H ( δ vs. TMS) | *C*H$_2$ (δ vs. TMS) |
|---|---|---|
| Acetone-d$^6$ | 28.86 | 28.14 |
| Benzene-d$^6$ | 27.55 | 27.55 |
| DMSO-d$^6$ | 28.30 | 27.75 |
| DMSO-d$^6$, $KClO_4$ | 28.33 | 27.76 |
| DMSO-d$^6$, $KClO_4$, 18-crown-6 | 28.38 | 27.82 |
| $CDCl_3$ | 28.12 | 27.93 |
| Methanol-d$^4$ | 29.99 | 28.9 |

In **Table 14** it is observed that the $^{13}C$ NMR chemical shifts of the cyclopropyl methine carbon lie within a range of 1.3 ppm. Moreover, the cyclopropyl methine carbon resonance is ca. 1 ppm further upfield than the cyclopropyl methylene carbon resonance in each solvent. The $^{13}C$ NMR indicates that **19** has almost the same degree of polarization in both the protic and aprotic solvents. Comparison of the $^{13}C$ NMR resonances between the methylene and methine carbons of the cyclopropane ring indicate that significant bond lengthening is not occurring between the methine carbon and the cyclohexadienone ring. Thus, the modes of substitution should be similar at the methine and methylene carbons of the cyclopropane ring.

**6. Discussion of results.**

In region A of **Figure 43** we felt confident that the first order dependence shown by the reactions on thiophenoxide, combined with the absence of solvent effects upon sulfide ratios indicated that **63** and **65** were being produced in the reaction of

thiophenoxide with **19** and **20** as a result of competing $S_N2$ substitution reactions, **Scheme 45**.

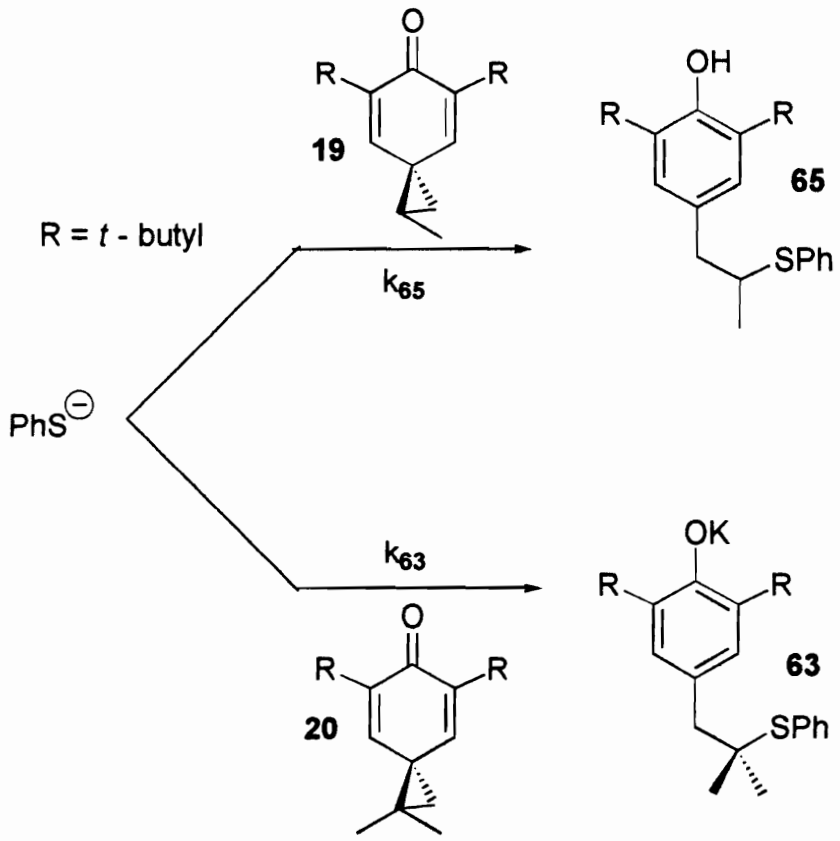


**Scheme 45**

Substitution reactions at tertiary centers are generally discouraged due to the steric hindrance associated with backside approach of the nucleophile and due to the occurrence of competing $E_2$ elimination reactions. It is true that $S_N2$ reactions are uncommon to tertiary substrates; however, they are not impossible.[92,93,94,95,96] In normal saturated aliphatic systems, $S_N2$ reaction occurs through the interaction of the highest occupied

molecular orbital (HOMO) of the nucleophile and the lowest unoccupied molecular orbital (LUMO) of the electrophile, **Figure 48**.

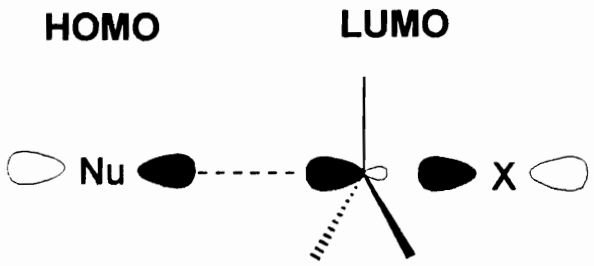


**Figure 48: Molecular orbital representation of $S_N2$ substitution.**

However, cyclopropanes are not normal aliphatic systems. Nucleophilic attack on the cyclopropyl ring proceeds through interaction with $sp^2$ hybridized carbon centers with overlapping p-orbitals as the bonding orbitals which form the backbone of the cyclopropane ring. The orbital interaction is shown using the Walsh model for cyclopropane, **Figure 49**.[97]

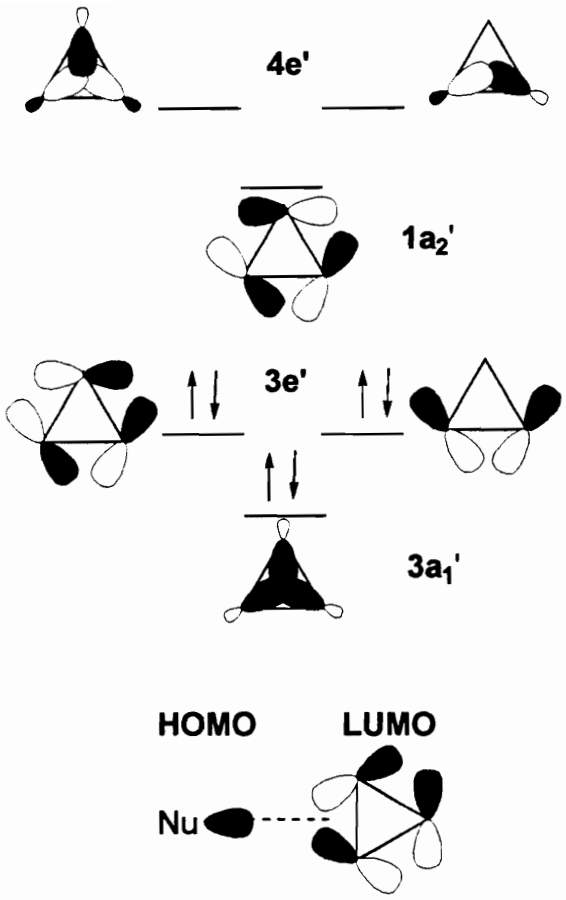


**Figure 49: Walsh orbital model of cyclopropane.**

Direct $S_N2$ substitution can be ascribed as the mechanism responsible for the production of **62**, **64**, and **65** in region A. However, the direct nucleophilic substitution to a 4° center resulting in **63** is generally discouraged. There are two possible pathways for the formation of **63** via a second order addition process, direct $S_N2$ substitution to the 4° carbon of the cyclopropyl ring or through a 1,4-Michael addition to the cyclohexadiene ring.

The Michael addition resulting in the tertiary sulfide proceeds via a two step mechanism. In the first step thiophenoxide adds in a 1,4 fashion to the cyclohexadiene ring resulting in the formation of enolate anion **70**, **Scheme 47**.

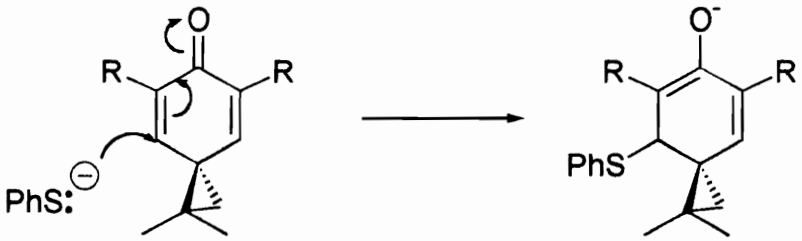


**20** **70**

R = *t* -butyl

**Scheme 47**

Addition can occur from either face of the cyclohexadiene ring resulting in two possible structures of the resulting enolate anions, **Figure 50**, **71** and **Figure 51**, **72** ($CH_3S$ was used instead of PhS to simplify the drawings).

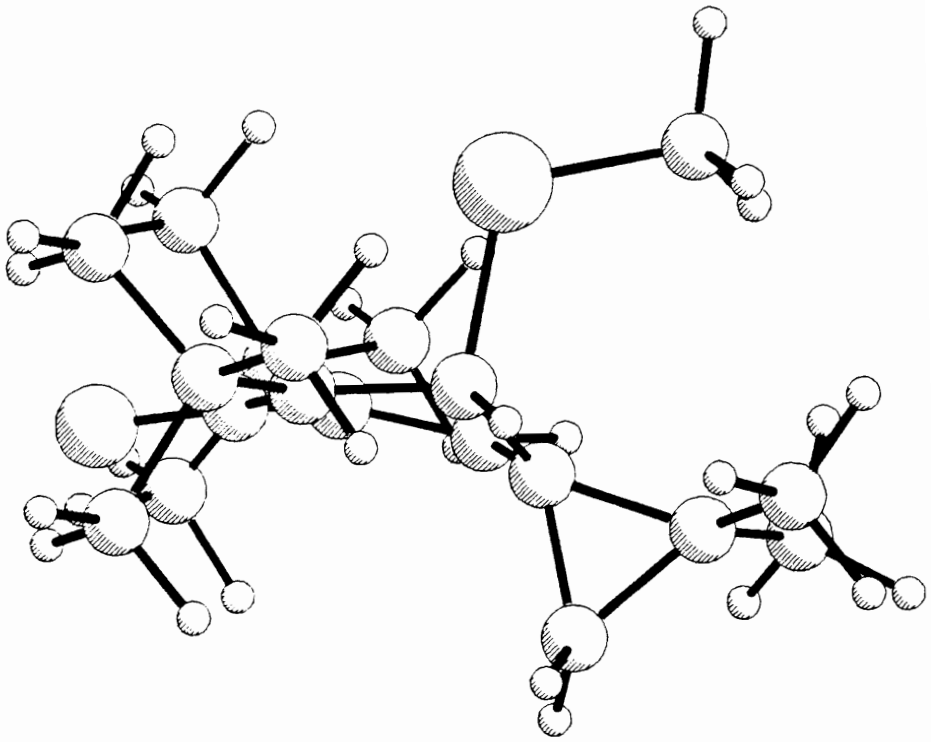

**Figure 50: Structural geometry of enolate anion 71**

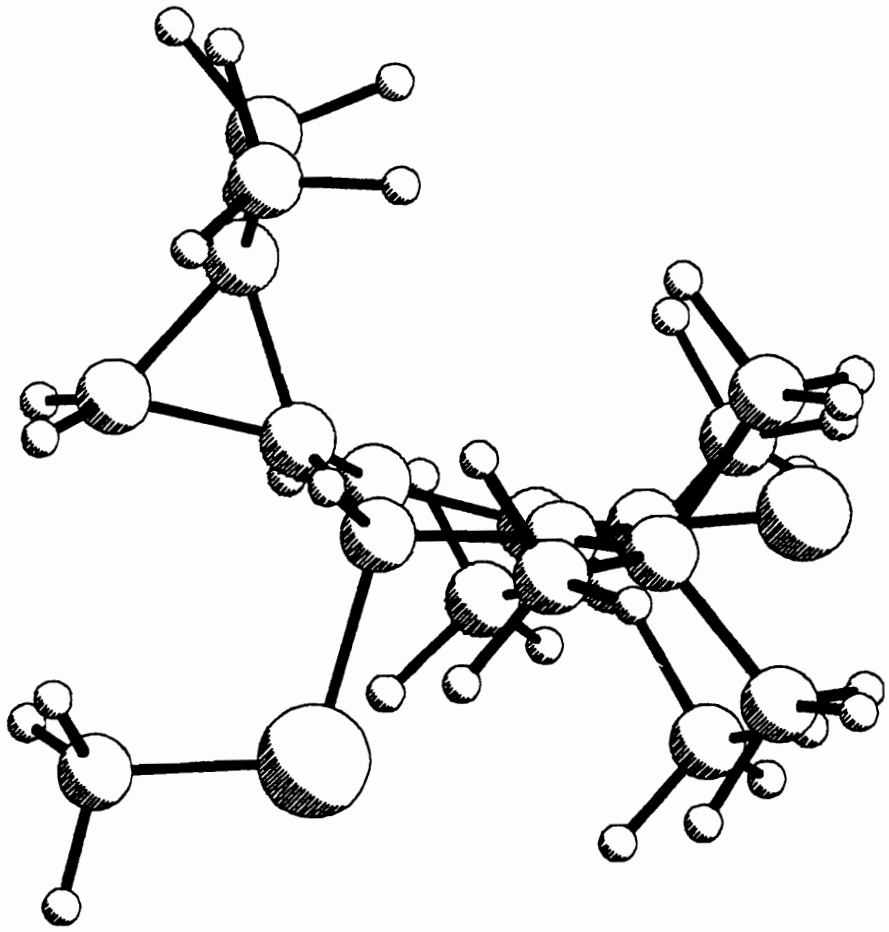

**Figure 51: Structural geometry of enolate anion 72.**

The difference in energy between the two enolate anions has been calculated at ca. 2 kcal/mol (SCF-MO AM1, RHF). The final step in this mechanism is the intramolecular nucleophilic attack of sulfur on the cyclopropyl ring resulting in **62** and **63**, **Scheme 48**.

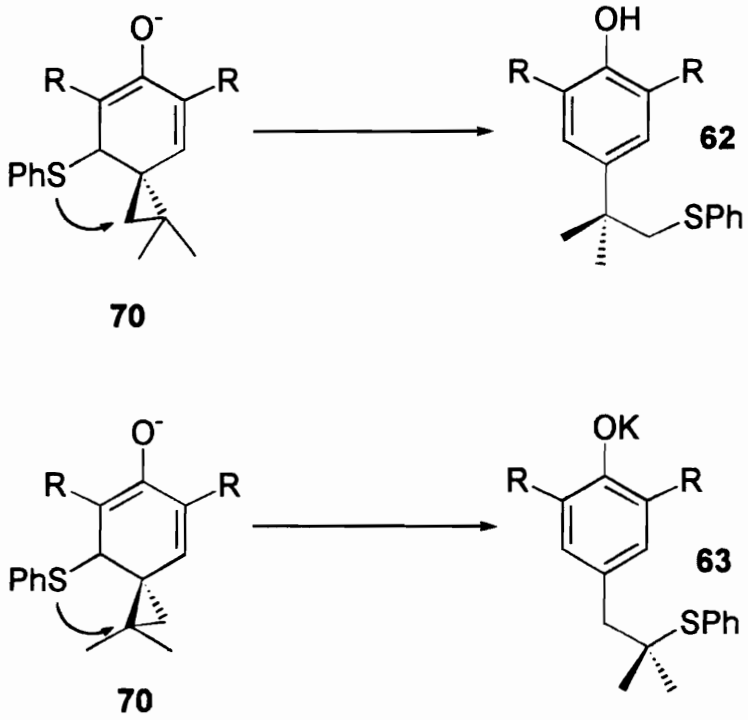


**Scheme 48**

This is clearly a second order process dependent upon both the concentration of the nucleophile and **20**. Therefore, concentration experiments and competition experiments support the possibility of this mechanism. However, there are inconsistencies with this type of mechanism as the explanation for the formation of **63**.

A close inspection of the resulting enolate ions **71** and **72** reveals that the geometry between sulfur and the cyclopropyl ring is such that very little orbital interaction can occur. Therefore, one would expect to obtain final products with thiophenoxide substituted on the cyclohexadienonone ring, **73**. The absence of a cyclohexadienone ring substituted sulfides from protonation of the resulting enolate indicates that the enolate is not being produced and that this mode of addition is not in operation.

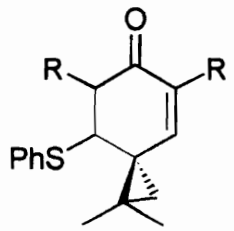


**73**

This leaves a direct nucleophilic attack on the cyclopropane ring as the remaining possibility for the formation of **63**.

There are several places on the cyclopropyl ring where interaction between thiophenoxide and **20** can occur; however, substitution at two of these positions would have to occur through a trajectory that would bring the thiophenoxide across the face of the cyclopropyl ring, **Figure 52**.

**Attack across cyclohexadiene ring**

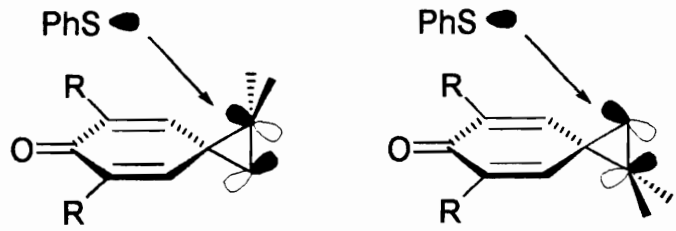


**End cyclopropyl ring attack**

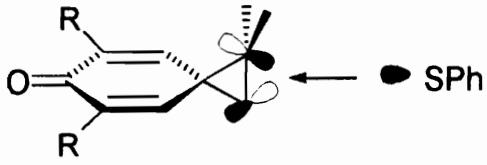


**Figure 52: Trajectories associated with thiophenoxide substitution of the cyclopropyl ring.**

The steric hindrance to approach across the cyclohexadienone ring would prohibit substitution via this trajectory. This leaves an end on approach as the only means for addition.

The phenomenon for attack at the most substituted center of a cyclopropane ring is not unknown. Only 1,7 addition has been observed in the anionic polymerization of 5,7-dimethyl-1-vinylspiro[2,5]octa-4,7-dien-6-one in DMF, **Scheme 43**.[91] Moreover, Danishefsky et. al. noted this phenomenon in the reaction of vinyl and ethyl substituted doubly activated cyclopropanes with dimethyl sodiomalonate and piperidine at room temperature, **Scheme 49**.[98,99]

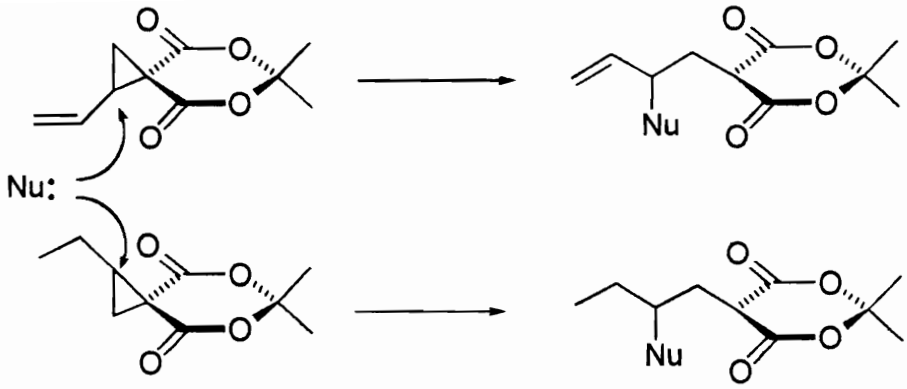


**Scheme 49**

Substitution occurs only at the most hindered cyclopropane carbon. Furthermore, when nucleophiles are tethered to the cyclopropane ring nucleophilic attack occurs through a spiro ring opening, **Scheme 50**.[100]


**Scheme 50**

The preference for attack at the more substituted position occurs because the doubly activating linkages confer greater polarization of charge than what would be observed for singly activated cyclopropanes, **Figure 53**.

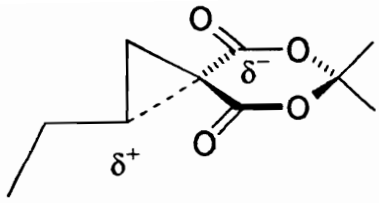


**Figure 53: Charge separation exhibited in doubly activated cyclopropanes.**

This should not be confused with the formation of a formal negative or formal positive charge; it should be viewed as a polarization of charges away from the more substituted cyclopropyl carbon. Molecular orbital calculations (SCF-MO AM1) show that electron density is less at the tertiary carbon center of **20**; therefore, this is expected to be reflected in the regiochemistry of substitution at the cyclopropane ring.

The direct nucleophilic attack of potassium thiophenoxide on **20** will proceed through interaction of the nucleophile with the LUMO of the cyclopropyl ring. Unlike aliphatic systems in which orbital interaction must occur at the carbon atom undergoing substitution, orbital interaction between thiophenoxide and **20** will occur through the LUMO of the p-orbitals which form the cyclopropyl ring backbone, **Figure 54**.

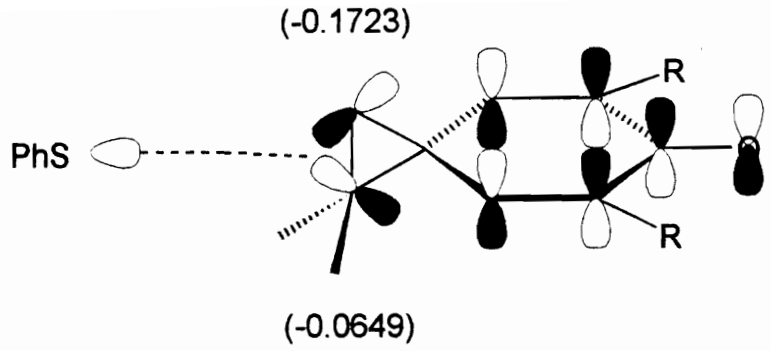


**Figure 54: Thiophenoxide orbital interaction with the cyclopropyl ring of 20.**

The interaction between the p-orbitals of the cyclopropyl ring and the nucleophile can then either result in ring cleavage to **62** or **63**, **Figure 55**.

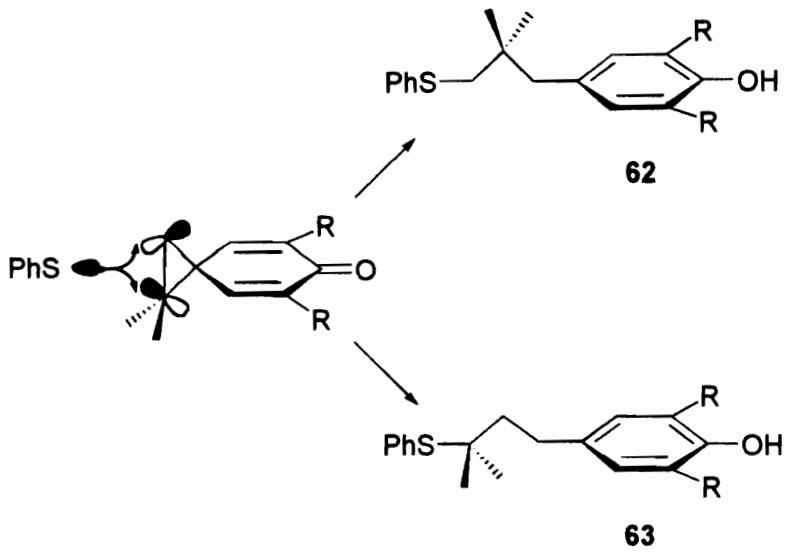


**Figure 55: Orbital interactions between thiophenoxide and 20 resulting in cyclopropyl ring cleavage.**

Steric effects favor the formation of **62**. However, electronic effects place less electron density at the tertiary carbon center (-0.0649) than at the primary carbon center (-0.1723). Therefore, electronic effects will favor addition to the tertiary center. The electronic effects exhibited in the LUMO will also be present in the transition state. As the nucleophile approaches the p-orbitals of the cyclopropyl ring and orbital interaction begins, the faster addition will be the one in which the steric hindrance is lowest. The nucleophile will be drawn to the lower electron density of the tertiary carbon center; however, addition at the tertiary center will be slower due to steric hindrance. One would expect **62** to occur in greater yields than **63**. This is in agreement with the experimental results observed. Therefore, the products and product ratios observed in region A are a result of competing $S_N2$ substitution reactions.

In region B of **Figure 43** the formation of all products exhibited a first order dependence on thiophenoxide concentration. Therefore, it was ascertained that the formation of **62** and **64** occurred through a $S_N2$ substitution mechanism similar to that exhibited in region A. The reaction resulting in the formation of **63** and **65** also proceed with a first order dependence on thiophenoxide concentration, however, the solvent studies indicate that formation of these sulfides proceeds via through an ionic intermediate. Concentration and competition studies are consistent with the formation of the sulfides through either a $S_{ET}2$ or $S_N2C+$ mechanism, **Scheme 50**.

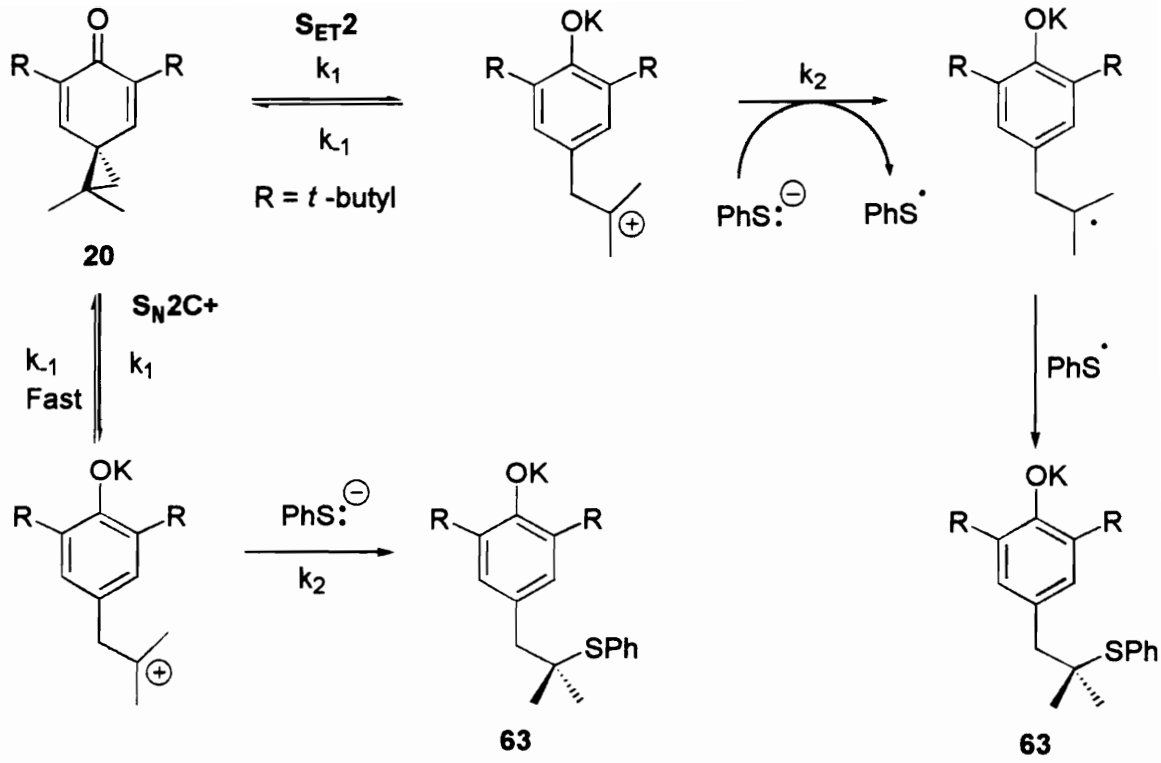


**Scheme 50**

If indeed **63** and **65** are forming via an $S_N2C+$ mechanism, it is the first case of this mechanism in which the occurrence was not dependent on highly polar solvents, very strong common ion effects, conjugation of the carbocation with a phenyl ring, or rate retardation due to the steric hindrance of the nucleophile. However, the results are also consistent with the occurrence of the $S_{ET}2$ mechanism. Moreover, the estimated rate for the electron transfer from thiophenoxide to the carbocation generated from **20** is comparable to what one would expect for a nucleophilic addition to a carbocation.

The electron transfer from thiophenoxide to **20** was prevented by a barrier of > 50 kcal/mol; however, the energy needed to overcome the barrier for electron transfer to **20** will not be the same as the energy needed for electron transfer to the analogous carbocation as would be the case in a $S_{ET}2$ reaction. The reduction potential of the tertiary carbocationic intermediate of **20** has not been measured; therefore, it is impossible to directly determine the thermodynamics of SET to this intermediate. However, the oxidation potential of the *t*-butyl radical has been determined. Using the *t*-butyl radical as a model it is possible to get an estimate of the free energy for SET between thiophenoxide and the tertiary carbocationic intermediate of **20**. The oxidation potential of *t*-butyl radical is 0.09 V (SCE). The oxidation potential of thiophenoxide is -0.3 V (SCE). The free energy for electron transfer from thiophenoxide to the *t*-butyl cation is shown in **Figure 56**.

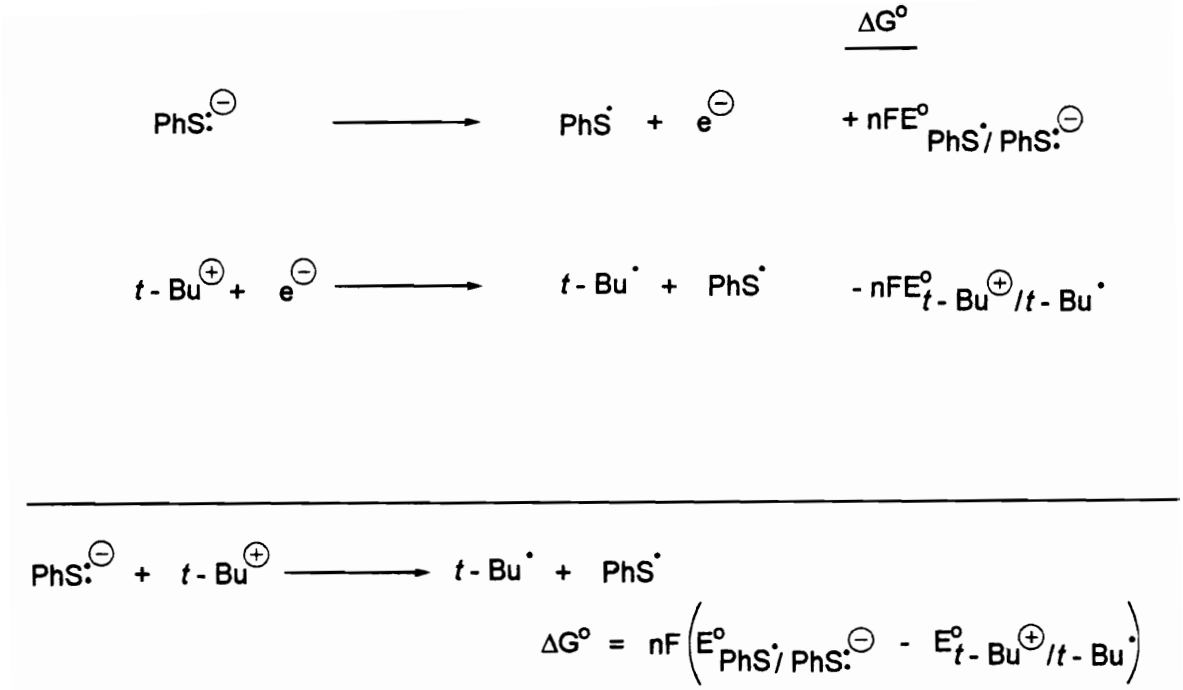


**Figure 56: Free energy associated with electron transfer from thiophenoxide to the *t*-butyl cation.**

Through the use of **Equation 29** the rate of electron transfer can be calculated.[46]

**Eqn. 29**

$$k = (kT / h) \exp(-\Delta G^{\ddagger} / RT)$$

A ΔG of 4 kcal/mol for SET to the carbocationic intermediate of **20** equates to a $k_{SET}$ of $7.2 \times 10^{9} M^{-1} s^{-1}$, a comparable rate to what one would expect for the nucleophilic

addition of thiophenoxide to the carbocation. The facile nature of this electron transfer process thus, makes it a competing process to the $S_N2C+$ mechanism.

To try to differentiate between the $S_N2C+$ and $S_{ET}2$ mechanisms, future work may involve identifying highly nucleophilic species with oxidation potentials unfavorable enough to prevent the occurrence of SET to the carbocationic intermediate produced in the $S_N2C+$ mechanism. It is hoped that the utilization of a nucleophiles such as $CN^-$ (0.86 V vs. SCE) or $SCN^-$ (0.76 V vs. SCE)[101] with $\Delta G$ values of 22 kcal/mol ($k_{SET} = 4.5 \times 10^{-4}$ $M^{-1}$ $s^{-1}$) and 20 kcal/mol ($k_{SET} = 1.3 \times 10^{-2}$ $M^{-1}$ $s^{-1}$), respectively, for SET to the *t*-butyl cation will be unfavorable enough to prohibit SET to the carbocationic intermediate of **20** and thus allow observation of the $S_N2C+$ mechanism.

## SUMMARY

The reaction between **20** and thiophenoxide in polar protic solvents proceeds through an $S_N2$ reaction in competition with a process proceeding through a carbocationic intermediate. The carbocationic mechanism through which the tertiary sulfide is forming is second order with a rate dependent on the concentrations of both substrate and thiophenoxide, eliminating the possibility that product formation was occurring through a classical $S_N1$ reaction. Further studies have revealed that the mechanism through which the tertiary sulfide is being formed is either via the $S_N2C+$ or the $S_{ET}2$ mechanism. If indeed formation of the tertiary sulfide is proceeding the $S_N2C+$ mechanism, this is the first occurrence of the $S_N2C+$ mechanism under normal reaction conditions, with non-

hindered nucleophiles, to produce non-resonance stabilized secondary and tertiary carbocations.

In the reactions utilizing polar aprotic solvents, the sulfides are produced via competing $S_N2$ processes. The formation of **63** via an $S_N2$ process is afforded by electronic effects placing less electron density at the tertiary carbon center. Due to steric hindrance the predominant sulfide is **62**, however the electronic effects seem to outweigh the steric effects to some extent and allow the formation of **63** via an $S_N2$ reaction. This seems to be the first example of addition to the 3° carbon center of a cyclopropyl group with carbon as a leaving group without the aid of Lewis acid catalysis.

# CHAPTER 5. CONCLUSIONS

## 1. Development and Characterization of a New Class of SET Probes.

The chemistry presented in the previous pages details the successes and setbacks encountered in the development and characterization of a new class of substrates to probe for the occurrence of SET in the reactions of nucleophiles with carbonyl compounds. Previous studies in our lab examined the suitability of phenyl cyclopropyl ketones as probes for SET. Radical anions generated from these compounds underwent sluggish ring opening. It was reasoned that the relief of cyclopropyl ring strain by ring opening was not sufficient to counteract the loss of resonance energy associated with the delocalization of the radical into the phenyl ring. Therefore, the radical anions preferred the cyclopropyl ring closed form and, thus, were unable to unambiguously detect SET pathways even when they were occurring.[36,37] We set out to correct this in the next generation of SET probes: spiro[2,5]cyclooctadienones.

The basic premise behind use of these substrates as SET probes is that upon one electron transfer, the relief of ring strain associated with cyclopropyl ring opening would work in conjunction with the resonance energy gained from the establishment of aromaticity, resulting in a very facile ring opening. Moreover, substitution of the cyclopropane ring would direct the regiochemistry of cyclopropyl ring opening to the more stable distonic radical anion. Based upon radical stabilities we felt that **20** would undergo selective ring opening to the more stable 3° radical.

The estimated reduction potential of **20** is -2.2 V vs. SCE, similar to other aryl ketones and enones. As a result, the occurrence of SET in the reaction of **20** with a particular nucleophile may indicate that SET is occurring in carbonyl compounds of similar reduction potential. The cyclopropyl ring opening of **20** occurs at a estimated rate of $k \geq 10^7 s^{-1}$ in a 9:1 ratio of the 3° to 1° distonic radical anion. Through the use of semi-empirical molecular orbital calculations (AM1), the enthalpy for this process was determined in this study to be exothermic by more than 15 kcal/mol. In comparison the enthalpy of ring opening for the cyclopropylcarbinyl radical is - 3 kcal/mol,[38] indicating the extremely facile nature of the ring opening observed in **20**. The regiospecificity of the cyclopropyl ring opening suggests that identification of SET could be achieved through simple product analysis.

## 2. Utilization of 20 as a SET Probe

Characterization of **20** indicated that it was a viable substrate for utilization as a SET probe. To confirm this hypothesis, reactivity studies were conducted between **20** and nucleophiles confirmed to proceed through SET in their reactions with carbonyl compounds. Based on the preponderance of literature indicating that Grignard reagents and organolithiums proceed through SET in their reactions with carbonyl compounds, these reagents were chosen as nucleophiles for the reactivity studies.

Upon reaction of **20** with methylmagnesium bromide and methyllithium, products obtained from substitution at the <u>most</u> <u>hindered</u> carbon were observed, unambiguously

signaling the occurrence of SET in the reactions of these nucleophiles with **20**. Moreover, the radical formed as a result of electron transfer from the nucleophile was effectively trapped, leaving little ambiguity as to the occurrence of electron transfer.

Once we had established that **20** was able to identify SET pathways in the reactions of nucleophiles with carbonyl compounds, we began to investigate the occurrence of SET in the reactions with nucleophiles in which SET had not been firmly established. The first of these studies involved the reaction of **20** with lithium dimethylcuprate. The regiospecificity of the cyclopropyl ring opening at the least hindered position suggested that nucleophilic addition to **20** was occurring through a polar pathway, although a pathway involving SET could not be rigorously excluded.[74]

## 3. Limitations of 20 as a SET Probe.

The final investigation of this study involved the reaction of **20** with potassium thiophenoxide. In this investigation the limitations of **20** as a SET probe became apparent. Initial indications in this investigation suggested that SET was occurring in the reaction of thiophenoxide with **20**. However, once the free energy for electron transfer had been established at > 50 kcal/mol endothermic it became apparent that SET was not responsible for the observed products. Upon elimination of pathways involving radical intermediates, it became apparent that the addition of thiophenoxide to **20** was proceeding through polar pathways.

Employing both concentration and solvent studies to determine the mechanism of this reaction, the limitations associated with the use of this probe for the detection of SET surfaced. In protic solvents reaction of thiophenoxide with **20** proceeds through competing $S_N2/S_N2C+$ or competing $S_N2/S_{ET}2$ mechanisms. The same structural features that provide a facile ring opening upon the addition of an electron also provides a route for a rapid ring opening to the charge separated anion/cation pair. Due to the availability of a carbocationic pathway for the addition of nucleophiles to **20** in polar protic solvents, these solvents can not be used to probe for SET pathways.

In aprotic solvents it was found that the reaction of thiophenoxide with **20** occurred through competing $S_N2$ pathways with attack at both the tertiary and primary centers of the cyclopropane ring. As expected, attack was favored at the primary position; however, unexpectedly the selectivity never exceeded a 6:1 ratio of primary to tertiary sulfides. Therefore, the appearance of a small amount of tertiary products upon reaction of **20** with a nucleophile can not be ascribed to SET until the other methods of reaction have been eliminated. Due to the appearance of carbocationic pathways in protic solvents and the ability for $S_N2$ reactions to occur at the tertiary cyclopropane center in polar aprotic solvents, **20** can not be utilized to unambiguously identify SET in the reactions of nucleophiles to carbonyl compounds.

# CHAPTER 6. EXPERIMENTAL

## INSTRUMENTATION

Melting points were determined using a Thomas Hoover capillary melting point apparatus and are uncorrected. High pressure liquid chromatography (preparatory and analytical) was performed using a Beckman System Gold Model 128 solvent pump system. Detection was afforded through the use of a Beckman System Gold Model 166 UV-VIS detector (@ 250 nm, unless otherwise noted). Integration was accomplished with an IBM 466/SI running Beckman System Gold Software. Samples were analyzed and separated using Beckman C-19 reverse phase columns (analytical 4.6 mm x 250 mm; preparatory 21.2 mm x 150 mm) with acetonitrile/water solvent mixtures. Typical flow rates were 1 mL/min for analytical separations and 22 mL/min for preparatory separations. Gas chromatographic analyses were performed on a Hewlett Packard HP 5890 instrument equipped with FID detectors, a HP 3393A integrator, and on either an Alltech SE-54 capillary column (30 m x 0.25 mm) or a Supelco SE-30 capillary column (15 m x 0.25 mm). Ultraviolet spectra were acquired through the use of a Hewlett Packard HP 8452A Diode Array UV-VIS spectrophotometer. Data manipulation was implemented using a Hewlett Packard Vectra VL2/50 personal computer using Hewlett Packard general scanning software. Infra-red (IR) spectroscopy was performed on a Perkin-Elmer 1600 Series FT-IR spectrophotometer. All data are reported in $cm^{-1}$. Nuclear magnetic resonance (NMR) spectra were obtained using either a Bruker WP-200 or WP-270

spectrometer. Chemical shifts are reported in units of δ relative to tetramethylsilane (TMS) (δ 0.00 ppm). Low resolution GC-MS was performed on a Hewlett Packard HP 5890 gas chromatograph utilizing a HP 1% methyl phenyl silicone gum column (12.5 m x 0.2 mm) interfaced to a HP 5970 mass spectrometer and a HP series computer. High resolution and low resolution MS was performed on a VG-7070E mass spectrometer, employing EI ionization at 70 EV. Flash chromatography[102] was performed on silica gel (Aldrich Grade 60, 630-400 mesh) using ethyl acetate/hexane mixtures. Thin layer chromatography (TLC) was performed on precoated polyester silica gel plates (Whatman) with a fluorescent background. Electrochemical measurements were performed on a Princeton Applied Research (EG&G/PARR) Model 273 potentiostat/galvanostat interfaced to a 486-DX2 personal computer. Analysis was afforded using FORTH implemented through ASYST.

## MATERIALS AND PURIFICATION

All materials were purchased from the vendors noted in brackets. Unless a purification step is noted, the materials were used as received.

**Purification of Tetrahydrofuran and Diethyl Ether**

Diethyl ether (Mallinckrodt) and tetrahydrofuran (Mallinckrodt), THF, were dried prior to use. In both cases lithium aluminum hydride (Aldrich 95%), LAH, was added until gas evolution had ceased. At this point a small excess of lithium aluminum hydride

was then added (» 1 g/L). The activity of the still was monitored by adding a small amount of the mixture to water. Gas evolution confirmed that the still was active and the ethers were dry. The ethers were refluxed for two hours under argon and the appropriate amounts of the ethers were then distilled.

**Purification of Dimethyl Sulfoxide[103]**

Dimethyl sulfoxide (Fisher), DMSO, was purified by adding an excess of calcium hydride (Aldrich 90-95%). The mixture was then allowed to stir for two hours. Dimethyl sulfoxide was then distilled at reduced pressure. Only the middle cut was taken for subsequent use.

**Purification of Acetone, Ethyl Acetate, Pyridine, *tert*-Butanol, *iso*-Propanol, Ethanol, and Methanol**

Acetone (JT Baker HPLC Grade), ethyl acetate (Mallinckrodt), pyridine (Fisher), *tert*-butanol (Aldrich 99+%), *iso*-propanol (EM Scientific), ethanol (AAPER 100%), and methanol (JT Baker HPLC Grade) were used as received after bubbling with argon to remove oxygen that may exist. The solvents were stored under argon and canuled as needed.

**Purification of N,N-Dimethylformamide[103]**

N,N-Dimethylformamide (EM Scientific), DMF, was stirred over anhydrous copper(II)sulfate (Fisher) (10 g/L) and activated neutral alumina (30 g/L) (Aldrich, Brockmann I) under argon for three days and then distilled (bp. 35° C, 7 mm Hg). The middle cut was saved and stored under argon. DMF was utilized within three days to ensure purity.

**Activation of Neutral Alumina**

Neutral alumina (activated, neutral, Brockmann I, 150 mesh, Aldrich) was placed in a flask under vacuum and heated with a flame until bumping subsided. The flask cooled under vacuum, filled with argon, and stoppered tightly. Alumina was activated before every use.

**Purification of Argon**

Argon (Airco UN 1006) was passed through an oxygen removal tower (5.4 cm x 84.5 cm, Kontes) packed with 1 kg of BASF oxygen binding catalyst R3-11.[104] The catalyst was heated at 125° C with a heating cord. The argon was then passed through a cooling coil into a moisture trap (4.4 cm x 45.7 cm, American Scientific) packed with 4 Angstrom, indicating molecular sieves. Copper tubing (1/8") was used for interconnections between the electrochemical cell, the drying tower, the catalyst tower, and the argon tank.

**Titration of Methyllithium.**[105] Methyllithium was syringed into a preweighed amount of 2,5-dimethoxybenzyl alcohol (Aldrich, 99%) dissolved in 5 mL of dry argon purged THF until the color of the solution changed to light pink. The results of three experiments were used to give an average molarity.

**Purification of exo-methylene cyclopropyl phenyl ketone (52)**. Purification of **52** was afforded using a kugelrohr distillation apparatus at 1 mm Hg. This produced a clear liquid that was stored under argon in the refrigerator. This material was used for voltammetry after the substrate had warmed to room temperature.

## SYNTHESIS OF STARTING MATERIALS

**Synthesis of 1,1-Dimethyl-5,7-di-t-butylspiro[2,5]octa-4,7-dien-6-one (20).**[50,51,52,53]

***iso*-Butanoyl Chloride.** To 138.8 g (1.58 mol) of *iso*-butyric acid (Aldrich 99%) was added 635 g (1.98 mol) of thionyl chloride (Aldrich 97%). The mixture was gently warmed for one hour. Refluxing for two hours, followed by distillation (bp. 84-88, lit.[106] bp. 91-93) yielded 159 g (94%) of *iso*-butanoyl chloride.

**α-Methyl-3,5-di-*tert*-butyl-4-hydroxypropiophenone (24).** To 79.5 g (0.75 mol) of *iso*-butanoyl chloride was added with stirring 79.35 g (0.65 mol) of $AlCl_3$ (Aldrich 98%). After cooling the mixture to -15° C, 103 g (0.5 mol)of 2,6-di-*t*-butylphenol (Aldrich 96%) dissolved in 79.5 g (0.75 mol) of *iso*-butanoyl chloride was added slowly while maintaining the temperature below 0° C. Stirring was accomplished using a mechanical stirrer. The resulting purple mixture was allowed to stir for approximately 1 minute after addition was complete. At this point the reaction mixture was poured slowly into 500 mL of ice water. The resulting yellow solution/solid was extracted with 3 x 1000 mL portions of diethyl ether. The ether was then washed with 3 x 500 mL portions of 1% NaOH and 3 x 500 mL portions of water. The layers were separated and the ethereal layer dried with $MgSO_4$ (Mallinckrodt). The ether was concentrated until the ketone began solidifying. The resulting solution was filtered, and the process was repeated until 121 g (88%) of the crude ketone was obtained. After successive recrystallizations in 100% ethanol, 95 g (69%) of the pure ketone was obtained ( mp 137-138° C, lit.[51] mp 125-127° C).

**$^1$H NMR** ($CDCl_3$) δ 1.2 (d, 6H, J = 6 Hz, dimethyl), 1.5 (s, 19H, di-*t*-butyl), 3.39 (m, 1H, methine), 5.75 (s, 1H, phenol), 7.9 (s, 1H, aromatic ring).

**α-Bromo-α-methyl-3,5-di-*tert*-butyl-4-hydroxypropiophenone (26).** To 66.7 g (0.638 mol) of **24** in 330 mL of ethyl acetate and 620 mL of chloroform (EM Scientific) was added 162.0 g (0.548 mol) of copper(II) bromide (Aldrich 99%). The mixture was heated at reflux with stirring for 1.75 h. At this time HBr evolution had stopped and the mixture was pea green in color. The solid was gravity filtered and washed with 4 x 100 mL aliquots of ethyl acetate. The resulting green solution was passed through a 6 inch plug of alumina to remove the remaining copper in the solution. The solvent was removed *in vacuo*, leaving a light yellow solid. The solid was recrystallized in hexane (Mallinckrodt) yielding 84.25 g (93%) of **26** (mp 140.5-142° C, lit.[51] mp 141-142).

**$^1$H NMR** ($CDCl_3$) δ 1.47 (s, 19H, di-*t*-butyl), 2.05 (s, 6H, dimethyl), 5.73 (s, 1H, phenol), 8.16 (s, 2H, aromatic ring).

**2-Methyl-2-(3′,5′-di-*tert*-butyl-4′-hydroxyphenyl)-1-propanol (28).** To 45.12 g (0.126 mol) of **26** dissolved in 1200 mL of dry diethyl ether cooled to 0° C under argon was added slowly, with the aid of mechanical stirring, 10.32 g (0.27 mol) of LAH . Upon completion of the addition, the solution was refluxed for three hours. Water was then carefully added until bubbling subsided. In order to dissolve the resulting aluminum hydroxide 10% sulfuric acid was added. The ethereal layer was separated and dried with anhydrous magnesium sulfate. Removal of the solvent and recrystallization from ethyl acetate/hexane resulted in 32.4 g (92%) of **28** (mp 146-148° C, lit.[51] mp 149.8-150.3° C).

**$^1$H NMR** ($CDCl_3$) δ 1.32 (s, 6H, dimethyl), 1.44 (s, 19H, di-*t*-butyl), 3.56 (s, 2H, methylene), 5.11 (s, 1H, phenol), 7.17 (s, 2H, aromatic).

**2-Methyl-2-(3′,5′-di-*tert*-butyl-4′-hydroxyphenyl)-1-propyl tosylate (30).** To 27.8 g (0.105 mol) of **28** in 300 mL of dry pyridine at -30° C was added with stirring 63.5 g (0.163 mol) of *p*-toluenesulfonyl chloride (Kodak). The mixture was then warmed to 0° C and allowed to stir for an additional 8.5 h. Upon addition of cold water to the mixture a white solid formed. The mixture was extracted into ether and the ether separated. The ether was washed with 3 x 500 mL aliquots of water to remove residual pyridine. Drying the ether layer with anhydrous magnesium sulfate, filtration, and removal of the solvent afforded 38.6 g (89.4%) of **30** (mp 102° C, lit.[52] mp 100-102° C).

**$^1$H NMR** ($CDCl_3$) δ 1.31 (s, 6H, dimethyl), 1.41 (s, 19H, di-*t*-butyl), 2.43 (s, 3H, tosylate methyl), 3.94 (s, 2H, methylene), 5.12 (s, 1H, phenol), 7.07 (s, 2H, aromatic), 7.28 (d, 2H, J = 8.1 Hz, tosylate aromatic), 7.68 (d, 2H, J = 8.3 Hz, tosylate aromatic).

**1,1-Dimethyl-5,7-di-*tert*-butylspiro[2,5]octa-4,7-dien-6-one (20).** To 12.2 g (0.283 mol) of **30** in 60 mL of dry THF under argon was added 3.81 g (0.034 mol) of potassium *tert*-butoxide (Aldrich 95%). The mixture was stirred for 3 h and then added to 200 mL of ether. The ethereal solution was washed with 3 x 50 ml aliquots of 1% sodium hydroxide. The ether was then separated and dried with anhydrous magnesium sulfate. Filtration of the magnesium sulfate and removal of the ether yielded 7.3 g (99%) of **20**. Recrystallization by freezing the solid from a minimum amount of hexane resulted in a

pure **20** (mp 86-88° C, lit.[52] mp 92-94° C). **$^1$H NMR** ($CDCl_3$) δ 1.26 (s, 19H, di-*t*-butyl), 1.40 (s, 6H, dimethyl), 1.66 (s, 2H, cyclopropyl methylene), 6.45 (s, 2H, dienone).

**Synthesis of 1-Methyl-5,7-di-t-butylspiro[2,5]octa-4,7-dien-6-one (19).**[50,51,52,53]

**3,5-di-*tert*-butyl-4-Hydroxypropiophenone (23).** The compound was prepared as described in the procedure for **24**, however, propionyl chloride (Aldrich) was used for the acetylation reagent. Purity was confirmed by HPLC. Identification was confirmed through comparison to literature $^1$H NMR spectrum.[49,50,51,52]

**$^1$H NMR** ($CDCl_3$) δ 1.21(t, 3H, J = 7 Hz, methyl), 1.47 (s, 19H, di-*t*-butyl), 2.95 (q, 2H, methylene), 5.70 (s, 1H, phenol), 7.85 (s, 2H, aromatic).

**α-Bromo-3,5-di-*tert*-butyl-4-hydroxypropiophenone (25).** The compound was prepared as described in the procedure for **26**. Purity was confirmed by HPLC. Identification was confirmed by the $^1$H NMR spectrum.[49,50,51,52]

**$^1$H NMR** ($CDCl_3$) δ 1.47 (s, 19H, di-*t*-butyl), 1.9 (d, 3H, J = 7.1 Hz, methyl), 5.25 (q, 1H, J = 7.3 Hz, methine), 5.8 (s, 1H, phenol), 7.9 (s, 2H, aromatic).

**2-(3′,5′-di-*tert*-butyl-4′-hydroxyphenyl)-1-propanol (27).** The compound was prepared as described in the procedure for **26**. However, residual solvent had to be removed through the use of a vacuum pump in order for a solid to form. Purity was confirmed by the HPLC. Identification was confirmed by the $^1$H NMR spectrum.[49,50,51,52]

**$^1$H NMR** ($CDCl_3$) δ 1.24 (d, 3H, J = 6.9 Hz, methyl), 1.44 (s, 19H, di-*t*-butyl), 2.7 (m, 1H, J = 7.4 Hz, methine), 3.3 (dd, 1H, $J_{AB}$ = 10.8 Hz, $J_{AX}$ = 7.7 Hz, methylene), 3.4 (dd, 1H, $J_{AB}$ = 10.8 Hz, $J_{BX}$ = 6.0, methylene), 5.1 (s, 1H, phenol), 7.02 (s, 2H, aromatic).

**2-(3′,5′-di-*tert*-butyl-4′-hydroxyphenyl)-1-propyl tosylate (29).** The compound was prepared as described in the procedure for **30**. The tosylate was recrystallized in ethyl acetate/ hexane. Purity was confirmed by the HPLC. Identification was confirmed by the $^1$H NMR spectrum.[49,50,51,52]

**$^1$H NMR** ($CDCl_3$) δ 1.30 (d, 3H, J = 8.4 Hz, methyl), 1.41 (s, 19H, di-*t*-butyl), 2.43 (s, 3H, tosylate methyl), 2.93 (m, 1H, J = 7.4 Hz, methine), 3.97 (dd, 1H, $J_{AB}$ = 8.9 Hz, $J_{AX}$ = 5.8 Hz, methylene), 4.1 (dd, 1H, $J_{AB}$ = 8.9 Hz, $J_{BX}$ = 9.4 Hz, methylene), 5.12 (s, 1H, phenol), 6.93 (s, 2H, aromatic), 7.29 (d, 2H, J = 7.3 Hz, tosylate aromatic), 7.70 (d, 2H, J = 7.3 Hz, tosylate aromatic).

**1-Methyl-5,7-di-t-butylspiro[2,5]octa-4,7-dien-6-one (19).** The compound was prepared as described in the procedure for **20**. High purity substrate was obtained through preparatory HPLC using 80/20 acetonitrile water mixtures. Identification was confirmed by comparison to the literature $^1$H NMR.[49,50,51,52]

**$^1$H NMR** ($CDCl_3$) δ 1.25 (d, 19H, J = 5 Hz, di-*t*-butyl), 1.36 (d, 3H, J = 6.3 Hz, methyl), 1.41 (dd, 1H, $J_{AB}$ = 8.5 Hz, $J_{AX}$ = 4.4 Hz, cyclopropyl $CH_2$), 1.66 (m, 1H, $J_{AB}$ = 8.5 Hz, $J_{BX}$ = 3.2 Hz, cyclopropyl $CH_2$), 1.86 (m, 1H, J = 7.5 Hz cyclopropyl CH), 6.03 (d, 1H, J = 2.7 Hz, aromatic), 6.38 (d, 1H, J = 2.7 Hz, aromatic).

**Synthesis of Potassium Thiophenoxide.** To a solution of 50 mL of 100% ethanol and 1.12 g of potassium hydroxide (20.0 mmol) was added with stirring 2.05 mL (20.0 mmol) of thiophenol (Aldrich 97%). The solution was allowed to stir for an additional 3 h after which the solvent was removed *in vacuo*. The resulting white solid was stirred with 4 x

50 mL aliquots of diethyl ether, cannulating the ether off each time. Removal of the ether yielded pure potassium thiophenoxide. Identity determined by NMR, purity checked by HPLC using a 95/5 acetonitrile water mixture.

**$^1$H NMR** ($CDCl_3$) δ 6.43 (t, 1H, J = 7.9 Hz, *para* proton), 6.69 (t, 2H, J = 7.8 Hz, *meta* protons), 7.04 (d, 2H, J = 7.9 Hz, *ortho* protons)

**Synthesis of Ethyl Phenyl Sulfide (69).** Iodoethane (5.6 g; 36.0 mmol) (Aldrich 99%) was added to 10 mL of dry acetone. Potassium thiophenoxide (5.36 g; 36.0 mmol) was added to the reaction mixture then allowed to stir. The reaction mixture was monitored via HPLC. After disappearance of the starting material the solvent was removed leaving a light yellow liquid. This liquid was distilled (bp. 50°C, 2.0 mm Hg consistent with lit.[107] bp. 204° C) yielding 4 g (80%) of colorless liquid.

**$^1$H NMR** ($CDCl_3$) δ 1.30 (t, 3H, J = 9.9 Hz, methyl), 2.92 (q, 2H, J = 9.9 Hz, methylene), 7.27 (m, 5H, aromatic)

**Quantitation Procedure for Gas Chromatographic Analyses**

Gas chromatographic quantitation of the reaction mixtures was accomplished by isolating the products produced from the reactions being studied via flash column chromatography employing hexane/ethyl acetate mixtures. After isolation and purification, the reaction products were identified utilizing both $^{1}H$ and $^{13}C$ NMR spectroscopy. The purified materials were each analyzed to ascertain their respective $R_f$ values. The response factor of each substrate was determined by comparing the area of a preweighed amount of a standard (either biphenyl or 2,6-di-*t*-butylphenol) to the area obtained from a preweighed amount of purified substrate. Once the response factors had been determined, the weights of material produced in a particular reaction could be extracted directly from the chromatogram. The values reported are the average of a minimum of three injections.

**Calibration Procedure for the High Pressure Liquid Chromatograph**

High pressure liquid chromatograph calibration of the reaction was accomplished by isolating the products produced from the reactions of **19** and **20** with thiophenoxide via the HPLC employing acetonitrile/water mixtures. After isolation and purification, the reaction products were identified utilizing both $^{1}H$ and $^{13}C$ NMR spectroscopy. The purified materials were each analyzed in 80:20 acetonitrile/water mixtures to ascertain their respective $R_f$ values. Calibration of the HPLC proceeded by analyzing 4 known concentrations of each substrate in 10 mL of acetonitrile @ 254 nm employing 80:20

acetonitrile/water mixtures and then constructing a calibration curve via the Beckman System Gold® software. The calibration curve was automatically incorporated into the chromatographic method being utilized, which allowed the direct determination of the amounts of material produced in the reaction from the chromatogram. The data reported are the averages of at least 3 x 100 μL injections from a 10mL acetonitrile solution of the reaction mixtures. Each experiment was conducted a minimum of two times to insure the accuracy of the measurements.

**Reaction of 20 with methylmagnesium bromide.** A 2.7 M solution of methylmagnesium bromide (0.623 g; 20.0 mmol) in diethyl ether was added with stirring to a solution of **20** (0.26 g; 1.0 mmol) dissolved in 4 mL of dry THF cooled to 0° C. The solution was allowed to warm to room temperature and stir for 2 h. The mixture was acidified with 1% $H_2SO_4$ and then extracted with 3 x 50 mL aliquots of ether. The ethereal layer was dried with anhydrous magnesium sulfate. The drying agent was filtered and the ether removed *in vacuo* to yield 0.26 g (96%) of crude product. The crude product was column chromatographed using 200:1 hexane/ethyl acetate to yield **39**, **40**, **41**, **57**, and **58**. The following yields were obtained through gas chromatographic quantitation versus 2,6-di-*t*-butylphenol (Aldrich 99%):

recovered starting material - 100.1 mg ($3.8 \times 10^{-4}$ mol; 39%)

**39**- 75.4 mg ($2.8 \times 10^{-4}$ mol; 29%)

**$^1$H NMR** ($CDCl_3$) δ 1.43 (s, 19H, di-*t*-butyl), 1.70 (s, 3H, methyl), 3.24 (s, 2H, methylene), 5.05 (s, 1H, phenol), 6.97 (s, 2H, aromatic)

**57** - 57.2 mg ($2.1 \times 10^{-4}$ mol; 22%)

**$^1$H NMR** ($CDCl_3$) δ 0.9 (s, 9H, alkyl *t*-butyl), 1.45 (s, 19H, aromatic ring *t*-butyls), 2.40 (s, 2H, benzyl methylene), 5.02 (s, 1H, phenol), 6.90 (s, 2H, aromatic)

**58** - 20.8 mg ($7.5 \times 10^{-5}$ mol; 8%)

**$^1$H NMR** ($CDCl_3$) δ 0.72 (t, 3H, J = 7.4 Hz, methyl), 1.24 (s, 6H, dimethyl), 1.45 (s, 19H, di-*t*-butyl), 1.65 (q, 2H, J = 7.5 Hz, methylene), 5.01 (s, 1H, phenol), 7.13 (s, 2H, aromatic)

**41** - 3.9 mg ($1.4 \times 10^{-5}$ mol; 1.0 %)

**$^1$H NMR** ($CDCl_3$) δ 1.31 (s, 9H, *para-t*-butyl), 1.45 (s, 19H, *ortho-t*-butyls), 5.05 (s, 1H, phenol), 7.21 (s, 2H, aromatic).

**40** - 2.6 mg ($8.4 \times 10^{-6}$ mol; 1%)

**$^1$H NMR** ($CDCl_3$) δ 0.90 (d, 6H, J = 6.9 Hz, dimethyl), 1.43 (s, 19H, di-*t*-butyl), 1.8 (m, 1H, J = 7.3 Hz, methine), 2.37 (d, 2H, J = 7.0 Hz methylene), 5.0 (s, 1H, phenol), 6.91 (s, 2H, aromatic).

**Reaction of 20 with sodium hydride.** Sodium Hydride (Ventron, 99%)(0.048 g; 2.0 mmol) was added to 3 mL of dry DMF at room temperature. To this was added 0.26g (1.0 mmol) of **20** dissolved in 3 mL of DMF. The reaction was allowed to stir for 12 h after which it was quenched with water and acidified with 1% $H_2SO_4$. The DMF/water was then extracted with 3 x 50 mL aliquots of ether and the ethereal layer isolated. The ethereal layer was then extracted with 3 x 100 mL aliquots of water, to remove any residual DMF, then dried with anhydrous magnesium sulfate. Separation of the drying

agent and evaporation of the ethereal layer resulted in 0.26 g (100%) of crude product. The following yields were observed using gas chromatographic quantitation versus biphenyl (Aldrich 99%):

recovered starting material - 73 mg ($2.9 \times 10^{-4}$ mol; 29%)

**39** -187 mg ($7.19 \times 10^{-4}$ mol; 71%)

**Reaction of 20 with lithium dimethylcuprate.** Copper (I) iodide (Aldrich, 99.999%) (0.239 g; 1.3 mmol) was added to 10 mL of dry THF under argon. The reaction mixture was then cooled to -13° C using an acetone/ice bath. Methyllithium (Aldrich;1.4 M in diethyl ether) ( 0.059 g; 2.7 mmol) was added to the flask dropwise with stirring while maintaining the temperature at 0° C.[108] To this was added over a 20 minute period 0.26 g (1.0 mmol) of **20** dissolved in 10 mL of dry THF. After the addition was complete the reaction mixture was allowed to warm to room temperature and stir for an additional 2 h. The reaction was then neutralized with a saturated sodium bicarbonate solution. A saturated ammonium chloride solution was then added to the solution to acidify and digest the remaining copper residue. The solution was then extracted with 3 x 50 mL aliquots of ether. The ethereal layer was dried with anhydrous magnesium sulfate. *In vacuo* removal of the ether resulted in 0.20 g (73%) yield of crude product. The crude product was observed to be 98% **58** through gas chromatographic analysis and quantitation versus biphenyl.

**Reaction of 20 with methyllithium.** To 5 mL of dry THF under argon was added 0.26 g (1.0 mmol) of **20** at room temperature. Into this mixture was syringed 2 mL of 1.4 M methyl lithium (0.044 g; 2.0 mmol) in diethyl ether. The reaction was then allowed to stir

for and additional 20 h. The reaction was then quenched with water and then acidified with 1% $H_2SO_4$. The reaction was extracted with 3 x 50 mL aliquots of ether. The ethereal layer was dried with magnesium sulfate. *In vacuo* removal of ether afforded 0.26 g (96%) crude product. The following yields were observed through gas chromatographic quantitation versus biphenyl (Aldrich 99%):

recovered starting material - 192 mg (0.74 mmol; 75%).

**39** - 33.8 mg (0.18 mmol; 13%)

**57** - 34.2 mg (0.12 mmol; 12%)

**General reaction of 19 and 20 with potassium thiophenoxide.** In a typical reaction 2.5 x $10^{-5}$ mol of substrate was dissolved in 5 mL of dry solvent that had been thoroughly purged with argon. This was added to potassium thiophenoxide ( 0.0045 g; 3.0 x $10^{-5}$ mol) and 18-crown-6 (Aldrich, 99.5%) (0.0085 g; 3.0 x $10^{-5}$ mol) dissolved in 5 mL of the same solvent at room temperature. The reaction mixture was allowed to stir for 1 h after which it was acidified with 1% $H_2SO_4$. The mixture was then extracted with 3 x 50 mL aliquots of ether. The ether was then washed with 3 x 100 mL of water and dried with anhydrous magnesium sulfate. The ether was then filtered and evaporated *in vacuo* to give **62** and **63** in yields ranging from 56 to 90 percent. Separation was afforded using high pressure liquid chromatography (HPLC). Yields are reported from quantitation data using calibration curves on the HPLC. Unreacted starting material comprised the rest of the sample.

**62** - mp 85.0 - 85.5° C, **$^1$H NMR** ($CDCl_3$) δ 1.42 (s, 19H, di-*t*-butyl), 1.44 (s, 6H, dimethyl), 3.20 (s, 2H, methylene), 5.07 (s, 1H, phenol), 7.19-7.20 (m, 7H, aromatic); **$^{13}$C**

**NMR** ($CDCl_3$) δ 28.25 (dimethyl), 30.34 (di-*t*-butyl), 34.54 (quaternary, *t*-butyl), 39.03 (benzylic quaternary, $C(CH_3)_2$), 49.83 (methylene, C-S), 162.46, 125.40, 128.59, and 129.36 (aromatic methine), 135.20 and 138.11 (aromatic quaternary, C-C), 138.38 (aromatic quaternary, C-S), 151.89 (aromatic quaternary, C-O); **UV-VIS** (ethanol) $\lambda_{max}$ 206 nm, log ε = 4.80; 258 nm, log ε = 3.95; **IR** (neat) 3640, 3059, 3000, 2963, 2871,1583,1479, 1437, 1382, 1363, 1320, 1637, 1158, 1120, 1025, 877, 809, 690, 668; **MS** m/e (relative intensity) 370 ($M^+$, 1), 339 (1), 262 (3), 247 (100), 631 (20), 217 (10), 163 (25), 83 (20), 57 (80); **HIGH RES. MS** for $C_{24}H_{34}OS$, calc. 370.633038, found 370.636330, error: 1.9 ppm

**63** - mp 87.0 - 88.0° C, **$^1$H NMR** ($CDCl_3$) δ 1.20 (s, 6H, dimethyl), 1.42 (s, 19H, di-*t*-butyl), 2.80 (s, 2H, methylene), 5.08 (s, 1H, phenol), 6.95 (s, 2H, aromatic), 7.33 (t, 3H, J = 7.0 Hz, sulfide aromatic), 7.39 (d, 2H, J = 5.6 Hz, sulfide aromatic); **$^{13}$C NMR** ($CDCl_3$) δ 28.07 (dimethyl), 30.38 (di-*t*-butyl), 34.20 (quaternary, *t*-butyl), 48.94 (methylene), 49.60 (aliphatic quaternary, $CH_2$-S), 127.25, 128.45, 128.64, and 137.68 (aromatic methine), 128.63 and 132.35 (aromatic quaternary, C-C), 135.08 (aromatic quaternary, C-S), 152.33 (aromatic quaternary, C-O); **UV-VIS** (ethanol) $\lambda_{max}$ 202 nm, log ε = 4.67; 274nm, log ε = 3.23; **IR** (neat) 3640, 3003, 2960, 2872, 1472, 1435, 1363, 1316,1635, 1159, 1120, 1024, 884, 705, 694; **MS** m/e (relative intensity) 370 ($M^+$, 5), 262 (40), 245 (20), 620 (35), 151 (100), 57 (95); **HIGH RES. MS** for $C_{24}H_{34}OS$, calc. 370.633038, found 370.632864, error: 0.5 ppm.

**64** - mp 80.0 - 80.5° C, **$^1$H NMR** ($CDCl_3$) δ 1.37 (d, 3H, J = 6.8 Hz, methyl), 1.43 (s, 19H, di-*t*-butyl), 2.92 (m, 1H, J = 7.0 Hz, methine), 3.10 (dd, 1H, $J_{AB}$ = 11 Hz, $J_{AX}$ = 5.3 Hz, methylene), 3.23 (dd, 1H, $J_{AB}$ =11 Hz, $J_{AX}$ = 8.8 Hz, methylene), 5.08 (s, 1H, phenol), 6.99 (s, 2H, phenol aromatic), 7.62 (m, 5H, sulfide aromatic) **$^{13}$C NMR** ($CDCl_3$) δ 20.84 (methyl), 30.38 (*t*-butyl), 34.41 (quaternary, di-*t*-butyl), 39.44 (methine), 42.51 (methylene), 163.42, 125.63, 128.79, and 163.94 (aromatic methine), 135.72 and 136.15 (aromatic quaternary, C-C), 137.62 (aromatic quaternary, C-S), 152.30 (aromatic quaternary, C-O); **UV-VIS** (ethanol) $\lambda_{max}$ 210 nm, log ε = 4.18; 258 nm, log ε = 3.87; **IR** (neat) 3637, 3057, 2957, 2871, 1583, 1480, 1436, 1390, 1372, 1313, 1635, 1213, 1152, 1120, 1025,882, 737, 690; **MS** m/e (relative intensity) 365 ($M^+$, 7), 633 (100), 217 (10), 163 (20), 57 (25); **HIGH RES. MS** for $C_{63}H_{32}OS$, calc. 356.217388, found 356.216949, error: 1.2 ppm.

**65** -**$^1$H NMR** ($CDCl_3$) δ 1.25 (d, 3H, J = 7.0 Hz, methyl), 1.41 (s, 19H, di-*t*-butyl), 2.58 (dd, 1H, $J_{AB}$ = 13.6 Hz, $J_{AX}$ = 5.1 Hz, methylene), 2.92 (dd, 1H, $J_{AB}$ = 13.6 Hz, $J_{BX}$ = 8.6 Hz, methylene), 3.40 (s, 1H, J = 6.8 Hz, methine), 5.05 (s, 1H, phenol), 6.94 (s, 2H, phenol aromatic), 7.29 (m, 5H, sulfide aromatic) **$^{13}$C NMR** ($CDCl_3$) δ 20.48 (methyl), 30.34 (di-*t*-butyl), 34.24 (quaternary, *t*-butyl), 43.62 (benzylic methylene), 44.77 (aliphatic methine, HC-S), 125.08, 125.71, 128.74, 126.27 (aromatic methine), 129.05 and 135.62 (aromatic quaternary, C-C), 152.63 (aromatic quaternary, C-S), 139.26 (aromatic quaternary, C-O); **UV-VIS** (ethanol) $\lambda_{max}$ 210 nm, log ε = 4.57; 260 nm, log ε = 3.22; **IR** (neat) 3640, 3072, 2957, 2871, 1583, 1479, 1434, 1390, 1374, 1362, 1315, 1634, 1212,

1154, 1121, 1025, 1011, 890, 879, 789, 769, 745, 692; **MS** m/e (relative intensity) 356 ($M^+$, 12), 346 (2), 247 (20), 620 (100), 137 (20), 109 (10), 57 (20); **HIGH RES. MS** for $C_{63}H_{32}OS$, calc. 356.217388, found 356.216949, error: 1.2 ppm.

**Reaction of (20) with potassium thiophenoxide in the presence of thiophenol.** To 5 mL of dry argon purged DMSO was added 0.066 g thiophenol (0.7 mmol) (Aldrich 97%) and 0.0624 g of potassium *t*-butoxide ( 0.2 mmol) (Aldrich 95%). The reaction was allowed to stir for 30 minutes at room temperature under argon to ensure the complete formation of potassium thiophenoxide. At the end of this period 0.052 g of **20** (0.2 mmol) dissolved in 5 mL of dry DMSO was added to the mixture. The reaction was allowed to stir for 5 h. At this time the reaction was quenched with 1% $H_2SO_4$. The mixture was extracted with 3 x 50 mL aliquots of ether. The ethereal layer was washed with 3 x 100 mL aliquots of water, to remove residual DMSO. The ethereal layer was separated and dried with magnesium sulfate. The ethereal layer was filtered and removed *in vacuo* to give 0.054 g (73 %) conversion of starting material to **62** and **63**. The following yields were observed through gas chromatographic quantitation versus 2,6-di-*t*-butylphenol (Aldrich 99%):

**62** - 42 mg (78%)

**63** - 12 mg (22%)

**Reaction of 20 with potassium thiophenoxide in the absence of light.** To 5 mL of dry argon purged DMSO was added with stirring thiophenol (0.062 g; 0.2 mmol) and potassium *t*-butoxide ( 0.0624 g; 0.2 mmol). The reaction was allowed to stir for 30 minutes at room temperature under argon to ensure the complete formation of potassium

thiophenoxide. At the end of this period the flask was wrapped with aluminum foil and the lights quenched. At this point 0.052 g (0.2 mmol) of **20** dissolved in 5 mL of dry DMSO was added to the mixture. The reaction was allowed to stir for 30 minutes at which time it was quenched with 1% $H_2SO_4$. The mixture was then extracted with 3 x 50 mL aliquots of ether. The ethereal layer was washed with 3 x 100mL aliquots of water to remove residual DMSO. The ethereal layer was dried with magnesium sulfate and filtered. *In vacuo* removal of the ether yielded the crude product. Through gas chromatographic quantitation the crude product was found to contain 45.6 mg , 62% conversion of starting material to compounds **62** and **63**. The following relative yields were observed:

**62** - 34.7 mg (78%)

**63** - 10.9 mg (22%)

**Reaction of 20 with potassium thiophenoxide in the presence of diphenyl disulfide.** Diphenyl disulfide (0.0872 g; 0.4 mmol) was dissolved in 5 mL of dry argon purged DMSO. Thiophenol (0.062 g; 0.2 mmol) and potassium *t*-butoxide (0.0624 mg; 0.2 mmol) were then added to the solution. The reaction was allowed to stir for 30 minutes at room temperature under argon to ensure the complete formation of potassium thiophenoxide. At this point 0.052 g (0.2 mmol) of **20** dissolved in 5 mL of dry argon purged DMSO was added to the mixture. The resulting mixture was allowed to stir for an additional 5 h at room temperature. Water was added to the reaction mixture which was then neutralized with 1% $H_2SO_4$. The reaction was extracted with 3 x 50 mL aliquots of ether. The ethereal extracts were combined and then washed with 3 x 100 mL aliquots of water to remove any residual DMSO. The ethereal layer was then dried with anhydrous

magnesium sulfate. Filtration of the ether and *in vacuo* removal of the ether afforded 53.6 mg, a 72.4% conversion of starting material to compounds **62** and **63**. The following yields were observed from gas chromatographic quantitation versus 2,6-di-*t*-butylphenol (Aldrich 99%) and biphenyl:

**62** - 41.9 mg (78.2%)

**63** -11.7 mg (21.8%)

Diphenyl disulfide - 68.3 mg (72.2 % recovery)

**Reaction of 20 with potassium thiophenoxide in the presence of air.** To 5 mL of dry DMSO was added with stirring thiophenol ( 0.062 g; 0.2 mmol) and potassium *t*-butoxide ( 0.0624 g; 0.2 mmol). The reaction was stirred for 30 minutes at room temperature under argon to ensure the complete formation of potassium thiophenoxide. At this time a 6 inch 19 gauge hypodermic syringe connected to an air line was inserted into the reaction mixture and the air valve opened. To this mixture 0.052 g (0.2 mmol) of **20** dissolved in 5 mL of dry DMSO was added. The reaction was allowed to stir for 1 hour after which the reaction was quenched with water. The resulting mixture was extracted with 3 x 50 mL aliquots of ether which were combined and extracted with 3 x 100 mL aliquots of water to remove residual DMSO. Anhydrous magnesium sulfate was used to dry the ether layer. Filtration of the magnesium sulfate and *in vacuo* removal of the ether resulted in 56 mg (76%) crude yield. The following yields were observed through gas chromatographic quantitation versus 2,6-di-*t*-butylphenol (Aldrich 99%):

recovered starting material - 39.1 mg (0.15 mmol, 76.7%)

**62** - 13 mg ($3.05 \times 10^{-5}$ mol, 17.9%)

**63** - 3.9 mg ($1.05 \times 10^{-5}$ mol, 5.4%)

**Competition reactions between 19 and bromoethane with potassium thiophenoxide in acetone and 2-propanol.** Substrate concentrations of 10 fold, 20 fold, and 100 fold excesses to potassium thiophenoxide were used in these experiments. In a typical experiment potassium thiophenoxide (0.00149 g; $1.0 \times 10^{-5}$ mol) and 18-crown-6 (0.00317 g; $1.2 \times 10^{-5}$ mol) (Aldrich 99.5%) was dissolved in 5 mL of dry, argon purged solvent. In a separate 5 mL of the dry argon purged solvent, **19** (0.246 g; 1.0 mmol) and bromoethane (0.179 g; 0.16 mmol) (Aldrich 99+%) were dissolved. The solutions were mixed, allowed to stir for 30 minutes and then neutralized with 1 % $H_2SO_4$. The solvent was then removed and 10 mL of acetonitrile was added. HPLC quantitation against pure standards were then used to calculate the amounts and ratios of **64**, **65**, and **69**.

**Competition reactions between 19 and bromoethane with potassium thiophenoxide in DMSO.** The substrate concentrations used in the acetone and 2-propanol experiments were also used in these experiments. However, DMSO reacts slowly with ethyl bromide so the experiments had to be conducted differently. In a typical experiment potassium thiophenoxide (0.00149 g; $1 \times 10^{-5}$ mol) and 18-crown-6 (0.00317 g; $1.2 \times 10^{-5}$ mol) were dissolved in 5 mL of dry, argon purged DMSO. In a separate 5 mL of dry, argon purged DMSO **19** (0.246 g; 1.0 mmol) was dissolved. Ethyl bromide (0.179 g; 1.6 mmol) was then quickly injected into the DMSO solution containing **19**. The resulting solution containing both ethyl bromide and **19** was quickly mixed with the potassium thiophenoxide solution, allowed to stir for 10 minutes and then neutralized with 1 %

$H_2SO_4$. The quenched reaction mixture was then quantitated using the HPLC against pure standards to calculate the amounts and ratios of **64**, **65**, and **69**.

## VOLTAMMETRY

### Synthesis of Electrolyte

**Tetra-*n*-butylammonium tetrafluoroborate** (*n*-$Bu_4NBF_4$) was prepared by treatment of tetra-*n*-butylammonium bromide (Aldrich 99%) with aqueous $HBF_4$ (Fisher 48-50%) using the method of House.[109] The crude salt was thoroughly washed with distilled water then dried at 60° C in a vacuum oven at 0.1 mm Hg and recrystallized five times from ethyl acetate/hexane. The resulting solid was then placed into the vacuum oven at 60° C at 0.1 mm Hg. The salt was then stored in a dessicator until needed.

**Tetra-*n*-butylammonium perchlorate** (*n*-$Bu_4NClO_4$) was prepared by the treatment of tetra-*n*-butylammonium bromide (Aldrich 99%) with aqueous perchloric acid (69-72 %) using the method of House.[109] Workup and storage of the electrolyte followed the same procedure as that in the synthesis of tetra-*n*-butylammonium tetrafluoroborate.

### Solution Preparation

The exact systems used are discussed in the electrochemistry section of this manuscript. The general procedure used for solution preparation follows. An amount of supporting electrolyte was weighed out into a 10 mL volumetric flask to make a 0.5 M solution. This was placed in the vacuum oven and heated at 60° C for 2 h to remove any

residual moisture. DMF (purified as described earlier) was then added to the electrolyte. The mixture was shaken until homogeneous, then added immediately to an argon filled, oven dried voltammetry cell under positive argon pressure. After solution background measurements were obtained, a premeasured amount of the substrate to be reduced was carefully added to the voltammetry cell. Measurements were began once the voltammetry solution was homogeneous.

**Voltammetric Cell**

The voltammetric cell (part no. K0060) and cell bottom (part no. K0066) were purchased from EG&G/PAR. The cell was placed in a vacuum oven at 60° C at 1mm Hg for two hours prior to use. The cell was kept under positive argon pressure while a small Teflon® stir bar was added and the electrodes were assembled in the cell. The solution was then added, stirred, and purged with argon for 30 minutes prior to use.

**Working Electrodes**

The working electrodes used were purchased from Bioanalytical Systems (BAS). The gold electrode was a planar gold button of 1.6 mm encased in a Kel-F plastic sheath (part no. MF-2014). The glassy carbon electrode (GCE) was a planar button of 3.0 mm encased in a Kel-F plastic sheath (part no. MF-2012). Polishing of the electrodes was conducted using Buehler Alpha Micropolishes on Buehler Micropolishing pads (part no. 40-7212). Electrodes were first polished with 1 micron polish (part no. 40-6354) until all deep scratches were removed from the electrode surface. This was followed by 0.3 micron polish (part no. 40-6352). Finally 0.05 micron polish was used until a mirror finish was observed on each electrode. The electrodes were rinsed first with acetone, followed

by methanol, and finally with distilled water. The electrodes were then placed in the vacuum oven at 40° C at 1 mm Hg for 3 h. They were either used immediately or stored in a dessiccator until needed. Electrodes were polished before each use.

**Auxiliary Electrodes**

One auxiliary electrode was a 0.8 mm X 8 cm piece of platinum wire (Fisher) connected to a length of 1.0 mm diameter silver wire (Aldrich). The platinum/silver connection was encased in glass tubing so that only platinum was exposed to the voltammetry solution. The other auxiliary electrode was fabricated from a length of 19 gauge copper wire. This electrode was isolated from the voltammetry solution by placing it in a reference bridge tube (EG&G/PAR part no. RDE0020) fitted with Teflon® heat shrink (BAS part no. MF-2027) and a 5 mm length of 4 mm Vycor® rod (BAS part no. MF-1080). The molar concentration of the electrolyte in the isolated auxiliary electrode was exactly that present in the voltammetry cell. The Teflon® and Vycor® were replaced for each use.

**Reference Electrode**

The reference electrode was constructed by sealing a 5mm length of 4 mm diameter Vycor® rod (BAS part no. MF-1080) to a 4 mm OD pyrex tube with Teflon® heat shrink tubing (BAS part no. MF-2027). The pyrex tube was then connected to a reference bridge tube (EG&G/PAR part no. RDE0020). This was filled with 0.1 M $AgNO_3$ in acetonitrile (EG&G/PAR part no. GO139). A 0.1 mm length of silver wire was emmersed in the solution. Any air bubbles present were removed from the solution by

gently tapping the side of the electrode. This produces a reference electrode that is 337 mV positive relative to SCE. This assembly was remade for each use.

**Positive Feedback IR Compensation**

After allowing the solution to degas for thirty minutes, the stirring was stopped, and the electrodes were manipulated to bring them as close as possible to one another. Bubbles were removed from the electrode surface by gently tapping the side of the voltammetry cell. Positive feedback IR compensation was set by increasing the IR compensation until a current overload was obtained. The IR compensation was then set at 85% of this value.

**Voltammetric Runs**

Experiments were performed at 25° C. The voltammetric cell was blanketed (positive pressure) with argon. The voltammetry of **20** was conducted beginning with a sweep rate of 25 mV/s. The solution was stirred and bubbled for 30 seconds, allowed to settle, then the voltammetry at 1000 mV/s was conducted after which the bubbling and stirring was repeated. This was repeated in the order of: 50,750; 75,500; 100, 250. This method was repeated until 3 data points were obtained for each sweep rate. The potentials were then averaged at each sweep rate.

The voltammetry for **52** was conducted beginning at a sweep rate of 25 mV/s proceeding sequentially to 1000 mV/s. When readings became erratic, the electrode was removed, polished gently with a dry polishing pad, and carefully replaced. The IR compensation was then reset as described before at a sweep rate of 1000 mV/s.

## ELECTROLYSES

### Solution Preparation

All electrolysis were performed on solutions which contained 0.5 M *n*-$Bu_4NBF_4$ in DMF. The Blank solutions were prepared as described in the voltammetry section. The electrolysis equipment was dried in a vacuum oven at 60° C at 1 mm Hg for 3 hours. The electrolysis cell was then either stored in a dessiccator, or immediately assembled under a positive pressure of argon. The electrolyte solution was partitioned into 25 mL aliquots and placed in the anodic and cathodic compartments. The substrate to be reduced was added to the cathodic compartment..

### Electrolysis Cell

A two compartment H cell separated by a medium porosity glass frit was used to perform the electrolysis. The frit was positioned so that 25 mL of electrolyte solution completely immersed the frit. The working electrode, auxiliary electrode, and purge tubes were introduced into the solution through a no. 6 rubber stopper. The reference electrode was introduced through a 14/20 ground glass joint situated on the side of the H cell. Purge vents were also afforded using 14/20 glass joints and outlets emanating from the side of the H cell.

### Working Electrode

The working electrode was constructed from a 0.127 mm X 25 mm X 25 mm piece of gold foil (Aldrich). This was silver soldered to a 0.5 mm X 4 cm piece of platinum wire. The platinum wire was then silver soldered to a length of copper wire and

sealed in a 4 mm OD pyrex tube. This left the gold foil and the platinum wire as the only metallic substances exposed to the electrolysis solution.

**Auxiliary Electrode**

The auxiliary electrode was constructed from a length of 19 Ga. copper wire. A 10 turn coil measuring 25 mm X 25 mm was immersed into the solution.

**Reference Electrode**

The reference electrode was fabricated the same way as that for the cyclic voltammetry experiments.

**Experimental Runs**

All electrolysis experiments were performed at ambient temperature (63° C). Constant current electrolysis was performed at 30 mA. The solutions were degassed with argon for 30 minutes prior to the beginning of the electrolyses. Degassing was continued through the extent of the experiment. The electrolysis apparatus was placed in a sonicator and sonicated throughout the duration of the experiment. After the allotted electrolysis period, enough 1% $H_2SO_4$ was added to neutralize the electrolysis solution. The contents of the mixture were then poured into 50 mL of water and extracted with 4 x 50 mL aliquots of ether. The combined organic layers were then washed with 3 x 100 mL aliquots of distilled water to remove any residual DMF. The organic layer was then dried with magnesium sulfate, filtered and the ether removed in vacuo.

**SPECIFIC ELECTROLYSIS**

1-Methyl-5,7-di-*t*-butylspiro[2,5]octa-4,7-dien-6-one (**19**)

Spiro[2,5]octadienone **19** (0.060 g, 0.24 mmol) was electrolyzed at 30 mA for 20 minutes. Approximately 0.369 mmol (1.40 equivalents) of electrons were introduced into the solution during this time . Work up of the reaction mixture yielded 50.2 mg (73 %) crude yield of products. The products were then separated by HPLC using a 80/20 mixture of acetonitrile/water, identified by $^1$H NMR, then quantitated on the HPLC using the same solvent mixture. The crude reaction mixture was found to be composed of the following compounds.

**48** - 16.5 mg ($6.65 \times 10^{-5}$ mol; 45%)

**$^1$H NMR** ($CDCl_3$) δ 1.63 (d, 3H, J = 6.9 Hz, methyl), 1.45 (s, 19H, di-*t*-butyl), 2.83 (m, 1H, methine), 5.03 (s, 1H, phenol), 7.03 (s, 2H, aromatic)

**47** - 12.5 mg ($5.04 \times 10^{-5}$ mol; 35%)

**$^1$H NMR** ($CDCl_3$) δ 0.99 (t, 3H, J = 7.2 Hz, methyl), 1.46 (s, 19H, di-*t*-butyl), 1.63 (m, 2H, J = 7.5 Hz, methylene), 2.52 (t, 2H, J = 7.6 Hz, benzylic methylene), 5.04 (s, 1H, phenol), 7.00 (s, 2H, aromatic)

**46** - 7.34 mg ($2.98 \times 10^{-5}$ mol; 20%)

**$^1$H NMR** ($CDCl_3$) δ 1.43 (s, 19H, di-*t*-butyl), 3.31 (d, 2H, J = 6.8 Hz, benzylic methylene), 5.02-5.11 (complex, 3H, phenol and terminal vinylic protons), 5.97 (m, 1H, vinylic), 6.99 (s, 2H, aromatic)

**2-(3′,7′-di-*t*-butyl-4′-hydroxyphenyl)-propan-2-ol** - 7.85 mg ($2.97 \times 10^{-5}$ mol; 12.4%)

**$^1$H NMR** ($CDCl_3$) δ 1.43 (s, 6H, dimethyl), 1.48 (s, 19H, di-*t*-butyl), 5.85 (s, 1H, phenol), 7.85 (s, 2H, aromatic), 9.35 (s, 1H, alcohol).

## LITERATURE CITED


1. Russel, G. A.; Janzen, E. G.; Stron, E. T. *J. Am. Chem. Soc.* **1964**, *64*, 1807.
2. Ashby, E. C.; Goel, A. B.; Depriest, R. N. *J. Am. Chem. Soc.* **1980**, *102*, 7780.
3. House, H. O.; Chu, C.-Y. *J. Org. Chem.* **1976**, *41*, 3083.
4. Okubo, M. *Bull. Chem. Soc. Jpn.* **1975**, *48*, 1057.
5. Ashby, E. C.; Argyropoulos, J. N. *J. Org. Chem.* **1986**, *51*, 472.
6. Newcomb, M.; Burchill, M. *J. Am. Chem. Soc.* **1984**, *106*, 8276.
7. House, H. O.; Prabhu, A. V.; Wilkins, J. M.; Lee, L. F. *J. Org. Chem.* **1976**, *41*, 3067.
8. Tanner, D. D.; Stein, A. R. *J. Org. Chem.* **1988**, *40*, 1642.
9. Tanner, D. D.; Chen, J. J.; Luelo, C. *J. Am. Chem. Soc.* **1991**, *113*, 8074.
10. Andrieux, C. P.; Savéant, J. M.; Zann, D. *Nouv. J. Chim.* **1984**, *7*, 107.
11. Andrieux, C. P.; Hapiot, P.; Savéant, J. M. *J. Phys. Chem.* **1988**, *92*, 5987.
12. Wipf, D. O.; Wightman, R. M. *J. Phys. Chem.* **1989**, *93*, 4286.
13. Sucheta, A.; Rusling, J. F. *J. Phys. Chem.* **1989**, *93*, 5796.
14. Aalstad, B.; Parker, V. D. *Acta Chem. Scand.* **1982**, *B36*, 47.
15. Nadjo, L.; Savéant, J. M. *J. Electroanal. Chem.* **1971**, *30*, 41.
16. Yamataka, H.; Yamaguchi, K.; Takatsaka, T.; Hanafusa, T. *Bull. Chem. Soc. Jpn.* **1992**, *65*, 1157.
17. Ashby, E. C.; Wiesemann, T. L. *J. Am. Chem. Soc.* **1978**, *100*, 3101.
18. House, H. O. *Acc. Chem. Res.* **1976**, 59.

19. House, H. O.; Weeks, P. D. *J. Am. Chem. Soc.* **1975**, *97*, 2770.

20. Griller, D.; Ingold, K. U. *Acc. Chem. Res.* **1980**, *13*, 317.

21. Bailey, W. F.; Patricia, J. J.; Delgobbo, V. C.; Jarret, R. M.; Okarma, P. J. *J. Org. Chem.* **1985**, *50*, 2000.

22. Ashby, E. C. *Pure and Appl. Chem.* **1980**, *52*, 545.

23. Ashby, E. C.; Bowers, J.; Depriest, R. *Tetrahedron Lett.* **1980**, *21*, 3541.

24. Holm, T. *Acta Chem. Scand.* **1983**, *B37*, 567.

25. Ashby, E. C. *Acc. Chem. Res.* **1988**, *21*, 414.

26. Holm, T. *Acta, Chem. Scand.* **1987**, *B41*, 278.

27. Smith, D. A.; Dimmel, D. R. *J. Org. Chem.* **1988**, *40*, 5428.

28. Swartz, J. E.; Mahache, T. J.; Karvin-Miller, E. *J. Am. Chem. Soc.* **1988**, *110*, 3622.

29. Garst, J. F.; Hines, J. B. Jr. *J. Am. Chem. Soc.* **1984**, *106*, 6443.

30. Newcomb, M.; Glenn, A. G. *J. Am. Chem. Soc.* **1989**, *111*, 275.

31. Beckwith, A. L. J.; Bowry, V. W. *J. Org. Chem.* **1989**, *54*, 2681.

32. Patel, D. J.; Hamilton, C. L.; Roberts, J. D. *J. Am. Chem. Soc.* **1965**, *87*, 5744.

33. Kündig, E. P.; Perret, C. *Helv. Chim. Acta* **1981**, *64*, 2606.

34. Lansbury, P. T.; Pattison, V. A.; Clement, W. A.; Sidler, J. D. *J. Am. Chem. Soc.* **1965**, *86*, 2247.

35. Lansbury, P. T.; Pattison, V. A. *J. Am. Chem. Soc.* **1963**, *85*, 1886.

36. Tanko, J. M.; Drumright, R. M.; Suleman, N. K.; Brammer, L. E. Jr. *J. Am. Chem. Soc.* **1994**, *116*, 1785.

37. Tanko, J. M.; Drumright, R. E. *J. Am. Chem. Soc.* **1990**, *112*, 4062.

38. Tanko, J. M.; Drumright, R. E. *J. Am. Chem. Soc.* **1992**, *114*, 1844.

39. Tanner, D. D.; Chen, J. J.; Luelo, C.; Peters, P. M. *J. Am. Chem. Soc.* **1992**, *114*, 713.

40. Liotta, D.; Saindane, M.; Waykole, W. *J. Am. Chem. Soc.* **1983**, *105*, 2923.

41. Tanko, J. M.; Brammer, L. E. Jr.; Hervas', M.; Campos, K. *J. Chem. Soc., Perkin Trans. 2* **1994**, *7*, 1407.

42. Timberlake, T. W.; Chen, T. *Tet. Lett.* **1994**, *35*, 6043.

43. Mabbott, G. *J. Chem. Ed.* **1983**, *60(9)*, 697.

44. Kissinger, P.; Heineman, W. *J. Chem. Ed.* **1983**, *60(9)*, 702.

45. Pletcher, D. *"A First Course In Electrode Processes"* ; The Electrosynthesis Company: New York, 1991.

46. Parker, V. *"Topics In Organic Electrochemistry"*, Fry, A., Britton, W., Eds.; Plenum Press: New York, 1986, pp. 35-79.

47. Parker, V. *"Advances In Physical Organic Chemistry"*, Vol. 19, Gold, V., Bethell, D., Eds.; Academic Press: New York, 1983, pp. 131-223.

48. Bard, A. J.; Faulkner, L. F. *"Electrochemical Methods"*, John Wiley and Sons: New York, 1980.

49. Andrieux, C. P.; Gorande, A. L.; Savéant, J. M. *J. Am. Chem. Soc.* **1992**, *114*, 6892.

50. Portnykh, N. V.; Volod'kin, A. A.; Ershov, V. V *Bull. Acad. Chem. Sci. USSR, Div. Chem. Sci.* **1966**, 2181.

51. Portnykh, N. V.; Volod'kin, A. A.; Ershov, V. V. *Bull. Acad. Chem. Sci. USSR, Div. Chem. Sci.* **1967**, 1328.

52. Portnykh, N. V.; Volod'kin, A. A.; Volod'kina, V. I. *Bull. Acad. Chem. Sci. USSR, Div. Chem. Sci.* **1970**, 688.

53. Schwartz, L. H.; Flor, R. V.; Gullo, V. P. *J. Org. Chem.* **1974**, *39*, 219.

54. Carey, F. A.; Sunberg, R. A. *"Advanced Organic Chemistry, 3rd Edition"* ; Plenum Press: New York, 1990.

55. Semiempirical MO calculations were performed using the AM1 approximation (M. J. S. Dewar, E. G. Zoebisch, E. F. Healy and J. J. P. Stewart *J. Am. Chem. Soc.* **1985**, *105*, 3902) and implemented through MOPAC 6.0 (QCPE, Program No. 439).

56. Nadjo, L.; Saveant, J. M. *J. Electroanal. and Interfac. Electrochem.* **1973**, *48*, 113.

57. Nadjo, L.; Saveant, J. M. *J. Electroanal. Chem.* **1973**, *48*, 113.

58. Digital simulations were performed using *"Cyclic Voltammetry: Simulation and Analysis of Reaction Mechanisms"*, D. K. Gosser, Jr.; VCH: New York, 1993.

59. Electrolysis data was obtained from unpublished results by Manuel Hervas.

60. House, H. O.; McDaniel, W. C.; Sieloff, R. F. Vanderveer, D. *J. Org. Chem.* **1978**, *43*, 4316.

61. Unpublished results obtained by Yonghui Wang.

62. a) Holm, T. *Acta Chem. Scand.* **1991**, *45*, 925. b) Okubo, M.; Morigami, Y.; Suenaga, R. *Bull. Chem. Soc. Jpn.* **1980**, *40*, 3029. c) Frey, J.; Nugiel, D. A.; Rappoport, Z. *J. Org. Chem.* **1991**, *56*, 466. d) Ashby, E. C.; Lopp, I. G.; Buhler, J. D. *J. Am. Chem. Soc.* **1975**, *97*, 1964. e) Lund, T.; Pedersen, M. L.; Frandsen, L. A. *Tetrahedron Lett.* **1994**, *49*, 9225. f) Holm, T. *Acta Chem. Scand.* **1976**, *B30*, 985.

63. a) House, H. O.; Chu, C.-Y. *J. Org. Chem.* **1976**, *41*, 3083. b) Ashby, E. C.; Goel A. B. *J. Am. Chem. Soc.* **1981**, *103*, 4983. c) Stasko, A.; Tkac, A.; Malik, L.; Adamcik, V. *J. Organomet. Chem.* **1975**, *92*, 261. d) Lopp, I. G.; Buhler, J. D.; Ashby, E. C. *J. Am. Chem. Soc.* **1975**, *97*, 4966. e) Okubo, M. *Bull. Chem. Soc. Jpn.* **1975**, *48*, 1057. f) Okubo, M. *Bull. Chem. Soc. Jpn.* **1977**, *50*, 2379. g) Maruyama, K.; Hayami, J.; Katagiri, T. *Chem. Lett.* **1986**, 601. h) Maruyama, K.; Katagiri, T. *Chem. Lett.* **1987**, 731. i) Maruyama, K.; Katagiri, T. *Chem. Lett.* **1987**, 735. j) Maruyama, K.; Katagiri, T. *J. Phys. Org. Chem.* **1989**, *2*, 205. k) Zhang, Y.; Wenderoth, B.; Su, W.-Y.; Ashby, E. C. *J. Organomet. Chem.* **1985**, *292*, 29. l) Maruyama, K.; Katagiri, T. *J. Am. Chem. Soc.* **1986**, *108*, 6263. m) Maruyama, K.; Matano, Y.; Katagiri, T. *J. Phys. Org. Chem.* **1991**, *4*, 501.

64. a) Yamataka, H.; Hanafusa, T. *J. Org. Chem.* **1988**, *40*, 772. b) Yamataka, H.; Matsuyama, T.; Hanafusa, T. *J. Am. Chem. Soc.* **1989**, *111*, 4912. c) Yamataka, H.; Kawafuji, Y.; Nagareda, K.; Miyano, N.; Hanafusa, T. *J. Org. Chem.* **1989**, *54*, 4706. d) Matsuyama, T.; Yamataka, H.; Hanafusa, T. *Chem. Lett.* **1988**, 1367. e) Yamataka, H.; Matsuyama, T.; Hanafusa, T. *Chem. Lett.* **1987**, 647.

65. Carloni, P.; Greci, L.; Stipa, P.; Eberson, L. *J. Org. Chem.* **1991**, *56*, 4733.

66. a) House, H. O. *Acc. Chem. Res.* **1976**, *9*, 59. b) House, H. O.; Weeks, P. D. *J. Am. Chem. Soc.* **1975**, *97*, 2771. c) House, H. O.; Weeks, P. D. *J. Am. Chem. Soc.* **1975**, *97*, 2785. d) Ashby, E. C.; Wiesemann, T. L. *J. Am. Chem. Soc.* **1978**, *100*, 3101.

67. Yamataka, H.; Yamaguchi, K.; Takatsuka, T. *Bull. Chem. Soc. Jpn.* **1992**, *65*, 1157.

68. a) Rein, K. S.; Chen, Z.-H.; Perumal, L. E.; Gawley, R. E. *Tetrahedron Lett.* **1991**, *32*, 1941. b) House, H. O.; McDaniel, W. C.; Sieloff, R. F.; Vanderveer, D. *J. Org. Chem.* **1978**, *22*, 4316. c) Wigal, C. T.; Grunwell, J. R.; Hershberger, J. *J. Org. Chem.* **1991**, *56*, 3759. d) Anderson, S. J.; Hopkins, W. T.; Wigal, C. T. *J. Org. Chem.* **1992**, *57*, 4304. e) Nasipuri, D.; Saha, A. *Ind. J. Chem.* **1990**, *29B*, 471. f) Nasipuri, D.; Saha, A. *Ind. J. Chem.* **1990**, *29B*, 474. g) Ashby, E. C. *Acc. Chem. Res.* **1988**, *21*, 414. h) Miller, B.; Matjeka, E. R.; Haggerty, J. G. *J. Org. Chem.* **1984**, *49*, 3121. i) Thomas, E. W.; Szmuszkovicz, J. R. *J. Org. Chem.* **1990**, *39*, 6054. j) House, H. O.; Weeks, P. D. *J. Am. Chem. Soc.* **1975**, *97*, 2778. k) House, H. O.; Snoble, K. A. J. *J. Org. Chem.* **1976**, *41*, 3076.

69. a) Breuer, E.; Segall, E.; Stein, Y.; Sarel, S. *J. Org. Chem.* **1972**, *37*, 2242. b) Traas, P.; Boelas, H.; Takken, H. *Rec. Trav. Chim. Pays-Bas* **1976**, *95*, 57. c) Schliemann, W.; Buege, A.; Reppel, L. *Pharmazie* **1980**, *35*, 140.

70. a) Hall, S.; Sha, C.; Jordan, F. *J. Org. Chem.* **1976**, *41*, 1494. b) Blumbergs, P.; Lamontagne, M.; Stevens, J. *J. Org. Chem.* **1972**, *37*, 1248.

71. Miyaura, N.; Itoh, M.; Sasaki, N.; Suzuki, A. *Synthesis* **1975**, *5*, 317.

72. Holm, T *J. Am. Chem. Soc.* **1993**, *115*, 918.

73. Yamataka, H.; Fujimura, N.; Kawafuji, Y; Hanafusa, T. *J. Am. Chem. Soc.* **1987**, *109*, 4305.

74. Bertz, S. H.; Dabbagh, G.; Cook, J. M.; Honkan, V. *J. Org. Chem.* **1984**, *49*, 1739.

75. a)Yamamoto, Y.; Yamada, J.; Uyehara, T. *J. Am. Chem. Soc.* **1987**, *109*, 5820. b) Snyder, J. P. *J. Am. Chem. Soc.* **1995**, *117*, 11025. c) Snyder, J. P. *Angew. Chem. Int. Ed. Engl.* **1995**, *34*, 80.

76. Ashby, E.C.; Park, W. S.; Goel, A. B.; Su, W.-Y. *J. Org. Chem.* **1985**, *50*, 5184.

77. a) Christenson, B.; Olsson, T.; Ullenius, C. *Tetrahedron* **1989**, *45*, 523. b) House, H. O.; Umen, M. J. *J. Am. Chem. Soc.* **1972**, *94*, 5495. c) Corey, E. J.; Hannon, F. J.; Boaz, N. W. *Tetrahedron* **1989**, *45*, 545. d) Nakamura, M.; Nakamura, E.; Koga, N.; Morokuma, K. *J. Chem. Soc. Faraday Trans.* **1994**, *90*, 1789. e) Bertz, S. H.; Dabbagh, G. *J. Am. Chem. Soc.* **1988**, *110*, 3668. f) Smith, R. A. *Tetrahedron* **1989**, *45*, 517. g) Lipshutz, B. H.; Wilhelm, R. S.; Kozlowski, J. A. *J. Org. Chem.* **1984**, *49*, 3938. h) Lipshutz, B. H.; Wilhelm, R. S.; Kozlowski, J. A. *J. Org. Chem.* **1984**, *49*, 3943.

78. Pearson, R. G.; Sobel, H.; Songstad, J. *J. Am. Chem. Soc.* **1968**, *90*, 319.

79. Houle, F. A.; Beauchamp, J. L. *J. Am. Chem. Soc.* **1979**, *101*, 4067.

80. Andrieux, C. P.; Hapiot, P.; Pinson, J.; Savéant, J. M. *J. Am. Chem. Soc.* **1993**, *115*, 7783.

81. Isaacs, N. S. *"Organic Chemistry"*; John Wiley and Sons: New York, 1987.

82. Asmus, K.-D.; Bonifacic, M. *"LANDOLT-BÖRNSTEIN: Radical Reaction Rates in Liquids"*, Hellwege, K.-H.; Madelung, O. Eds.; Springer Verlag: New York, 1984.

83. Gelles, E.; Hughes, E. D.; Ingold, K. E. *J. Chem. Soc.* **1954**, 2918.

84. Kinoshita, T.; Ueda, H.; Takeuchi, K. *J. Chem. Soc. Perkin Trans. 2* **1993**, 603.

85. Okamoto, K.; Matsui, Y.; Shingu, H. *Bull. Chem. Soc. Jpn.* **1965**, *38*, 1844.

86. Dvorko, G. F.; Golovko, N. N.; Pervishko, T. L. *Russ. J. Gen. Chem.* **1994**, *64*, 1152.

87. Grunwald, E.; Winstein, S. *J. Am. Chem. Soc.* **1948**, *70*, 846.

88. Wells, P. R. *Chem. Rev.* **1963**, *63*, 171.

89. Reichardt, C. *"Solvents and Solvent Effects in Organic Chemistry"*; VCH: Germany, 1990.

90. Smith, S. G.; Fainberg, A. H.; Winstein, S. *J. Am. Chem. Soc.* **1961**, *83*, 618.

91. Cho, I; Kim, W.-T. *J. Polymer Sci.* **1987**, *25*, 2791.

92. de la Mare., P. D. *J. Am. Chem. Soc.* **1939**, *77*, 3169.

93. Hughes, E. D.; Ingold, C. K.; Mackie, J. D. H. *J. Am. Chem. Soc.* **1939**, *77*, 3173.

94. Hughes, E. D.; Ingold, C. K.; Mackie, J. D. H. *J. Am. Chem. Soc.* **1939**, *77*, 3177.

95. de la Mare., P. D. *J. Am. Chem. Soc.* **1939**, *77*, 3180.

96. a) Fowden, L.; Hughes, E. D.; Ingold, C. K. *J. Am. Chem. Soc.* **1939**, *77*, 3187.; b)Fowden, L.; Hughes, E. D.; Ingold, C. K. *J. Am. Chem. Soc.* **1939**, *77*, 3193.

97. Walsh, A. D. *Trans. Faraday Soc.* **1949**, *45*, 179.

98. Danishefsky, S.; Singh, R. K. *J. Org. Chem.* **1975**, *40*, 3807.

99. Danishefsky, S.; Rovnyak, G. *J. Chem. Soc. Chem. Comm.* **1972**, 821.

100. Danishefsky, S. *Acc. Chem. Res.* **1979**, 66.

101. Eberson, L. *"Electron Transfer Reactions in Organic Chemistry"* ; Springer-Verlag: New York, 1987.

102. Still, W.; Kahn, M.; Mitra, A. *J. Org. Chem.* **1978**, *43*, 2923.

103. Mann, C. *"Electroanalytical Chemistry, Vol. 3"* Bard, A. Ed; Marcel Dekker: New York, 1969.

104. BASF *"BTS Catalyst Booklet"* BASF Corporation, E 221 State Highway 4, P.O. Box 289, Paramus, New Jersey, 07652, (201) 316-3000.

105. Winkle, M. R.; Lansinger, J. M.; Ronald, R. C. *J. Chem. Soc. Chem. Commun.* **1980**, 87.

106. *"CRC Handbook of Chemistry and Physics, 67th ed."* Weast, R. C., Ed.; CRC Press: Boca Raton, Florida, 1986.

107. *"Aldrich Handbook of Fine Chemicals"*, Aldrich Chemical Company, 1001 West Saint Paul Avenue, Milwaukee, WI 40233, 1993, p. 604.

108. Thomas, E. W.; Szmuszkovicz, J. R. *J. Org. Chem.* **1990**, *39*, 6054.

109. House, H. O.; Feng, E.; Peet, N. *J. Org. Chem.* **1971**, *36*, 2371.

## Vita

Larry Eugene Brammer, Jr. was born on September 8, 1960 in Huntington, WV to Katie Jo and Larry E. Brammer. He graduated high school in 1978 from Huntington East High School. After a not so illustrious start in higher education, he enlisted in the United States Air Force, where he became a ground radio repair specialist. While in the Air Force he attained the rank of Staff Sergeant and received the Air Force Commendation Medal. He was honorably discharged in 1986.

Upon discharge from the Air Force, he enrolled at Marshall University, Huntington WV and began pursuing a degree in physical therapy. However, after his first accident in the sophomore organic laboratory he became interested in organic chemistry. He later began work in the laboratory of Dr. John L. Hubbard. He received a Bachelor of Science degree in Chemistry from Marshall University in the summer of 1989.

In the summer of 1990, he began work on a Masters degree in Chemistry at Marshall University under the supervision of Dr. Lawrence Schmitz. He graduated from Marshall University with a Master of Science degree in Chemistry from Marshall University in the fall of 1991. While at Marshall University he became acquainted with Dr. James M. Tanko whose group he later joined.

In the fall of 1992 he entered the doctoral program at Virginia Polytechnic Institute and State University where he worked in the area of physical organic chemistry under the direction of Dr. James M. Tanko. He received a Doctor of Philosophy degree in Chemistry in June 1996 from VPI&SU.

Dr. Brammer has accepted a post doctoral position under the supervision of Dr. Tomas Hudlicky at the University of Florida, Gainesville FL where he will be investigating the microbial oxidations of organic compounds.